Title:	**Mission Operation Concept Document part C**
Reference :	EUCL-IAUL-RP-8-001
Issue :	4.4
Date :	14/02/2025
Custodian:	Ismael Tereno

Authors	**Role**	**Signature**
João Dinis Ismael Tereno	EC, SOST EC, SOST lead	
Contributors		**Signature**
Carlo Burigana Jean-Charles Cuillandre Roberto Scaramella Tiziana Trombetti	EC, ECSURV EC, ECSURV EC, ECSURV lead EC, SOST	
Approved		**Signature**
Y. Mellier	EC, EC lead	

The presented document is Proprietary information of the Euclid Consortium.
This document shall be used and disclosed by the receiving Party and its related entities (e.g. contractors and subcontractors) only for the purposes of fulfilling the receiving Party's responsibilities under the Euclid Project and that the identified and marked technical data shall not be disclosed or retransferred to any other entity without prior written permission of the document preparer.

Document version tracking

Issue	Date	Page	Description
1.0	30/09/20	All	New document. Partially replaces the former MOCD-B whose contents are now split in two new documents: CRSDIV and MOCD-C. Companion document to RSD_2020B. Delivered for the SCOMT review.
2.0	18/01/22	All	Companion document to RSD_2022A. Revised layout.
2.1	08/02/22	10, 28-29, 36, 51-57	Second issue of the companion document to RSD_2022A. Delivered for the MKP review. Includes expanded compliance tables, revised Figs. 4.2, 5.5, Tab. 5.4, and revised associated discussions. Also known as MOCDC_v2022A.1 (this temporary style for versioning was later abandoned).
3.0	08/02/22	All	Companion document to RSD_2022B. Delivered for the MKP review. Introduces a major novelty in the survey: a larger Euclid Deep Survey. Change of institutional reference to IAUL. Also known as MOCDC_v2022B.0 (this temporary style for versioning was later abandoned).
4.0	10/05/2023	All	Companion document to RSD_2023A. Delivered for the FAR review.
4.1	12/06/2023	All	Companion document to RSD_2023B. Revised layout. Implements a new scientific merit function. It is the first SOST delivery and an outcome of the first SOST rehearsal. It is also the first RSD under configuration control and introduces the RSD configuration model. Endorsed by the RSD CCB.
4.2	19/01/2024	All	Companion document to RSD_2024A, the first operational sky survey. Introduces RSD tags. Expanded section on RSD inputs.
4.3	24/09/2024	All	Companion document to RSD_2024C, the first replanned sky survey.
4.4	14/02/2025	All	Companion document to RSD_2024A, the first sky survey with field recovery.

Table of Contents

The presented document is Proprietary information of the Euclid Consortium.
This document shall be used and disclosed by the receiving Party and its related entities (e.g. contractors and subcontractors) only for the purposes of fulfilling the receiving Party's responsibilities under the Euclid Project and that the identified and marked technical data shall not be disclosed or retransferred to any other entity without prior written permission of the document preparer.

1 Introduction

1.1 Purpose and scope

The Mission Operations Concept Document part C version 4.4 describes the **Reference Survey Definition RSD_2025A**.

An RSD is a sequence of pointings of EWS, EDS, auxiliary fields, and calibration observations, as well as S/C slews, to be followed by Euclid as it operates in a step-and-stare mode from its orbital position, starting at the end of PDCC and finishing at the end of the nominal mission. Its ultimate goal is to fulfill the high-level science objectives of the Euclid mission. The corresponding RSDF is generated with the current version of ECTile and uses an XML format conformant to the XML Schema defined in [AD04].

The first RSD to be used for actual Euclid sky survey observations was RSD_2024A. It was followed by RSD_2024B, the first RSD generated with observations already executed. RSD_2024B introduced the repair capability, which enabled us to make corrections to a small number of non-EWS observations of RSD_2024A. The next RSD, RSD_2024C, was the first replanned survey, i.e., it computed a new survey after a restarting date while keeping the schedule of the observations already executed unchanged. The present RSD_2025A introduces the recovering capability. In contrast with replanning, recovering allows us to reschedule, after a restarting date, observations already scheduled in the previous RSD before the restarting date.

After this introduction, the present MOCD-C defines a list of RSD relevant parameters (tags) and provides their values. References and acronyms are found in Sect.2. The process of mission planning and RSD computation is documented in Sect. 3, which also keeps a tracking record of the modifications in planning strategy and software development that were implemented in each RSD. Section 3 also defines a list of RSD relevant parameters (tags) and provides their values. To construct a feasible RSD compliant with the science requirements, a large number of constraints need to be considered as input for its computation. There are three classes of inputs, defined in three applicable documents [AD01, AD02, AD03]. Their most relevant contents to the computation of the RSD are summarized in Sect. 4: system and operational constraints from [AD02] in Sect. 4.1, calibration requirements from [AD03] in Sect. 4.2, and guidelines for science optimization from [AD01] in Sect. 4.3. The RSD implementation is described in Sect. 5, while Sect. 6 presents an analysis of its results. Finally, Sect. 7 verifies the compliance of the current RSD with the system and top-level science requirements defined in [AD02] and with the calibration implementation procedures given in [AD03].

1.2 RSD parameters

RSD parameters are relevant input and output properties of #version_rsd collected here for ease of reference. These parameters appear throughout the MOCD-C document as recurring tags.

#bgs_brratio = 5:3
#bgs_selfcal = 1.4 deg

#count_fields_calib = 17 064
#count_fields_deep = 4309
#count_fields_polar = 1345

The presented document is Proprietary information of the Euclid Consortium.
This document shall be used and disclosed by the receiving Party and its related entities (e.g. contractors and subcontractors) only for the purposes of fulfilling the receiving Party's responsibilities under the Euclid Project and that the identified and marked technical data shall not be disclosed or retransferred to any other entity without prior written permission of the document preparer.

#count_fields_total = 50 526
#count_fields_wide = 27 957
#count_patches_total = 953
#count_patches_wide = 327
#count_slews_dither = 110 306
#count_slews_field = 42 956
#count_slews_large = 563
#count_slews_large_month_max = 14
#count_slews_total = 153 825

#ews_area_observed = 12 858.4 deg^2
#ews_area_enclosed = 13 025.4 deg^2
#ews_area_overlapfree = 11 031.6 deg^2

#fov_common = 0.5248 deg^2
#fov_dithered = 0.6880 deg^2
#fov_tile = 0.5508 deg^2
#fov_tile_effective = 0.4922 deg^2
#fov_tolerance = 3.5 deg

#overlap_f2f_mean = 504.6 arcmin^2
#overlap_global = 14.2%
#overlap_global_area = 1826.8 deg^2

#quality_q_min = 0.68
#quality_snr_j_mean = 8.11
#quality_snr_h_mean = 7.51
#quality_snr_rg_mean = 4.63
#quality_snr_vis_mean = 16.51
#quality_snr_y_mean = 6.72

#replan_basis = RSD_2024C
#replan_breakpoint = 2025-02-24T12:04:36Z
#replan_breakpoint_mjd = 9186.50362
#replan_patch = 142
#replan_restart = 2025-02-28T11:15:03Z
#replan_restart_mjd = 9190.46921

#roi_total = 16 220 deg^2
#roi_mainlandnorth = 7142 deg^2
#roi_mainlandsouth = 6877 deg^2
#roi_islandnorth = 148 deg^2
#roi_islandsouth = 2053 deg^2

#ros_d1 = 1073 s

The presented document is Proprietary information of the Euclid Consortium.
This document shall be used and disclosed by the receiving Party and its related entities (e.g. contractors and subcontractors) only for the purposes of fulfilling the receiving Party's responsibilities under the Euclid Project and that the identified and marked technical data shall not be disclosed or retransferred to any other entity without prior written permission of the document preparer.

#ros_duration = 4204 s
#ros_leadtime = 20 s
#ros_total = 4438 s

#slewtime_dither = 70 s
#slewtime_field_min = 170 s
#slewtime_field_typical = 214 s
#slewtime_total = 200.0 days
#slewtime_total_dither = 87.3 days
#slewtime_total_field = 106.9 days
#slewtime_total_large = 5.7 days

#solar_aamax = -2.9 deg
#solar_aamax_used = -3.054 deg
#solar_aamin = -8.5 deg
#solar_aamin_used = -8.331 deg
#solar_aapeak = 83%
#solar_aatarget = -4.5 deg
#solar_margin = 0.15 deg
#solar_saamax = 120.0 deg
#solar_saamax_used = 112.995 deg
#solar_saamin = 87.0 deg
#solar_saamin_used = 87.168 deg
#solar_saapeak = 40%
#solar_saadelta_outlier = 0.5%

#sop_aamin = -6.4 deg
#sop_aamax = -3.0 deg
#sop_cadence = 28 days
#sop_duration = 6 h
#sop_saamin = 89.1 deg
#sop_saamax = 118.9 deg

#stars_allsky = 3843
#stars_roi = 967
#starsholes_roi = 849
#starsholes_enclosed = 681
#starsholes_enclosed_area = 167.0 deg^2
#starsholes_enclosed_areafrac = 1.26 %

#threshold_cpcmin = 4 deg
#threshold_ext = 1.2 years
#threshold_polarcap = 77.8 deg
#threshold_thermalization = 7 days

#time_2500_ext = 1.44 years

The presented document is Proprietary information of the Euclid Consortium.
This document shall be used and disclosed by the receiving Party and its related entities (e.g. contractors and subcontractors) only for the purposes of fulfilling the receiving Party's responsibilities under the Euclid Project and that the identified and marked technical data shall not be disclosed or retransferred to any other entity without prior written permission of the document preparer.

#time_2500_ews = 1.32 years
#time_duration = 5 years and 10 months
#time_duration_days = 2134.5
#time_startingdate = 2024-02-14T00:00:00Z
#time_startingdate_mjd = 8810.0

#unallocated_time = 106.3 days
#unallocated_area = 1018.6 deg^2

#version_calf = 1.11
#version_crsdiv = 2.0
#version_ectile = 2.2
#version_mocda = 4.9
#version_mocdc = 4.4
#version_roi = 3
#version_rsd = RSD_2025A

2 Documents and acronyms

2.1 Applicable documents

Ref	Title	Reference	Issue ; Date
AD01	Criteria for RSD Implementation and Verification (CRSDIV)	EUCL-OAR-RP-8-001	2.0; 10/05/23
AD02	Mission Operations Concept Document - part A (MOCDA)	EUCL-EST-RD-1-010	4.9; 01/12/23
AD03	Calibration Framework	EUCL-MPIA-INF-8-002	1.11 ; 19/12/24
AD04	SOC-ECSURV ICD	EUCL-ESAC-ICD-8-001	2.6; 20/04/23

2.2 Reference documents

Ref	Title	Reference	Issue; Date
RD01	Euclid Reference Observation Sequence	EUCL-EST-TN-1-019	2.0; 29/11/23
RD02	Euclid S/C Slew Time Estimator	EUCL-EST-TN-1-018	2.0; 27/11/23
RD03	The Euclid wide survey region of interest v3	Report to EST (J.C. Cuillandre et al)	1.0; 09/01/23
RD04	Bright star and Self-cal limitations for ECSURV	EUCL-MPIA-TN-8-001	1.0; 29/03/21
RD05	Assessment of the instruments as-built FoVs	EUCL-EST-TN-3-016	1.1; 02/12/21
RD06	Euclid mission budget and requirements justification document	EUCL-EST-TN-1-004	3.0; 30/08/18
RD07	Calibration Concept Document – part B (CalCD-B)	EUCL-MPIA-RD-1-001	3.1; 26/09/18
RD08	VIS PSF variations from the STOP analysis	EUCL-OXF-TN-8-006	3.0; 08/01/22
RD09	Euclid preparation I. The Euclid Wide Survey	A&A 662, A112	xx; 28/06/22
RD10	ECTile users guide	User manual (J. Dinis)	2.0; 05/03/24
RD11	Assessment of the scheduling restrictions from the reduced	Report to ESOM (J. Dinis)	4; 01/09/23

The presented document is Proprietary information of the Euclid Consortium.
This document shall be used and disclosed by the receiving Party and its related entities (e.g. contractors and subcontractors) only for the purposes of fulfilling the receiving Party's responsibilities under the Euclid Project and that the identified and marked technical data shall not be disclosed or retransferred to any other entity without prior written permission of the document preparer.

	alpha-range		
RD12	RSD Document Change Request	EUCL-IAUL-xx	1.1; 21/01/25
RD13	SOST issues Redmine page	https://euclid.roe.ac.uk/projects/sost/issues	retrieved on 09/01/25
RD14	F-blocks on-target times	Summary table (R. Kohley)	8.1; 07/01/25
RD15	MCRR report: Verification steps for MRD 06 and 07	EUCL-IFA-TN-8-004	1.1; 8/01/24

2.3 Acronyms

AA	Alpha Angle
APE	Absolute Pointing Error
BGS	Blue Grism
CalF	Calibration Framework
CalWG	Calibration Working Group
CDR	Critical Design Review
CPC	Completeness Purity Calibration
CRSDIV	Criteria for RSD Implementation and Verification
DCR	Document Change Request
DES	Dark Energy Survey
DR1	Data Release #1
EAFs	Euclid Auxiliary Fields
ECSURV	Euclid Consortium Survey Group
EDF	Euclid Deep Field
EDF-F	Euclid Deep Field Fornax
EDF-N	Euclid Deep Field North
EDF-S	Euclid Deep Field South
EDS	Euclid Deep Survey
EGBS	Euclid Galactic Bulge Survey
ESOM	Euclid Survey Operations Meeting
ESOP	Early Science Operation Phase
ESSOT	Euclid Sky Survey Operational Tool
EST	Euclid Science Team

ESSWG	Euclid Sky Survey Working Group
EWS	Euclid Wide Survey
FAR	Flight Acceptance Review
FoV	Field of View
GC	Galaxy Clustering
LMC	Large Magellanic Cloud
LSST	Legacy Survey of Space and Time
MACC	Multi-accumulate
MKP	Mission Key Point
MOC	Mission Operations Center
NEP	North Ecliptic Pole
NISP	Near Infrared Spectroscopy and Photometry Instrument
OCF	Observation Configuration File
PDCC	Phase diversity calibration campaign
PLM	Payload Module
PSF	Point Spread Function
RGS	Red Grism
RoI	Region of Interest
ROS	Reference Observation Sequence
RSD	Reference Survey Definition
RSDF	Reference survey Definition File
S/C	Spacecraft
S/N	Signal to Noise Ratio
SAA	Solar Aspect Angle
SCCI	Spacecraft Constraints and Capability Information
SCOMT	Survey and Calibration Operations Mid-Term
SEP	South Ecliptic Pole
SMC	Small Magellanic Cloud
SOPS	Spacecraft Operations
SOST	Survey Operations Support Team
SOST-RH-01	SOST Rehearsal #1
SPV	Science Performance Verification
STOP	Structural Thermal Optical Performance
TBD	To Be Defined

TBC	To Be Confirmed
UNIONS	Ultraviolet Near-Infrared Optical Northern Survey
VCD	Verification Control Document
VIS	Visible Imaging Instrument
WL	Weak Lensing
wrt	with respect to

3 RSD configuration model

ECTile is the software purposely made to generate RSDs. Its development started in 2014. The implementation of a new RSD requires a planning process that usually does not change significantly from the previous one, and may or may not require new features in ECTile. The process is done in three stages. In a preparatory stage-zero, the inputs are defined. After that, in stage-one, a skeleton of the schedule of the various calibration and EDFs is manually planned and it is then computed in detail by ECTile. The core of ECTile is stage-two, where ECTile computes the EWS by generating patches for each survey window, automatically selecting one of the patches and scheduling it by defining a connection path between its inner fields, as detailed in [RD09]. The process is iterated many times in an optimization loop.

3.1 ECTile versions

- ECTile 1.0 (May 2023): prepared to generate the first operational RSD, compliant with all constraints and limitations known at the time of the Euclid launch.

- ECTile 2.0 (December 2023): major update following the detection in commissioning of straylight from the Sun in the optical system that led to a change in the operating AA range. Introduces tilted FoVs to cope with the new restricted and offset AA range.

- ECTile 2.1 (September 2024): prepared to generate the first RSD replanning. Introduces an interactive mode increasing the user's control of the survey patches.

- ECTile 2.2 (January 2025): prepared to generate the first RSD planning with recovery of lost observations. Introduced the backlog file and improved the interactive mode.

3.2 Mission planning and RSD computation

The procedure of RSD planning and computation with ECTile is summarized in Figure 3.1 and is described in more detail in Sects. 3.2.1 to 3.2.3. The configuration file and input data are shown in the left. The procedure flows with the green arrows. An ECTile tool named in green next to an arrow is applied to an input file, and uses information from the configuration and data files connected with thin lines to produce an output. Output binary files are shown in yellow and output plots in white. A red arrow indicates the output is manually constructed using information of the previous file and not mechanically computed by an ECTile tool. Blue boxes are the five core input files that are manually modified by the mission planner and are the stepping stones of the RSD computation. The orange arrows indicate the optimization loop: the monitoring on-screen of the step by step computation of the RSD guides the mission planner in the manual modification of the files *plan.d* and *wide-plan.d.* At the end of the process, the final RSD file is generated in xml format (brown box).

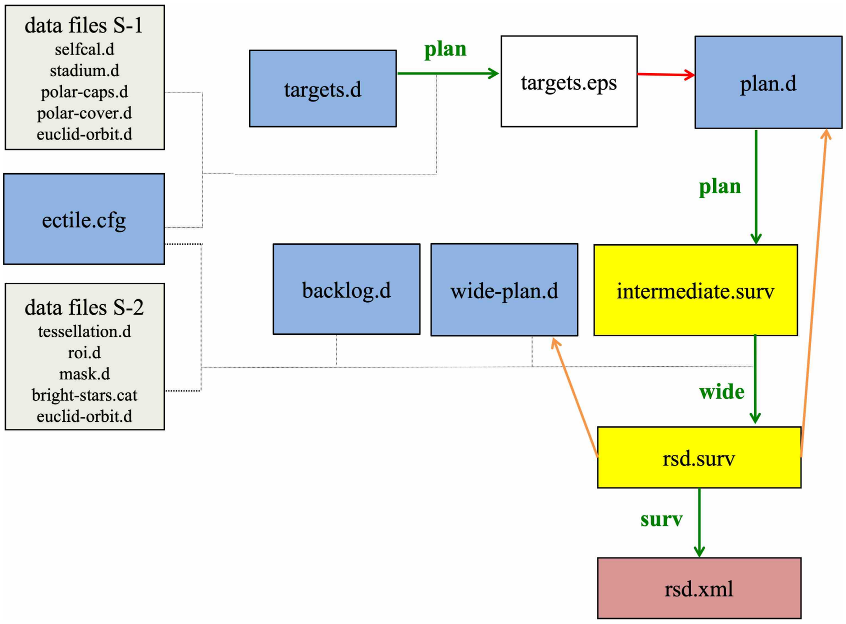

Figure 3.1: RSD configuration model for ECTile 2.2 (see text for a description)

3.2.1 Stage-zero: configuration file

The input parameters are defined in the configuration file *ectile.cfg*. Other input information is present in additional data files. The parameter values in *ectile.cfg* can be modified by the mission planner. Some of the parameters reflect the inputs from MOCD-A [AD02], CalF [AD03] and CRSDIV [AD01]. A summary list is given below. A low-level full list and description of all parameters is given in [RD10], while a high-level description and justification of the main RSD inputs is given in Sect. 4.

- RSD dates: starting date and duration
- Orbit file: Euclid orbit around L2
- FoV: VIS and NISP corners and gap sizes, APE, tile tolerance
- Slews: thresholds and durations
- Spacecraft: SAA and AA ranges, orbital margin, target AA
- S-pattern: dither off-sets
- Blinding stars: exclusion radius per magnitude, proper motions
- RoI: quadrants, polar caps, masks for RoI clipping
- Stadium: parameters of the EDFS shape
- PSF: stabilization period, cadence, pointing restrictions
- SOPS: duration, cadence
- Selfcal: cadence, base-longitude
- Scheduling optimization: margins, merge separation, quadrant selector
- Observing timings: for all elements of each sequence used (ROS, PN-scan, VIS-NL, etc)
- Locations: coordinates of all targets

The presented document is Proprietary information of the Euclid Consortium.
This document shall be used and disclosed by the receiving Party and its related entities (e.g. contractors and subcontractors) only for the purposes of fulfilling the receiving Party's responsibilities under the Euclid Project and that the identified and marked technical data shall not be disclosed or retransferred to any other entity without prior written permission of the document preparer.

- Targets table: location, position angle, pattern (geometry, number of passes, smearing, blue:red ratio), observing sequence

The additional input files include information on: RoI footprint, tessellation, polar caps patches, blinding stars catalog, self-cal pointings, stadium shape, orbit file, masks.

3.2.2 Stage-one: planning calibrations

The next step in computing an RSD is to place all the targeted observations, i.e, the calibration and sample characterization fields, the deep fields, and the polar caps. These include all the non-EWS observations plus the EWS polar observations, which are treated separately from the rest of the EWS. The complete set of targets is declared in *ectile.cfg*, together with the definition of its parameters (location, position angle, geometry, number of passes, smearing, blue:red ratio, observing sequence timings).

Stage-one is a process that is mostly manual and is done in two steps. In the first step, composite targets are assembled by combining one or more targets. The list of composite targets is stored in the file *targets.d.* The composite targets defined in this file form the set of all possibilities that will be available for scheduling. Their definition is an optimization choice that is not expected to change much. A unique code is assigned to each composite target. A few examples are:

- DeepNorthTwo 2100 2100: a sequence of two full visits to EDF-N
- DeepNorthTwo 2100 -2100: a sequence of two full visits to EDF-N, with the two visits traversing the EDFN fields in opposite directions
- M1-1: 1101 1900: the first monthly block, consisting of the CALBLOCK-F-001 observation assigned to the first observing instance, followed by the CALBLOCK-F-007 observation.
- PN-7: 7107 7207 7300 7300 7207 7207 7300 7300 7207 7207 7300: the CALBLOCK-F-010 sequence, assembled from its element observations (preliminary scan, PN observations and self-cal observations).

The ECTile tool *plan* computes a visual chart (*targets.eps*) of the visibility window of each composite target given as an interval of Sun ecliptic longitude, showing also within the interval the duration of each observation. Targets may have a single perennial visibility window (for targets near the ecliptic poles), or two visibility windows 180 deg apart (leading and trailing).

From this information the mission planner creates an ordered list of the composite targets, clustering them in groups, in terms of the Sun longitude of their visibility windows. The manually construction of this calibration plan file, *plan.d*, is the second step of the stage-one process. Each composite target is placed in the list making sure there are no overlaps in the observation periods of targets. For this, they can be placed either in the leading or trailing window, and can be manually shifted to any longitude within the visibility window. The composite targets are distributed throughout the six years of the mission, hence in practice six sequences ordered in longitude need to be defined (one per year). As an optimization strategy, a number of composite targets are grouped together in a block to be observed back-to-back. In this case, one of the targets is assigned the role of anchor and the observing longitudes of the neighboring targets are shifted (within the visibility windows) to ensure no time gaps exist between the targets of a block.

The placement of the composite targets is a core aspect of strategic planning of an RSD. It is made with two goals in mind: (i) respecting CalF cadences and priorities requirements, (ii) building

The presented document is Proprietary information of the Euclid Consortium.
This document shall be used and disclosed by the receiving Party and its related entities (e.g. contractors and subcontractors) only for the purposes of fulfilling the receiving Party's responsibilities under the Euclid Project and that the identified and marked technical data shall not be disclosed or retransferred to any other entity without prior written permission of the document preparer.

a plan that enables an optimal implementation of the EWS in the next stage, avoiding leaving gaps too small for the EWS and ensuring the EWS coverage in the first year (where many calibrations need to be scheduled) is capable of reaching the expected area for DR1 and has sufficient overlap with the ground-based coverage. Following these two guidelines we devise the optimized general strategy sketched below. In the first year of observations the optimized strategy is the following.

- Place all ten CPC-South visits. These are the most demanding targets.
- Place 11 monthly calibration blocks per year at an approximate step of 360°/11 = 32°.73. This promotes a synergy with CPC-North.
- Place all ten CPC-North visits.
- Place part of the northern polar cap patches. The particular solution implemented for the partition of the northern polar cap in patches (i.e. the width of these patches and the angular offset between them) was constructed to create a synergy with the monthly blocks cadence, allowing them to be placed in sequence.
- Place part of the southern polar cap patches.
- Place half of the COSMOS field, in two separate epochs (one observed with the blue ROS variant), covering half of the COSMOS area to the full depth.
- Place a double pass on EDF-F to have a minimal coverage of the full depth of the EDS in the first year.
- Place the F-004 priority field (AEGIS), separated in two epochs to apply red and blue grism ROS variants.
- Place the F-005 priority field (CDFS), separated in two epochs to apply red and blue grism ROS variants.
- Place the biannual calibration blocks. Because these are freely placeable, the choice is to place them within two monthly blocks occurring on the low-stress periods.
- Place additional visits to EDF-N to avoid small gaps of time between other targets. Since it can be placed all year round, the visits to EDF-N may be used as a filler.

In the second year of the optimized plan, the most demanding targets are EDF-F and EDF-S, which have short visibility due to their low ecliptic latitudes. The COSMOS field is finalized, as are the remaining polar caps. Besides continuing the EDS visits and the regular monthly-block and biannual visits, the second year contains the F-010 observation made when the preferred target is visible (which is not in a low-stress period). The second year also starts the annual calibration block which is placed as early as possible in the year.

The remaining years follow a common strategy, with most of the targets (EDF-F, EDF-S, recurring calibrations) being scheduled almost exactly in the same way every year, with the exception of the EAFs targets, each visible at a different longitude, and EDF-N that is scheduled with several visits in sequence during low-stress periods.

Variations on this optimized plan may be implemented for different reasons, notably the need for rescheduling of failed observations will create delays in the plan.

The plan is then executed by the ECTile tool *plan* that produces a visual chart (*plan.eps*) for inspection. If there are no clashes in the targets placement, the tool *plan* is used once more to generate the intermediate survey binary file (*intermediate.surv*), where the longitudes are converted to time assuming a given starting date. This survey does not follow *plan.d* strictly but performs optimization steps by automatically making small shifts in time and merging of neighboring blocks of targets according to optimization parameters defined in *ectile.cfg*. Finally, a chronogram of the schedule (*intermediate.eps*) is also produced.

3.2.3 Stage-two: computing the wide survey

The computation of the EWS by ECTile is the process that leads to the scheduling of ROS observations in Euclid FoVs placed on the tiles of the global tessellation. The process is described in detail in [RD09] and proceeds by gradually scheduling each *survey window* chronologically. A survey window is a contiguous interval of time left unscheduled in stage-one.

The ECTile tool *wide* takes the *intermediate.surv* file as input and computes a visibility window (with leading and trailing sides) for the first survey window. For this survey window, and as function of its duration, it generates four or more *patches* (one per quadrant of the RoI) that are possible to observe within the available time; a patch being a connected set of tiles. One or more of the patches are mechanically selected according to a hard-coded strategy (priority to higher latitudes, priority to south versus north hemisphere early in the mission). Then, a search is done to find PSF calibration fields within reach from that patch. If the search is successful, an observation of a PSF field (plus the other calibrations associated in the PSF block) is scheduled within the survey window with SAA and AA values matching the ones of the contemporary EWS patch. SOPS interruptions are also scheduled at this stage. These various placements use some of the time of the survey window, hence leaving less time for the scheduling of the patch and thus the selected patch is reduced by a few tiles.

The tiles within the patch are geometrically connected by the diffusion algorithm and time stamps are assigned to each tile, according to a set of hard-coded rules aiming to minimize solar angles variations. The tile sequence is usually separated in multiple sub-sequences, defining several *patch-segments* within a patch. A map is produced on-screen with the resulting scheduled patches of the survey window. Often, the map and associated displayed information, show imperfections. Common cases are patches that do not use the full time available in the survey window, or patches with irregular shapes that difficult a smooth fit with neighbors, or a small set of tiles left unscheduled between two patches; the scheduling of a patch may also fail and no patch is produced. The mission planner can then redo the patch generation by modifying the time *margin* parameters of the problematic survey window in an optimization loop. This allows patches to increase/decrease their spread in longitude, making them shorter/taller in latitude, hence adjusting the time it takes to traverse them with respect to the orbital speed. This results in longitudinal shifts of the patch or in spatial modifications of its shape. The user can also select the patches from a different quadrant than the one suggested by ECTile, impacting the RSD progression. These optimization choices are added to the *wide-plan.d* file that lists the parameters used for each survey window.

Sometimes, adjusting the margins is not enough to solve the problem. An alternative is to increase/decrease the size of the survey window. For that, we need to go back to *plan.d* and shift a target, e.g. slightly delaying a calibration or moving a polar cap observation for several months; any valid option that would modify the size of the relevant survey window. We note that modifications in *plan.d* are also made with other optimization goals. For example, shifting calibrations is a way to free space to increase the success of finding a PSF opportunity and avoiding low cadences.

When the mission planner is happy with the result, the process continues to the next survey window; an RSD containing around 100 survey windows. We note that a modification in *plan.d* implies restarting the process from start.

In stage-two, the *wide* tool also takes the input from the file *backlog.d*. This file is manually filled with the list of observations to be repeated. This is part of the recovery procedure that allows one to reschedule lost observations that had been scheduled in the previous RSD but are required to be re-observed for various reasons (e.g. failed executions, low-quality flags). This applies to observations scheduled in a date prior to the restarting date of the RSD under construction, and to be re-observed in a date after the restarting date. This set of observations is registered in the file with their original obs-id identifiers. They are grouped in composite targets, that may be a full EWS patch or a smaller group of neighboring fields. A unique code is assigned to each of these composite targets. The codes are inserted in the *wide-plan.d* indicating the survey windows where they will be observed and the re-observation mechanism: *large infill* or *small infill.* Large infill means the reobservations are scheduled as a patch of the relevant survey window, while small infill indicates that after patch creation, some time will be carved to insert the missing fields, similar to the PSF and SOPS insertion mechanisms. Alternatively, the EWS composite targets for reobservation can be scheduled in stage-one, by including them in *plan.d*; this alternative being more appropriate for small targets.

After processing the last survey window, the *surv* tool is applied to generate the final *rsd.xml* file.

3.3 Changelog

This section keeps track of the modifications on ECTile (development), as well as changes in input parameters and optimization strategies (mission planning) introduced by each RSD.

RSD_2025A (27/01/2025) reported in MOCD-C 4.4 [First recovered survey]

ECTile version: 2.2

ECTile development	
Modification	**Justification**
Implementation of recovery capability*	To be able to reschedule already executed failed EWS observations. Introduces a fourth core input file (backlog.d)
Improvement of the interactive mode	The interactive mode is now an integral part of stage-two of RSD computation. Introduces a fifth core input file (wide-plan.d). Expanded patch trimming options, enabling a more robust optimization procedure
New PSF and SOPS placement algorithm	Improved mechanism to introduce PSF and SOPS windows in the survey window. Same mechanism implemented for small infills. Verification of PSF-SOPS separation and of occurrence of SOPS in non-ROS observations
Red and Blue grism tracking	To keep track of the color of missed observations, ensuring the correct balance after rescheduling
Revised F-010 implementation, including computing the new pointings from input off-set values specified in the	There is a new set of dither off-sets specified for the quincunx pattern. The pattern is different for each grism (some are identical), and it gets closer to the edges of the

focal plane array.	detectors.
ObsID scheme	To be fully compliant with the ICD: one obsid per ROS tile, one obsid per non-ROS observation with the exception of F-010 (11 obsids), one obsid for the EGBS

Mission Planning

Item	Location	Modification	Justification
Intra-decontamination period EWS	wide-plan.d backlog.d	All EWS observations from 23/3/2024 to 7/6/2024 scheduled in RSD_2024A are rescheduled in similar dates in 2025 (3 survey windows)	Approved by the EST (Dec. 2024) cf. [RD12]
Intra-decontamination period: other observations	plan.d backlog.d	Reschedule of all other observations from that period: COSMOS, CPC-N-02, CPC-N-06, Northcap-06, Northcap-10, Northcap-11, EDF-N. Shifts in time can be applied to ensure enough time is left for the reobservation of the EWS patches.	cf. [RD12]
Galactic bulge survey	plan.d ectile.cfg	Unallocated time slot reserved for SOC implementation of this new component of the Euclid surveys (28h)	The “Euclid Galactic Bulge Survey” for the purpose of microlensing, has been approved by the ESA director of science (19/12/2024)
F-003 CPC-N	plan.d	Reschedule CPC-N-01 and CPC-N-07, quality damaged by solar activity	cf. [RD12]
F-002 EDF-N	plan.d	Add 3 more visits to EDF-N	cf. [RD12]: there are 3 EDF-N executed patches affected in different ways
F-006 EWS	backlog.d wide-plan.d plan.d	Infill of 85 EWS tiles scheduled in previous RSDs that had been skipped (6 + 8), or lost (13), or part of the intra-decontamination rescheduled patches for which there was not enough time available to reschedule the full patch	cf. [RD12]

The presented document is Proprietary information of the Euclid Consortium.
This document shall be used and disclosed by the receiving Party and its related entities (e.g. contractors and subcontractors) only for the purposes of fulfilling the receiving Party's responsibilities under the Euclid Project and that the identified and marked technical data shall not be disclosed or retransferred to any other entity without prior written permission of the document preparer.

		in the same period (58)	
F-009 incomplete sequence	ectile.cfg	Implementation of the correct sequence	cf. [RD12]: RSD_2024C only scheduled 188 of the required 212 pointings
F-013: newcalblock	ectile.cfg plan.d	Implemented in the new "PSF block": F-012+F-015+F-013+F-008	Compliant with [AD03] and timings defined in [RD14]
Grism sanity	ectile.cfg	Start all F-004/5 B/R visits with the Red grism	Compliant with [AD03]
F-017: newcalblock	ectile.cfg plan.d	Introduce F-017 together with some blue F-002 when needed	To ensure grism sanity
F-018: newcalblock	ectile.cfg plan.d	Implemented in the monthly block: F-001+F-018+F-007	Compliant with [AD03] and timings defined in [RD14]
SOPS of 19/05/2025	wide-plan.d	Implemented 9 hours after the required time	If implemented at the required time it would prevent the observation of 8 EWS tiles or interrupt non-ROS calibrations. Waiver awarded by MOC
DES footprint	mask.d	Slight reduction of the DES coverage at the [320, 350] ecliptic longitude range	To be consistent with the footprint used by OU-EXT

*Note on Survey Recovery: Recovery is a new feature of a replanned survey. Similar to a replanned survey, a replanned survey with recovery is identical to a previous basis survey up to a restarting date and independent from the basis survey afterwards, where a new EWS is generated. However, in contrast with the simple replanned survey, the replanned survey with recovery introduces the possibility to repeat observations of EWS tiles already observed in the basis survey. We note that in the simple replanned survey it was only possible to repeat non-EWS observations. The EWS recovery can be made through three different mechanisms: stage-two large infill, stage-two small infill, and stage-one. The survey statistics merge the information of the rsd after the restarting date with the information on the executed survey before the restart, avoiding multiple counts of the same observations. The restarting date of RSD_2025A is *#replan_restart* and the basis survey is *#replan_basis*.

RSD_2024C (17/09/2024) reported in MOCD-C 4.3 [First replanned survey]

ECTile version: 2.1

The presented document is Proprietary information of the Euclid Consortium.
This document shall be used and disclosed by the receiving Party and its related entities (e.g. contractors and subcontractors) only for the purposes of fulfilling the receiving Party's responsibilities under the Euclid Project and that the identified and marked technical data shall not be disclosed or retransferred to any other entity without prior written permission of the document preparer.

ECTile development

Modification	Justification
Implementation of replanning capability*	To be able to reschedule failed observations (listed below under Mission Planning)
Interactive mode for patch trimming**	Patch trimming is an optimization technique that was implemented to increase the compactness of the survey, decreasing the number of failed patches. With a user interface it can be done in the fly, which speeds up the process
Routine to translate between SOC's ObsID system and ECTile's ObsID system	Internally, ECTile does not implement the official ObsID system, counting consecutive non-ROS pointings as different ObsIDs. However, the systems must be in sync when ingesting external information on missing observations for replanning purposes

Mission Planning

Item	Location	Modification	Justification
F-002 EDF-N	plan.d	Inclusion of one additional visit to EDF-N	cf. [RD12]: replacing the lost visit of 2024-06-21 reported in task #27043 [RD13]
F-003 CPC-N	plan.d	Inclusion of one additional visit to CPC-N	cf. [RD12]: replacing the lost visit of 2024-05-09, reported in task #26483 [RD13]
F-006 polar patch	plan.d	Rescheduling of patch North-cap-06	cf. [RD12]: replacing the 2024-06-06 visit that had been skipped due to decontamination, reported in task #27063 [RD13]
F-005 COSMOS	targets.d	Replanning of the four COSMOS visits with a new strategy	cf. [RD12]: after the loss of visit #1, reported in task #26543 [RD13], the four visits where replanned prioritizing area completion over depth, which is important in the presence of Solar activity, according to the updated CalF requirement [AD03]
F-005 SXDS	targets.d	Replanning of the four SXDS visits with a new strategy	cf. [RD12]: according to the updated CalF requirement [AD03] SXDS must follow the same strategy used for COSMOS to ensure a uniform distribution of blue-grism

The presented document is Proprietary information of the Euclid Consortium.
This document shall be used and disclosed by the receiving Party and its related entities (e.g. contractors and subcontractors) only for the purposes of fulfilling the receiving Party's responsibilities under the Euclid Project and that the identified and marked technical data shall not be disclosed or retransferred to any other entity without prior written permission of the document preparer.

			angles
F-007 first on-target time	ectile.cfg	Time decreased from 2730s to 2480s	cf. [RD12]: the excess time had been partially reduced to 2730s using the survey repair strategy in RSD_2024B, but the full reduction is only implemented now with replanning. Issue reported in task #26397 [RD13]
F-007 timings	ectile.cfg	Implementation of new timings	cf. [RD12]: following a modification of the FLAT parameters in the PTC and BFE sections of F-007 [AD03] new timings are defined in [RD14]
F-009 timings	ectile.cfg	Implementation of new timings	cf. [RD12]: more fluences were added, resulting in two variants that should be alternated [AD03], with associated updated timings [RD14]
F-012 timings	ectile.cfg	Implementation of new timings	Defined in [RD14]
F-015 timings	ectile.cfg	Implementation of new timings	Defined in [RD14]
F-016 timings	ectile.cfg	Implementation of new timings	Defined in [RD14]
F-012 and F-015 cadences	plan.d	Implementation of new cadence. F-012-015-008 are always observed in sequence. The cadence is set by F-008.	cf. [RD12]: increased Solar activity requires increased cadences of F-012 and F-015. This supersedes the previously planned modification of F-015 cadence reported in task #26399 [RD13]

*Note on Survey Replanning: Like a repaired survey, a replanned survey is identical to a baseline previous survey up to a breakpoint. But differently from a repaired survey, the calibrations plan file (plan.d) and associated targets file (targets.d) may be completely redefined after the breakpoint. This creates survey windows that may be different from the baseline survey and a new wide survey is generated after the breakpoint. The survey statistics merge the information of the rsd after the breakpoint with the information on the executed survey before the breakpoint. The replanned survey includes rescheduling of lost observations that are present in the rsd before the breakpoint, hence the merging needs to avoid multiple counts of the same observations. The breakpoint of RSD_2024C was 16th November 2024 and its baseline survey was RSD_2024B.

**Note on interactive mode: The patches of the EWS are computed with the maximum possible extension in longitude (for a given survey window and within the solar angles restrictions) to allow for a seamless covering in the case of interruption for non-EWS observations. However, this strategy often leads to scheduling of tiles that shoulder an adjacent patch. This creates an irregular border prone to produce failures in subsequent patches. ECTile 2.1 implements a new interface where the user can control the EWS generation, patch by patch, by altering the extent of each patch on the fly. This avoids the shouldering effect (increasing the patch extent in latitude), increases the user control on the survey generation process and in addition speeds up the process of survey optimization.

RSD_2024B (29/05/2024) no MOCD-C issued [First repaired survey]

ECTile version: 2.0 + survey repair tool

ECTile development	
Modification	**Justification**
Creation of the survey repair tool*	To quickly repair F-001 observations that had been mistakenly scheduled in RSD_2024A with a blue grism separation of 1.2 deg instead of 1.4 deg, avoiding regenerating the whole survey that was already in execution, and avoiding altering the schedule of the observations already taken.
Smearing offsets	Pre-computed relative offsets are applied to the pointing quaternion of a target. However, the pointing quaternion of a given pointing flips if the observation is made in the leading or trailing side. This was not taken into account, making the offset shift in the opposite direction in some cases, producing smeared visits but with a different pattern than intended.

Mission Planning			
Item	**Location**	**Modification**	**Justification**
F-001 blue grism separation	ectile.cfg	Separation changed from 1.2 deg to 1.4 deg (in all instances after July 15th 2024)	Mistakenly implemented as 1.2 deg in RSD_2024A
F-007 first on-target time	ectile.cfg	Time decreased from 2840s to 2730s	The required time is 2480s. It had been over-allocated as 2840s in RSD_2024A due to a typo in ectile.cfg. The repair procedure was only able to reduce it to 2730s, without impacting the survey.
F-010 first on-target time	ectile.cfg	Time changed from 1125s to 1225s	Typo in RSD_2024A's ectile.cfg

The presented document is Proprietary information of the Euclid Consortium.
This document shall be used and disclosed by the receiving Party and its related entities (e.g. contractors and subcontractors) only for the purposes of fulfilling the receiving Party's responsibilities under the Euclid Project and that the identified and marked technical data shall not be disclosed or retransferred to any other entity without prior written permission of the document preparer.

F-012 first on-target time	ectile.cfg	Time increased by 450s, from 1710s to 2160s	Following CalF update to avoid possible truncation of VIS secondary exposures
F-015 first on-target time	ectile.cfg	Time increased by 450s, from 1981s to 2431s	Following CalF update to avoid possible truncation of VIS secondary exposures
F-016 first on-target time	ectile.cfg	Time increased by 450s, from 1107s to 1557s	Following CalF update to avoid possible truncation of VIS secondary exposures
Smearing offsets in multi-visited EAFs and EDFs	targets.d	Smearing offsets corrected	Implemented differently to requirement due to the leading/trailing flip of the pointing quaternion
EAFs COSMOS and SXDS sequence	targets.d	Visiting order of the 4 sub-visits to each of these EAFs corrected	Wrongly implemented as part A (4x depth), part B (3x depth), part B (4x), part A (3x), instead of A-A-B-B. The wrong shift of direction was due to the leading/trailing flip of the pointing quaternion

*Note on Survey Repairing: A repaired survey is a survey computed from a previous one by recomputing patches from a breakpoint onwards, while the schedule before the breakpoint remains unchanged. The survey repairing process replaces wrong patches by new repaired ones, and regenerates the subsequent patches of the original survey. Subsequent wide patches are traversed with the same sequence as before, only with updated timestamps. New timestamps can only differ by up to a few hours from the original timestamps, within survey time margins, otherwise the repairing is not possible. The calibration plan is kept unchanged, but the corresponding calibrations, deep fields and polar patches are regenerated from scratch. PSF calibrations and SOPS are recomputed from scratch. Repairing is done one patch at a time, in chronological order, from the breakpoint of July 19th 2024. The regenerated RSD_2024B contains a few repaired calibrations and is otherwise very similar to RSD_2024A, with identical global statistics.

RSD_2024A (19/01/2024) reported in MOCD-C 4.2 [First operational survey]

ECTile version: 2.0

- Inclusion of s/c orbit file (orbit 0044). Solar angles and planetary positions computed for the actual S/C position (previously the S/C was assumed to be at L2).
- Used starting date 14-02-2024.
- Assumes the s/c FoV starts centered at NEP, with an orientation that makes AA = 4.5 deg.
- Reduced the orbital margin from 0.41 deg to 0.1 deg. Also added an extra margin of 0.05 deg to this parameter, totaling 0.15 deg, to cope with a mismatch in AA and SAA computation between ECTile and ESSPT 6.1.5.

- Restricted SAA range in EWS to [87, 104] deg, to avoid large deviations from transit, and also restricted AA to [-8.0, -3.0].
- Slight relaxation of the AA limits to [-8.5, -2.9] deg to increase reach (upper limit was -3.0).
- Recomputed the tessellation to be compatible with FoVs tilted up to 3.5 deg (increased from 3.0 deg to increase reach at low latitudes).
- Priority given to southern hemisphere vs northern in the first year (previously it was in the first two years).
- Introduced the sop-start parameter defining the time of the first SOP of the survey.

RSD_2023D (15/12/2023) no MOCD-C issued

ECTile version: 2.0

- Implemented all SOPS, some were missing in RSD_2023C due to a conflict between SOPS and self-cal.
- Updated to CalF 1.9, introducing the new calibrations F-015 and F-016.
- Included F-10 calibrations that were mistakenly absent from RSD_2023C.
- Implemented BGS self-cal observations misaligned by 1.4 deg with respect to the RGS ones (the previous requirement of 2 deg is no longer possible with the restricted AA range).
- Redesigned the calibration schedule to avoid observations inside the regions defined by AA < -6 deg if SAA in [88, 92] deg, according to the newly found stray light leak.
- Reverted PV timings, adopting the new version of the slew time estimator [RD02]

RSD_2023C (02/11/2023) no MOCD-C issued [Testing ECTile 2.0]

ECTile version: 2.0

- Updated to MOCD-A 4.9, which introduces the restricted AA range of [-8.5, -3.0] deg and the SAA range of [87, 120] deg.
- Added the capability of placing tilted FoVs to enable scheduling with the restricted AA range.
- Adapted the diffusion algorithm to cope with tilted FoVs in the EWS, including the usage of a target AA.
- Recomputed the tessellation to be compatible with FoVs tilted up to 3 deg.
- Redesigned the CPC-N and CPC-S orientations to allow for a +/-1 deg of tolerance (in orientation), needed to artificially enlarge these targets windows of visibility. The minimum separation between spectra directions was reduced from 5 to 4 deg.
- Redesigned the polar caps using FoV-level tilts with tolerance of 3 deg.
- Reverted the F-009 and F-011 target to selfcal-center (RSD_2023B used selfcal-faint).
- Used starting date 24-01-2024.
- Used the slew times defined for the PV phase.

RSD_2023B (12/06/2023) reported in MOCD-C 4.1 [SOST-RH-01]

ECTile version: 1.0

The presented document is Proprietary information of the Euclid Consortium.
This document shall be used and disclosed by the receiving Party and its related entities (e.g. contractors and subcontractors) only for the purposes of fulfilling the receiving Party's responsibilities under the Euclid Project and that the identified and marked technical data shall not be disclosed or retransferred to any other entity without prior written permission of the document preparer.

ECTile development	
Modification	**Justification**
Resolution of a bug affecting the choice of PSF fields	In RSD_2023A, F-007 was not always performed on the PSF field that minimized SAA and AA variation.
A new scientific merit function is produced. It is a sky quality score that combines VIS (I_E) S/N and NISP (RG_E) S/N	A new merit function introduced in [AD01] replaces the previous weight given by the number density of GC galaxies. The previous proxy relied on outdated simulations and were representative of only one of the two Euclid core probes.

Mission Planning			
Item	**Location**	**Modification**	**Justification**
Starting date	ectile.cfg	Delay of 1 day, from 2023-12-04T12:00:00.000 to 2023-12-05T12:00:00.000	Consistent with assumptions of earlier launch date and longer PDC campaign.
PN block	targets.d	Removal of four PV-scan elements from the F-010 observation block	These extra observations were present in RSD_2023A due to a misinterpretation of the CalF description
Observing types	ectile.cfg	Selfcal-faint target assigned to CALBLOCKS F-009 and F-011	Following CalF update (in RSD_2023A selfcal-center was used)
Longitude shifts	plan.d	Slight changes in M1 and NISP-NON-LIN placements	To decrease the pressure at lon ~80, homogeneizing the EWS coverage
Patch selection	pick-switch.d	Enforce the choice of patches in the quadrants Q2 and Q3	To ensure the full coverage of the northern island and a connected coverage of the southern island

RSD_2023A (10/05/2023) reported in MOCD-C 4.0 [FAR review]

ECTile version: 1.0

- RoI v3 used.
- Computed for a duration of 5 years 10 months (previously 6 years).
- New common FoV and tile implemented.
- Takes into account proper motion of blinding stars by considering their coordinates at the middle of the survey routine phase and incrementing the exclusion radius in the tile computation.

The presented document is Proprietary information of the Euclid Consortium.
This document shall be used and disclosed by the receiving Party and its related entities (e.g. contractors and subcontractors) only for the purposes of fulfilling the receiving Party's responsibilities under the Euclid Project and that the identified and marked technical data shall not be disclosed or retransferred to any other entity without prior written permission of the document preparer.

- Implemented the precise on-target times for non-ROS observations specified in the OCF files.
- Added grism type to observations (RED or BLUE).
- Split the previously single visit to the EAFs AEGIS, GOODS-NORTH, VVDS and CDFS in two visits separated by 6 months, in order to obtain blue grism line separations.
- Implemented a fixed order traversal of the 60 self-cal pointings, and added 16 visits for blue grism observations.
- Adjusted the patterns covering the deep-fields to avoid nearby blinding stars.
- Added smearing to CALBLOCK-002/3/4/5, with the pattern of FoVs being slightly offset from its nominal center at each visit, and to CALBLOCK-F007/8/9/11 single FoV visits, previously made with repeated observations to the same location. The smear offset is taken from a set of points along a spiral around the nominal center.
- Zero length slews, previously present, were eliminated. Their need was circumvented with the addition of smearing offsets.
- Fixed description of patch boundaries. Previously some were wrongly split into two contours (caused by the presence of SOPS).
- Implemented all other specifications of MOCD-A 4.5 and CalF 1.5.0 not discriminated above, including updated observing sequences and new calibration blocks F-011/12.

RSD_2022B (12/01/2022) reported in MOCD-C 3.0 [MKP review]

- Increased the EDF-N area from 10 deg^2 to 20 deg^2.

RSD_2022A (12/01/2022) reported in MOCD-C 2.0 and revised in MOCD-C 2.1 [MKP review]

- Improved blinding-star avoidance with adaptable tessellations. Instead of simply skipping a tile (of a regular tessellation), tiles are placed closer to surrounding blinding stars (to reduce the footprint of holes created by blinding stars).
- Used part of the unallocated time to complete EDF-N earlier. This pushed the first occurrence of unallocated time to later times.
- Adapted to the latest dither S-pattern.
- Adapted to the latest FoV specifications.
- Introduced new computation of common FoV (resulting in a smaller FoV).
- Added a new algorithm for scheduling the self-calibration pattern (for an arbitrary orientation).

RSD_2021C (07/10/2021) no MOCD-C issued

- Updated SOPS implementation: slew following the SOP is a large slew with extra 5 minutes of idle time.
- Updated slew time computation (to the formulas specified in SCCI).

RSD_2021B (20/09/2021) no MOCD-C issued

- Updated slew time computation: enforced a minimum delta time from slew to slew (it may require additional idle time).
- Updated slew time computation: lead time of 22s at the start of the first frame of ROS taken out of ROS and added to the slew time (if followed by a ROS observation).
- Updated SOPS implementation: pointing complies with a reduced SAA and AA range.
- Reduced the SAA and AA range by 2 x 0.5 deg (previously 0.41 deg).
- Added null slews (with zero length and null duration) to minimise usage of idle time.
- Updated the weight map to a healpix of increased resolution (NSIDE changed from 64 to 256).

RSD_2021A (12/07/2021) no MOCD-C issued

- Added new input: blinding-star catalogue.
- Added blinding-star avoidance (by marking tiles containing a blinding-star and skipping them).
- SOPS implemented as required.
- Changed the tessellation to follow the RoI tightly (removing a one tile strip around the borders).
- Replaced the covering of the stadium shape with a tighter set of patterns (to produce patches at various orientations).
- Updated the ROS to the latest specification: increased dither-slews to 66 seconds (from 60 seconds), increased ROS by 21 seconds overall.
- Implemented field-to-field slews duration of 170 seconds for slews with amplitude smaller than 0.11 deg (previously considered a 60 s dither-slew).
- Changed the large slew threshold to 3.6 deg (previously was 3.7 deg).
- Reduced the SAA and AA range by 2 x 0.41 deg.
- Changed the limiting ecliptic latitude for polar-caps from +/-79 deg to +/-78 deg (to reduce pressure at the scheduling stage) and extended the polar-caps accordingly.
- Changed the tessellation in the southern polar-cap to avoid the R Dor blinding-star.
- Added 1% FOV overlap.
- Changed the logic of survey-window processing to cope with the insertion of SOPS and PSF calibrations.
- Changed the EWS build up to grow evenly between hemispheres.
- Changed the patch-source partitioning to extend adaptively as a function of latitude (the maximum reach to observe away from transit varies with latitude).
- Changed the diffusion algorithm to cope with borderline cases (in particular with patches that are intersected by the RoI, resulting in an odd shape).

RSD_2020B (20/09/2020) reported in MOCD-C 1.0 [SCOMT review]

- RoI input as polygonal contours.
- Guided build-up of EWS (to favour early observation of selected regions, implementing a layered build-up).
- New survey-window partitioning algorithm (to improve the placement of patches)

The presented document is Proprietary information of the Euclid Consortium.
This document shall be used and disclosed by the receiving Party and its related entities (e.g. contractors and subcontractors) only for the purposes of fulfilling the receiving Party's responsibilities under the Euclid Project and that the identified and marked technical data shall not be disclosed or retransferred to any other entity without prior written permission of the document preparer.

- Integration of the diffusion algorithm (to decrease patch-filling CPU time, and decrease SAA and AA field-to-field variation).
- Adapt to latest calibration specifications on the Calibration Framework.
- Inclusion of new CPC K-pattern following the RGS270 problem.
- New strategy for scheduling of PSF calibration fields.

The presented document is Proprietary information of the Euclid Consortium.
This document shall be used and disclosed by the receiving Party and its related entities (e.g. contractors and subcontractors) only for the purposes of fulfilling the receiving Party's responsibilities under the Euclid Project and that the identified and marked technical data shall not be disclosed or retransferred to any other entity without prior written permission of the document preparer.

4 Inputs

This section summarizes the main inputs to be considered for an RSD implementation.

4.1 System constraints

A first class of inputs originates from spacecraft constraints and system requirements. We present a summary of the MOCD-A information that is relevant to the computation of the RSD. The information is taken from the applicable version *#version_mocda* [AD02].

4.1.1 Pointing constraints

The S/C reference frame is shown in [AD01, AD02]. Rotations around two out of the three axis that define the orientation of the S/C are strongly constrained during observations. According to the requirements of [AD02], the solar aspect angle (SAA, the pitch that allows the satellite to depoint) is limited to the range *[#solar_saamin*, *#solar_saamax*] and the alpha angle (AA, the roll) is limited to the range *[#solar_aamin*, *#solar_aamax*]. We reduce this default range by introducing a safety margin of *#solar_margin* on every limit to account for the nominal maximum deviation between the assumed and actual orbit of 0.1 deg and to cope with differences between the computation of ephemerides by ECTile and SOC's ESSOT. Given these constraints, observations are mostly done by varying the third angle (yaw) sweeping along ecliptic meridians, and can be made either towards the direction of the orbit movement (leading side) or on the opposite direction (trailing side).

The AA range was strongly reduced and off-set from the pre-launch range of [-5, 5] following the commissioning phase findings that VIS was affected by considerable amounts of stray light. The root cause identified is a thruster nozzle that is illuminated by the Sun, from which the light enters the VIS focal plane through a triple scattering process. The amount of stray light present was measured by taking darks with the telescope rotated at various AA and SAA values. Figure 4.1 shows that stray light reaches high levels above AA ~ -3 deg, prompting a modification of the AA range. Figure 4.1 also shows a stray light leak at SAA ~ 90 deg when AA is below -6 deg. We further reduce the AA range by avoiding the SAA range [88, 92] if AA < -6 deg.

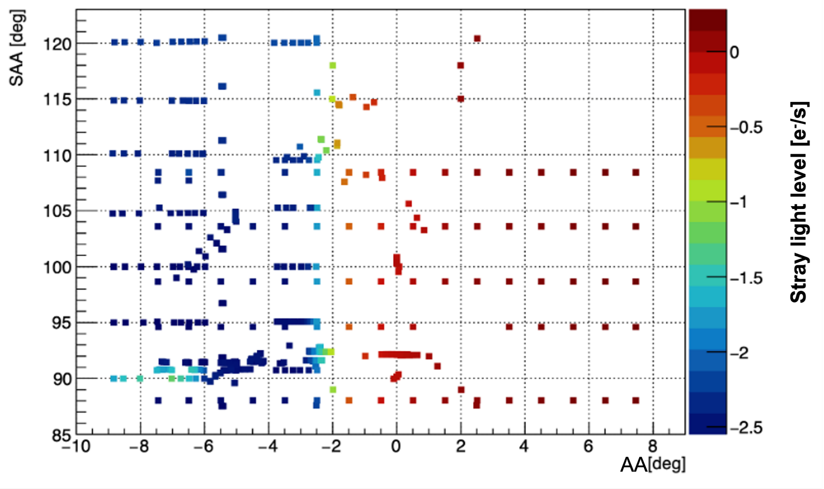

Figure 4.1: Stray light SAA/AA scan

The presented document is Proprietary information of the Euclid Consortium.
This document shall be used and disclosed by the receiving Party and its related entities (e.g. contractors and subcontractors) only for the purposes of fulfilling the receiving Party's responsibilities under the Euclid Project and that the identified and marked technical data shall not be disclosed or retransferred to any other entity without prior written permission of the document preparer.

4.1.2 Euclid tile

As required in [AD02], the sky must be tessellated with geometrically contiguous tiles of size determined from the VIS and NISP common FoV.

The *as-built* VIS and NISP FoVs [RD05] are off-centered, do not intersect each other completely leaving a NISP gap, and their geometry is trapezoidal. In order to define the tile, a rectangular intersection of NISP and VIS (the common FoV) must be considered. This is achieved by computing the inscribed rectangles of each FoV, thus creating "NISP and VIS boxes". These boxes are the maximal spherical rectangles that fit inside the trapezoidal shapes of each of the two FoVs. The common FoV is then given by the intersection of the VIS and NISP boxes, matching the pair of sides defining the shortest width with the pair of sides defining the shortest height, as detailed in [AD01]. The area of the common FoV is *#fov_common*.

Differently from originally planned, we do not implement a tessellation tile identical to the common FoV but larger, obtained by extending NISP downwards, mimicking the covering of the missed gap by the pointing immediately below. In this way, the tile covers the area that is observed in a single pointing. The tile is further extended to include the APE and a margin for rounding errors, ensuring no gaps between pointings. The adopted Euclid tile is a latitude–longitude rectangle with an area of *#fov_tile*.

One ROS observation of the EWS corresponds to placing the VIS and NISP FoVs on one tile of the tessellated sky and move it along the dither S-pattern (cf. Sect. 4.1.3). The rectangular area enclosed by the dither pattern has an area of *#fov_dithered* (naturally not all observed by each of the four dithered pointings).

4.1.3 Reference observation sequence

The Euclid ROS is defined in detail in [RD01]. It is used in all EWS observations and in part of the sample characterization observations (in the EDFs and EAFs). The ROS consists of four dithered frames as illustrated in Figure 4.2. The frames are off-set according to the "S" dither pattern defined in [AD01, AD02] and shown in Figure 4.3, implemented with dither slews of *#slewtime_dither duration*.

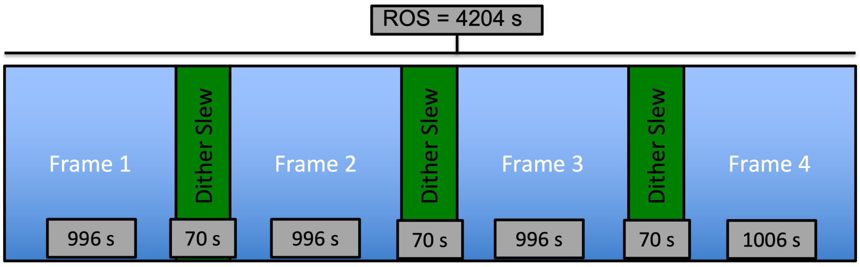

Figure 4.2: Schematic view of the ROS. The ROS does not include the final field-to-field slew and the initial lead time

Each frame starts with one NISP Spectrometer exposure in one of the red grisms RG_E done in parallel to a VIS band I_E exposure (that starts 8 seconds after the start of the NISP-S exposure to account for the opening of the shutter), followed by three NISP Photometry exposures in the J_E, H_E, Y_E bands. At the end of the ROS, the spectra main direction will form a K-pattern: RGS 000, RGS 180 rotated by -4 deg, RGS 000 rotated by 4 deg and RGS 180. VIS short science exposures are taken in parallel to the Y band exposures of the first and second frames, and a flat field is taken at the end of the fourth frame, increasing its duration by 10 s. In between exposures, the Filter Wheel (FWA) and Grism Wheel (GWA) must be rotated to correctly configure the NIPS instrument for the following exposure. As these movements will disturb the spacecraft pointing, a stabilization time (Stab) must be allocated. Extra idle time is also needed for tele-command (TC).

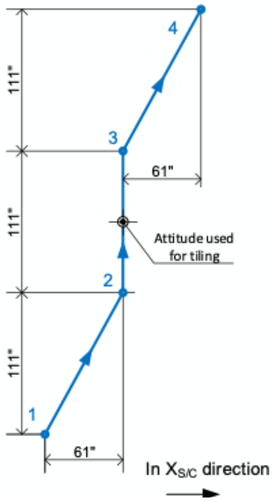

Figure 4.3: The nominal “S” dither pattern

The standard ROS as applied to the RSD computation is shown in Figure 4.4, and has a total duration of *#ros_duration*. In addition to the VIS nominal science and short science, the VIS instrument can perform other activities in parallel throughout the survey for calibration and image quality purposes without increasing the ROS duration. These are short dark (SD) and bias sequence, in dither 3, and flat field, dark, charge injection, serial trap pumping and vertical trap pumping (VTP) in dither 4.

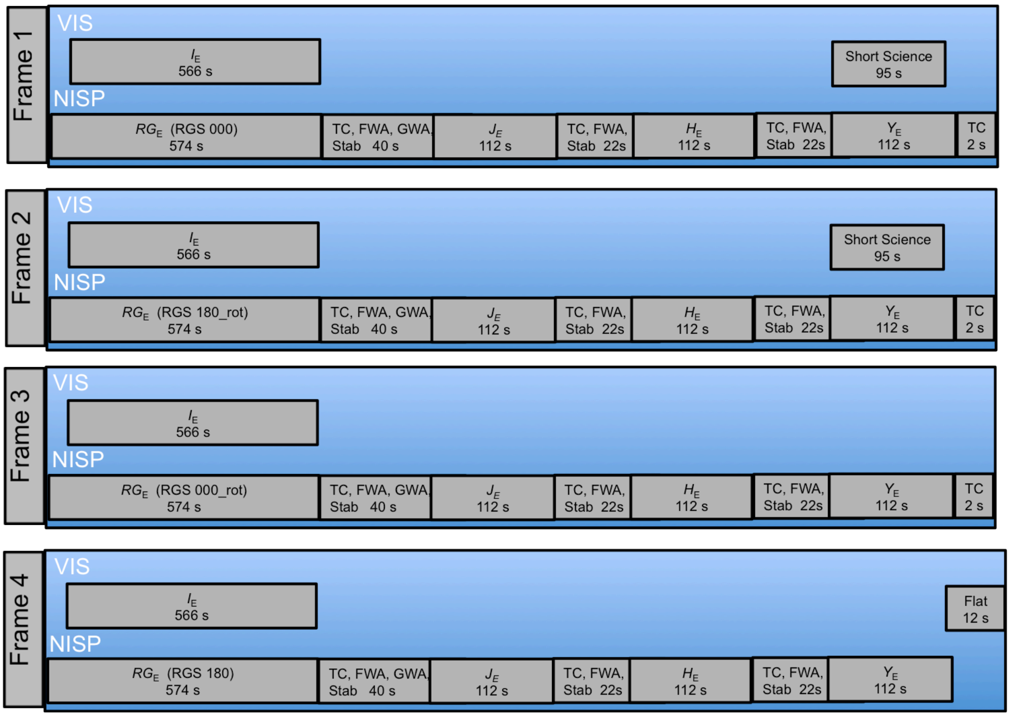

Figure 4.4: Detailed sequence of each of the four dithered frames of the ROS

The presented document is Proprietary information of the Euclid Consortium.
This document shall be used and disclosed by the receiving Party and its related entities (e.g. contractors and subcontractors) only for the purposes of fulfilling the receiving Party's responsibilities under the Euclid Project and that the identified and marked technical data shall not be disclosed or retransferred to any other entity without prior written permission of the document preparer.

After the ROS sequence the telescope slews to the next target with the filter wheel in the closed position. At the end of the slew the filter wheel moves to the open position, which requires an additional *#ros_leadtime* (TC+FWA+Stab) before the start of the first frame. This "lead time" is not part of the RSD ROS but is added to the field-to-field slew duration that leads to the first frame of the next ROS observation. Therefore, the total time of a ROS EWS, including lead time and average field-to-field slew of *#slewtime_field_typical* (cf. Sect 4.1.433) is *#ros_total*.

The specified observation sequence in RSD is encoded in a survey schedule by assigning time stamps and quaternions to the beginning of each frame, plus adding dither slew time between frames. Extra time, such as the *#ros_leadtime* lead, but also additional waiting times that may be required in non-ROS observations are added to the preceding slew.

A fraction of the visits to the EDFs and EAFs are made with the blue ROS variant in which the four exposures are taken in a single GWA position BGS 000, using the blue grism, instead of taking four exposures of the red grisms in a K-pattern.

Calibration observations are made with non-ROS sequences. One of the sequences used is known as ROS_D1. It consists of only one frame of ROS, but with an increased duration of *#ros_d1* because it contains all instrument activities during the on-target duration.

4.1.4 Field-to-field slews

The time it takes to slew from one pointing to the next one depends on the eigen-rotation between the two pointings (including angular separation and change in attitude). Rotations between 130 arcsec and 3.5 deg are named field slews, while larger rotations are known as large slews. The durations of field and large slews are computed with the formulae given in [RD02].

In short, the duration of a field slew is a minimum of *#slewtime_field_min* for eigen-slews below 0.13 deg and increases with the square-root of the eigen-slew for larger field slews, ranging from *#slewtime_field_min* to 283 s. The duration of a typical field slew of 0.9 deg between two neighboring fields is *#slewtime_field_typical*. A lead time of *#ros_leadtime* is added to this value in the cases when the S/C slews to a ROS observation.

The duration of a large slew increases linearly with the eigen-slew, ranging from 5.8 minutes for an eigen-slew of 3.5 deg up to around 34 min for eigen-slews of 180 deg. The total number of large slews is constrained in [AD02]. The strategies used to implement *#version_rsd* minimize the use of large slews, both in the scheduling of the EWS and by grouping calibration observations of the same cadence.

The scheduling always needs to include a minimum required time between two consecutive slews, also defined in [RD02]. This is to guarantee that, in the unlikely event the FGS acquisition takes long, there is margin to apply an extra attitude correction. This is especially relevant for short non-ROS sequences.

4.1.5 SOPS windows

MOCD-A [AD02] requires the survey to be interrupted every Monday at 12:00 UTC, plus or minus a margin of 2h during *#sop_duration* for spacecraft orbit and platform maintenance. The RSD leaves the spacecraft pointing to a position mid-way between the last pre-SOPS observation and the first post-SOPS observation, with an SAA between *#sop_saamin* and *#sop_saamax*, and an AA between *#sop_aamin* and *#sop_aamax*. Then the S/C returns to the next scheduled pointing applying a large slew that takes 5 minutes longer than it would be required for that eigen-rotation.

Non-ROS calibration sequences must not be interrupted by other activities, which implies they cannot be scheduled around a SOPS window.

4.2 Calibration requirements

A second class of inputs originates from calibration requirements. The in-flight observation procedures (known as calibration blocks) that need to be implemented to acquire the data required to fulfill calibration and characterization products defined in CalCD-B [RD07], are defined in the calibration framework (CalF). Calibration blocks F-002 to F-006 are the ones related with sample characterization. Their data is obtained with repeated observations of the Euclid Deep fields and of well-known astronomical fields with available external data, which we refer to as the Euclid Auxiliary fields. In contrast to the other calibration blocks they use the ROS sequence, and the timings are not defined in observation configuration files.

We present a summary of the CalF information that is relevant to the computation of the RSD, extracted from the applicable version *#version_calf* [AD03]. Since its publication, SOST made two requests for modifications to enable scheduling. These were accepted and are indicated explicitly in footnotes in MOCD-C. The summary includes the target, cadence, description of the required sequence, observing times as defined in the OCFs when applicable, and the time allocation for the sequence including slew times. Detailed information on the EDFs and EAFs is provided in [AD01].

4.2.1 CALBLOCK-F-001: Self-calibration

Procedure and Target: Perform the self-cal sequence observing 60 pointings within the standard self-cal field, also known as the SELFCAL-CENTER field. The coordinates of the 60 pointings are given in Table 4.1, where they are presented in observation order. The total observed area, when all pointings are covered with observations from transit longitudes distributed along all year, is enclosed in a circle of radius 0.9 deg.

Cadence: Perform this calblock with a monthly cadence (25 to 40 days). For efficiency this calibration can be scheduled in a monthly block consisting of the sequence F-001+F-018+F-007.

Sequence: The self-cal sequence consists in executing ROS_D1, i.e. the first frame of ROS, with a specific grism, at each of the 60 pre-defined pointings within the self-cal field. On a given visit, the pointings are observed with the same orientation, determined by the mean AA of the contemporary EWS patch. In the first visit, start by observing 8 pointings with AA ~ AA_mean - *#bgs_selfcal*, actuating the BGS000 blue grism (targets D42, 44, 45, 48, 2, 3, 30, 32). In practice, AA will slowly move with orbit progression, with the target AA being reached at the middle of the observation sequence. Then observe the full set 60 pointings, following their order, but with AA ~ AA_mean and using alternately the four red grisms, i.e., RGS000 for pointing 1, RGS180_rot for pointing 2, RGS000_rot for pointing 3, RGS180 for pointing 4, and repeating the loop over the red grisms until reaching the 60th pointing. Finally, observe targets D41, 43, 47, 46, 1, 4, 29, 31 again with BGS000, but now with AA ~ AA_mean + *#bgs_selfcal*. This concludes the first F-001 visit. In the second visit, roughly one month later, the sequence is repeated in the same order, but this time the blue grism will observe targets D53, 54, 49, 50, 37, 39, 26, 25 (AA-1.4) and targets D56, 55, 51, 52, 38, 40, 28, 27 (AA+1.4), while the red grisms are actuated alternating along the full set (pointings 1 to 60) but with a different sequence: RGS180_rot, RGS000_rot, RGS180, RGS000. The third visit uses the BGS000 in targets D10, 11, 5, 7, 23, 21, 18, 19 (AA-1.4) and targets D9, 12, 6, 8, 22, 24, 17, 20 (AA+1.4), while the sequence of red grisms alternating over the 60 pointings is now RGS000_rot, RGS180, RGS000, RGS180_rot. The fourth visit uses the BGS000 for targets D13, 14, 33, 36, 57, 58, 41, 42 (AA-1.4)

The presented document is Proprietary information of the Euclid Consortium.
This document shall be used and disclosed by the receiving Party and its related entities (e.g. contractors and subcontractors) only for the purposes of fulfilling the receiving Party's responsibilities under the Euclid Project and that the identified and marked technical data shall not be disclosed or retransferred to any other entity without prior written permission of the document preparer.

and targets D16, 15, 34, 35, 59, 60, 43, 44 (AA+1.4), notice the repetition of D41, D42, D43, D44. The sequence of red grisms is now RGS180, RGS000, RGS180_rot, RGS000_rot. After 4 visits, all grisms are observed at all 60 targets, and the cycle restarts in the 5th visit.

OCF on-target times: [1225s],7x[1073s],60x[1073s],7x[1073s], [1450s] (the first and last observation have increased durations due to the transition from/to calibration-EWS observations, which require FWA/GWA additional rotations and closing of the mass memory unit).

Time allocation: The time allocation for the Self-cal sequence, including ROS_D1 duration and slews is 24.3 h.

ID	Order (for RGS)	R.A.	Dec
SELFCAL-D42	1	2.687735891523070109e+02	6.530917643607952527e+01
SELFCAL-D44	2	2.688126993571971184e+02	6.524637462922721909e+01
SELFCAL-D41	3	2.686686314897860939e+02	6.523697025927710058e+01
SELFCAL-D43	4	2.687350627161707166e+02	6.530175872647558322e+01
SELFCAL-D45	5	2.686068072534315547e+02	6.510582790074464299e+01
SELFCAL-D48	6	2.687127003974289892e+02	6.512406655460813454e+01
SELFCAL-D47	7	2.687857019957170905e+02	6.516362823146603489e+01
SELFCAL-D46	8	2.686770401524764793e+02	6.517721666356210619e+01
SELFCAL-D2	9	2.684026628412527771e+02	6.514448912433289252e+01
SELFCAL-D3	10	2.683931502337825350e+02	6.510564042116952521e+01
SELFCAL-D1	11	2.683338328607711105e+02	6.509167096802160302e+01
SELFCAL-D4	12	2.683724432645189495e+02	6.515940267239214734e+01
SELFCAL-D30	13	2.684684023037730753e+02	6.502250766181664687e+01
SELFCAL-D32	14	2.683137099628377200e+02	6.505519342738520550e+01
SELFCAL-D29	15	2.682700451664400134e+02	6.499379247643648227e+01
SELFCAL-D31	16	2.683163691697626518e+02	6.506855497692339441e+01
SELFCAL-D53	17	2.683453369074656507e+02	6.493994321638432154e+01
SELFCAL-D54	18	2.683699843900433848e+02	6.498170960629329329e+01
SELFCAL-D56	19	2.683715449801671866e+02	6.494600491851031165e+01
SELFCAL-D55	20	2.684699686767491471e+02	6.500827516920598725e+01
SELFCAL-D49	21	2.679967371109335659e+02	6.496166516890818343e+01
SELFCAL-D50	22	2.680153333445846329e+02	6.500346526558708149e+01
SELFCAL-D51	23	2.680305437013537926e+02	6.503284755458345501e+01
SELFCAL-D52	24	2.681203407976814788e+02	6.503080538892940865e+01
SELFCAL-D37	25	2.682922781032415855e+02	6.547497088421729927e+01

The presented document is Proprietary information of the Euclid Consortium.
This document shall be used and disclosed by the receiving Party and its related entities (e.g. contractors and subcontractors) only for the purposes of fulfilling the receiving Party's responsibilities under the Euclid Project and that the identified and marked technical data shall not be disclosed or retransferred to any other entity without prior written permission of the document preparer.

SELFCAL-D39	26	2.684343895012351595e+02	6.555034223931107817e+01
SELFCAL-D38	27	2.683673440127335539e+02	6.552108163079601866e+01
SELFCAL-D40	28	2.684576982323557672e+02	6.554724900095493467e+01
SELFCAL-D26	29	2.685027894692535142e+02	6.561728721869499736e+01
SELFCAL-D25	30	2.684726214651515193e+02	6.557526008670906492e+01
SELFCAL-D28	31	2.685203260774594582e+02	6.560298149023091696e+01
SELFCAL-D27	32	2.684964154838451122e+02	6.563122831841930349e+01
SELFCAL-D10	33	2.687507063392295663e+02	6.554516643854840652e+01
SELFCAL-D11	34	2.687013880839363651e+02	6.547678032862189923e+01
SELFCAL-D9	35	2.685798066818130678e+02	6.547210447750491369e+01
SELFCAL-D12	36	2.687482759547385172e+02	6.555292402772255400e+01
SELFCAL-D5	37	2.688603113604480086e+02	6.536531490991127669e+01
SELFCAL-D7	38	2.690264629141197474e+02	6.537991923234400815e+01
SELFCAL-D6	39	2.689598214980393891e+02	6.541335746184520872e+01
SELFCAL-D8	40	2.690505697500939846e+02	6.543449797960043668e+01
SELFCAL-D23	41	2.689021948295654170e+02	6.531342792110351070e+01
SELFCAL-D21	42	2.688016342074652130e+02	6.527379055155755339e+01
SELFCAL-D22	43	2.689107295388272405e+02	6.529866671696800040e+01
SELFCAL-D24	44	2.689010128673028248e+02	6.533161660102703649e+01
SELFCAL-D18	45	2.693883003527739675e+02	6.535200896390244907e+01
SELFCAL-D19	46	2.693135987943638838e+02	6.531934953410414835e+01
SELFCAL-D17	47	2.691905182269963461e+02	6.531092390365220979e+01
SELFCAL-D20	48	2.692059477188362848e+02	6.538687999476010759e+01
SELFCAL-D13	49	2.692492266179530702e+02	6.534772696988548546e+01
SELFCAL-D14	50	2.693359182919091950e+02	6.535383872089019519e+01
SELFCAL-D16	51	2.694362345162348902e+02	6.535741350765979973e+01
SELFCAL-D15	52	2.694462357455213350e+02	6.542786910216231888e+01
SELFCAL-D33	53	2.694242525563329309e+02	6.531825851578717845e+01
SELFCAL-D36	54	2.696011250280964191e+02	6.536400576361720027e+01
SELFCAL-D34	55	2.695143151008379050e+02	6.537653260264035282e+01
SELFCAL-D35	56	2.694316216534356272e+02	6.533287838391977687e+01
SELFCAL-D57	57	2.694530201388830051e+02	6.504781893761530398e+01
SELFCAL-D58	58	2.694955734727524259e+02	6.509672497787576617e+01

The presented document is Proprietary information of the Euclid Consortium.
This document shall be used and disclosed by the receiving Party and its related entities (e.g. contractors and subcontractors) only for the purposes of fulfilling the receiving Party's responsibilities under the Euclid Project and that the identified and marked technical data shall not be disclosed or retransferred to any other entity without prior written permission of the document preparer.

SELFCAL-D59	59	2.695827737126971897e+02	6.512629080980971708e+01
SELFCAL-D60	60	2.696287536782168672e+02	6.511398358785062612e+01

Table 4.1: Self-cal pointings (in observing order for the RGS observations)

Field	R.A.	Dec
SELFCAL-CENTER	268.812745	65.2855857
SELFCAL-FAINT	268.000	64.900
EDF-N	269.733	66.018
NEP	270.000	66.561

Table 4.2: Coordinates of the northern polar fields: Selfcal-center (used in F-009, F-010, F-011), Selfcal-faint (used in F-007) and EDF-N. NEP is also listed for comparison

4.2.2 CALBLOCK-F-002: Noise bias (Euclid Deep Fields)

The EDS is required to have at least 40 deg^2, in two or more disjoint EDFs, and be two magnitudes deeper than the average EWS, requiring 40 ROS visits to each field. [AD01] describes in detail the process of selecting the best sky locations for the EDFs. One key element is visibility; long visibility is required since many visits are needed. Two EDFs were initially defined: EDF-N and EDF-S. EDF-N was placed close to NEP, but EDF-S cannot be close to SEP due to the presence of LMC and the Galactic plane. The field was thus moved further north, finding a location free from out of field stray light from bright stars and large extinction gradients. The EDF-S location will also be observed by the LSST survey of the Rubin observatory, and its shape was devised to increase the synergy between the two observations (Figure 4.5). One problem with high ecliptic latitude fields is the low visibility from ground facilities which makes the follow up difficult. To maximize the overall science return of the mission, a third deep field was created on lower ecliptic latitudes, the EDF-F that encloses the Chandra Deep Field South. The total area of the EDS thus increased to 53 deg^2.

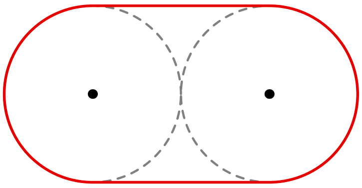

Figure 4.5: The 23 deg^2 EDF-S stadium, enclosing two adjacent circles of 10 deg^2 and the area between them

Field	Size	Shape	R.A.	Dec	lon_ecl	lat_ecl	Visits
EDF-N	20 deg^2	circle	269.733	+66.018	258.690	89.446	40
EDF-S	23 deg^2	stadium	61.241	-48.423	36.493	-66.599	45

EDF-F	10 deg^2	circle	52.932	-28.088	40.772	-45.397	52

Table 4.3: The Euclid Deep fields

Procedure and Target: Observe the three EDFs repeatedly with the ROS sequence. The number of visits depends on the background and is a function of ecliptic latitude. For each one of the three EDS fields, Table 4.3 gives the coordinates of the center, its size, shape and the number of visits needed to reach the required depth compensating for the zodiacal background, i.e. 40 g(β) (Sect. 4.3.11).

Cadence: The observations do not have a specified cadence, but the total observed area must grow at a relative pace similar to the area growth of the wide survey. Each visit must observe one of the deep fields completely. The first 10 visits to EDF-N and EDF-S fulfill CPC and are done according to the specifications of CALBLOCK-F-003.

Sequence: Each visit covers the field shape completely with a tessellated pattern with no inner holes. Fields in the tessellated pattern must overlap the same amount as in the wide survey. The pattern is offset at every visit, using the smearing pattern described in Sect.4.3.10. Each visit is made with one of the ROS spectra variants (blue or red, Sect. 4.1.3), such that over the total number of visits for each EDF, the ROS variants are applied in the ratio of *#bgs_brratio*. This translates to the following ratio between the number of BGS:RGS visits: EDF-F (32:20), EDF-N (25:15, divided in 25:5 with CALBLOCK-F-002 specifications and 0:10 with CALBLOCK-F-003 specifications), EDF-S (28:17, divided in 28:7 with CALBLOCK-F-002 specifications and 0:10 with CALBLOCK-F-003 specifications). The visits made immediately after or before a non-ROS sequence are required to respectively start or end with a ROS (red) pointing. So, an additional single ROS (red) may need to be inserted in some of the blue ROS variant visits.

Time allocation: The time allocation for one full visit of EDF-N, including ROS duration and field slews is 40 x (*#ros_leadtime* + *#ros_duration* + *#slewtime_field_typical*) = 2.1 days. One full visit of EDF-S takes 2.4 days, while one full visit of EDF-F takes 1.0 days.

4.2.3 CALBLOCK-F-003: Completeness and purity calibration

The main objective of CPC is to observe the target field with various orientations such that the slitless spectra of the sources can be fully disentangled. This requires the target field to have a long visibility throughout the year to enable repeated observations that ensure a variety of position angles and a large number of sources. To save survey time, part of the observations of EDF-N and EDF-S are made with the CPC position angle restrictions and no additional dedicated observations are needed, as justified in [AD01].

Procedure and Target: Observe EDF-N and EDF-S, presented in Table 4.3, 10 times each, with the ROS sequence and with constrained orientations.

Cadence: The requirements on the orientations restrict the cadence. The visits must be made and completed as soon as possible.

Sequence: Each visit covers the field shape completely with a tessellated pattern with no inner holes. Fields in the tessellated pattern must overlap the same amount as in the wide survey. All visits must be made with a distinct reference orientation. Given the set of four red grisms, a visit made with a reference angle θ observes four spectral directions: θ, $\theta - 4$, $\theta + 180$, $\theta + 184$ (denominated a K-pattern). The 10 visits for each field must be made with a minimum separation of their reference angles of *#threshold_cpcmin*. The first 10 visits to EDF-N and EDF-S are made with

The presented document is Proprietary information of the Euclid Consortium.
This document shall be used and disclosed by the receiving Party and its related entities (e.g. contractors and subcontractors) only for the purposes of fulfilling the receiving Party's responsibilities under the Euclid Project and that the identified and marked technical data shall not be disclosed or retransferred to any other entity without prior written permission of the document preparer.

this constraint and the resulting fields are known as CPC-N and CPC-S, respectively. All visits are made with the red ROS variant. The remaining visits to EDF-N and EDF-S are made according to CALBLOCK-F-002. Contrary to CALBLOCK-F-002 visits, the 10 CALBLOCK-F-003 visits are not off-set along the spiral described in Sect. 4.3.10.

Time allocation: The time allocation for one full visit of EDF-N, including ROS duration and field slews is 40 x *(#ros_leadtime* + *#ros_duration* + *#slewtime_field_typical*) = 2.1 days. One full visit of EDF-S takes 2.4 days.

4.2.4 CALBLOCK-F-004: Color gradient calibration fields

The shear measurements need to consider color gradients within galaxies because the PSF depends on wavelength. To characterize the galaxy sample, VIS and NISP observe five fields with ancillary HST data to four times the S/N of the EWS [AD01].

Procedure and Target: Observe the 5 color calibration fields with the ROS to at least four times the mean imaging S/N of the wide survey area. Three of these fields are also required to be observed to five times the imaging S/N of EWS as part of CALBLOCK-F-005 and hence do not need to be observed a second time. The fields are presented in Table 4.4, including the number of visits needed to achieve the required depth, which depends on the backgrounds (Sect. 4.3.11).

Cadence: The AEGIS field should be completed in the first year, and at least one field must be observed every following year.

Sequence: In each visit, the center of the field is off set along a smearing spiral (Sect. 4.3.10). Both ROS spectra variants must be used, with a ratio of *#bgs_brratio*. The blue ROS variant must be scheduled with at least two different reference spectral angles. This cannot be done by changing SAA and AA between contemporary visits, which use create a thermal instability of the telescope. The solution implemented is to schedule the visits in two periods 6 month apart, resulting in a variation of 180 deg in the reference angle. Each period includes the two ROS spectra variants, with the sequence always starting with the blue ROS.

Time allocation: The time allocation for the color gradient sequence is *#ros_total* x visits x pattern = 66.6 h or 2.8 days.

Field	Pattern	R.A.	Dec	lon_ecl	lat_ecl	Visits	Time allocation
CANDELS/AEGIS	2x1	214.827	+52.82	179.968	60.26	18	44.4 h
CANDELS/ GOODS-N	1x1	189.250	+62.25	148.342	57.32	18	22.2 h
CANDELS/ COSMOS	1x1	150.120	+02.35	151.366	-9.23	(46)	0; replaced by COSMOS in F-005
CANDELS/ GOODS-S	1x1	53.125	-27.80	41.140	-45.18	(22)	0; replaced by CDFS in F-005
CANDELS/ UDS	1x1	34.407	-05.22	30.300	-17.90	(37)	0; replaced by SXDS in F-005

Table 4.4: The five color gradient calibration fields

The presented document is Proprietary information of the Euclid Consortium.
This document shall be used and disclosed by the receiving Party and its related entities (e.g. contractors and subcontractors) only for the purposes of fulfilling the receiving Party's responsibilities under the Euclid Project and that the identified and marked technical data shall not be disclosed or retransferred to any other entity without prior written permission of the document preparer.

4.2.5 CALBLOCK-F-005: Photo-z calibration fields

The purpose of these observations is to obtain NISP-P photometry for a sample of galaxies with existing visible and near-infrared ground-based spectroscopy, in order to calibrate Euclid photometric redshift methods. To this end, NISP-P will observe four fields to five times the S/N of the EWS. VIS data are also needed to perform the target detection and selection in an identical manner as in the EWS.

Procedure and Target: Observe the 4 photo-z calibration fields with the ROS to five times the mean imaging S/N of the wide survey area. The fields are presented in Table 4.5, including the number of visits needed to achieve the required depth, which depends on the backgrounds (Sect. 4.3.11).

Cadence: COSMOS and CDFS are the priority in the first two years, and at least one other field must be observed every following year.

Sequence: In each visit, the center of the field is off set along a smearing spiral (Sect. 4.3.10). Both ROS spectra variants must be used, with a ratio of *#bgs_brratio*. The blue ROS variant must be scheduled with at least two different reference spectral angles. This cannot be done by changing SAA and AA between contemporary visits, which would create a thermal instability of the telescope. The solution implemented is to schedule the visits in two periods 6 month apart, resulting in a variation of 180 deg in the reference angle. Each period includes the two ROS spectra variants, with the sequence always starting with the blue ROS. The largest fields COSMOS and SXDS are observed in four visits, each visit observing the full area (2×2) to a certain depth. The first visit should reach at least 3x the imaging S/N of EWS and the remaining visits may increase the depth at a slower rate if needed.

Time allocation: The time allocation for the photo-z sequence is *#ros_total* x visits x pattern = 769.4 h or 32 days.

Field	**Pattern**	**R.A.**	**Dec**	**lon_ecl**	**lat_ecl**	**Visits**	**Time allocation**
COSMOS	2x2	150.119	+02.21	151.415	-9.36	75	370.0 h
VVDS	1x1	36.500	-04.50	32.617	-17.93	58	71.5 h
CDFS	1x1	53.117	-27.81	41.126	-45.19	34	41.9 h
SXDS	2x2	34.500	-05.00	30.470	-17.72	58	286.0 h

Table 4.5: The four photo-z calibration fields

4.2.6 CALBLOCK-F-006: Wide survey

These are the observations for the completion of the EWS. They are made by placing the Euclid FoV once on each of the tessellation and polar caps tiles. Observations are made with the standard ROS (red grism), taking *#ros_duration* each, aiming to cover as much of the RoI area as possible during *#time_duration*.

The presented document is Proprietary information of the Euclid Consortium.
This document shall be used and disclosed by the receiving Party and its related entities (e.g. contractors and subcontractors) only for the purposes of fulfilling the receiving Party's responsibilities under the Euclid Project and that the identified and marked technical data shall not be disclosed or retransferred to any other entity without prior written permission of the document preparer.

4.2.7 CALBLOCK-F-007: VIS non-linearity, PTC, BFE and NISP LED flats

Procedure and Target: Perform the VIS non-linearity sequence in the SELFCAL-FAINT field and then the FLAT sequence (for photon transfer curve, PTC, and brighter-fatter effect, BFE) in the same field, which is an area within the Self-cal field without bright stars, centered on (r.a., dec) = (268.000, 64.900). At the same time, a NISP LED flats sequence (of shorter duration) is taken, not interfering with the VIS observations and not relevant for the RSD computation.

Cadence: Perform this calblock with a monthly cadence (25 to 40 days). For efficiency this calibration can be scheduled in a monthly block consisting of the sequence F-001+F-018+F-007.

Sequence: The VIS non-linearity sequence starts with a BIAS, followed by 8 observations with four exposures each. After each set of 4 exposures an off-set is applied along the smear spiral described in Sect. 4.3.10, with a corresponding *#slewtime_field_min* slew. The eight observations are followed by a BIAS, then a second set of 8 observations, and finally a third BIAS, in a total of 19 pointings. Afterwards, the FLAT sequence is performed with LEDs, also including short science exposures. The FLAT sequence consists on 3 blocks and 3 slews. There are two variants of this calblock with identical timings (cycling done at SOC).

OCF on-target times: VIS NL = 5x[2480s, 1665s], 5x[1710s], [1955s]. VIS FLAT = [2085s], [2540s], [2270s]

Time allocation: Including slews, the time allocation for the VIS non-linearity sequence is 9.4 h and the time allocation for the VIS FLAT sequence is 2.1 h.

4.2.8 CALBLOCK-F-008: VIS PSF calibration and NISP-P non-linearity

Procedure and Target: Perform the VIS PSF sequence in an available VIS PSF calibration field taken from the list shown in Table 4.6. All fields are at similar ecliptic latitudes (in the two ecliptic hemispheres). At the same time NISP will take a shorter duration sequence of off-sky parallel ramps with no pointing constraints, which is not relevant for the RSD computation.

Cadence: Perform this calblock with a loose monthly cadence (two to six weeks). The observations must be made within the time allocation of an EWS survey patch, interrupting the patch no less than *#threshold_thermalization* days after the start of the patch. This ensures thermal equilibrium is achieved at the start of the observations. The observations must then be made with solar angles close to the mean of the values used to observe the patch, to keep thermal stabilization. Moreover, and also for the sake of thermal stability, F-008 must not be scheduled less than 3 days after a SOPS window.

Sequence: The PSF sequence consists in 100 observations of a PSF field with an exposure time of 289 s. The first pointing of a PSF calibration must be made with an orientation such that the AA and SAA variations when slewing from a preceding EWS pointing to the PSF target do not exceed 1 deg. The pointings must be oriented in a way that keeps AA and SAA constant (and equal to the values of first pointing). To avoid clustering of random pointings, the pointings are placed along the spiral described in Sect. 4.3.10. There are twelve variants of this calblock with identical timings (cycling done at SOC).

OCF on-target times: [500s], 98x[335s], [670s] (the first and last observation have increased durations due to the transition from/to calibration-EWS observations, which require FWA/GWA additional rotations and closing of the mass memory unit).

Time allocation: The time allocation for the VIS PSF sequence, excluding slews along the smearing spiral is 9.5 h.

The presented document is Proprietary information of the Euclid Consortium.
This document shall be used and disclosed by the receiving Party and its related entities (e.g. contractors and subcontractors) only for the purposes of fulfilling the receiving Party's responsibilities under the Euclid Project and that the identified and marked technical data shall not be disclosed or retransferred to any other entity without prior written permission of the document preparer.

Field	R.A.	Dec	lon_ecl	lat_ecl	lon_gal	lat_gal
VIS-PSF-1	292.48	53.53	321.00	73.00	85.33	16.16
VIS-PSF-2	285.03	49.83	302.00	71.60	79.93	19.07
VIS-PSF-3	275.78	47.80	282.00	71.00	75.93	24.30
VIS-PSF-4	265.72	48.09	261.00	71.40	74.83	30.97
VIS-PSF-5	254.20	49.37	237.00	71.00	75.94	38.61
VIS-PSF-6	247.27	52.69	220.00	72.20	80.91	42.58
VIS-PSF-7	239.80	56.89	200.00	73.00	88.18	45.55
VIS-PSF-8	235.16	60.85	184.00	73.80	94.79	45.96
VIS-PSF-9	225.35	61.91	172.50	70.50	100.21	49.09
VIS-PSF-10	221.47	67.43	155.00	71.50	107.55	46.13
VIS-PSF-11	215.61	73.55	135.00	71.00	114.45	42.05
VIS-PSF-12	218.16	82.06	109.00	70.50	118.83	34.25
VIS-PSF-13	43.34	-66.36	339.00	-71.80	285.75	-46.49
VIS-PSF-14	45.21	-61.46	353.50	-70.20	279.78	-49.44
VIS-PSF-15	54.60	-58.77	9.00	-72.30	272.38	-47.24
VIS-PSF-16	59.25	-55.16	23.00	-71.50	266.02	-46.46
VIS-PSF-17	65.30	-51.89	38.00	-70.90	260.15	-43.91
VIS-PSF-18	73.52	-49.10	56.00	-70.60	255.62	-39.06
VIS-PSF-19	81.34	-48.10	72.00	-71.00	254.49	-33.88
VIS-PSF-20	63.55	-49.19	39.00	-68.00	256.73	-45.53

Table 4.6: The 20 VIS PSF calibration fields, to be chosen according to visibility

4.2.9 CALBLOCK-F-009: NISP-S non-linearity

Procedure and Target: Perform the NISP-P non-linearity validation procedure in the SELFCAL-CENTER field and then the NISP-S non-linearity measurement of acquiring LED ramps.

Cadence: There are two variants of this calblock with identical timings (cycling done at SOC). The two variants must be scheduled with an annual cadence, either scheduled back-to-back or at different times. For efficiency this calibration can be scheduled right before CALBLOCK-F-016 forming a biannual block.

Sequence: The NISP non-linearity validation procedure consists in taking one NISP photometry exposure in one of the J_E, H_E, Y_E bands, followed by another exposure in the same band with a non-standard MACC mode of longer exposure time (after a repointing on the smear spiral). This sequence is done 4 times for each of the 3 bands. Then move to the LED ramps acquisition consisting of 48 measurements on each of 2 low-flux settings, 40 measurements on each of 2 medium-flux settings, 24 measurements on 1 high-flux setting, and 12 darks.

OCF on-target times: NL validation = 3x[[500s],3x[640s,280s],[820s]] already including *#slewtime_field_min* between pointings and increased durations for the first and last observations. NL measurements = 2x[[2950s], 7x[4x[2930s], [2995s], [2940s]], 4x[2930s], [2995s]] + 2x[[2950s], 7x[3x[2930s], [2995s], [2940s]], 3x[2930s], [2995s]] + [2950s], 7x[2930, 2995s, 2940s], [2930s], [2995s] + 5x[1760s, 1185s], [1760s], [1430s]

Time allocation: The time allocation for the NISP-P non-linearity validation procedure is 3.4 h. The time allocation for the NISP-S non-linearity procedure is 6.9 days.

4.2.10 CALBLOCK-F-010: NISP-S wavelength dispersion and VIS BFE

Procedure and Target: Perform the NISP-S wavelength dispersion sequence that includes observations of a planetary nebula (PN) from the list shown in Table 4.7 and observations of the SELFCAL-CENTER field. At the same time VIS will take pairs of flats and very short science exposures, which are not relevant for the RSD computation.

Cadence: Perform this calblock once, within 12-15 months after the start of the routine survey and depending on PN visibility.

Sequence: The NISP-S wavelength dispersion sequence consists in several observations of a PN interspaced with observations of the self-cal field. First, the ROS is executed four times, performing a PN scan with the PN placed near the four corners of the FoV. Then, the first grism is selected and the PN is observed at 5 locations of each of the 16 NISP detectors, with a dither sequence defined in [AD03]. We note the sequence no longer forms a quicunx shape as in previous RSD versions. At each location two NISP-S exposures without off-set are acquired. The 80 observations can be done in any order. Once this is done, the S/C must slew to the self-cal field where it must observe a 2x2 pattern centered on this field, where at each of the four pointings two slightly dithered NISP-S exposures are acquired. The orientation of the 2×2 pattern must be chosen in a way such that AA is not changed from the preceding PN exposure (with a margin of 0.5 deg), while SAA may differ by up to 10 deg. Then the next grism (out of the 5 grisms in total) is selected and process resumes, but in reverse order: the self-cal is observed followed by the PN observation. For efficiency, when the grism is changed for the next iteration, the orientation of the spacecraft may also change. However, like stated above, when slewing from the self-cal to the PN field AA must be kept constant. The process is iterated, moving between the two fields until all 5 grisms

The presented document is Proprietary information of the Euclid Consortium.
This document shall be used and disclosed by the receiving Party and its related entities (e.g. contractors and subcontractors) only for the purposes of fulfilling the receiving Party's responsibilities under the Euclid Project and that the identified and marked technical data shall not be disclosed or retransferred to any other entity without prior written permission of the document preparer.

have been actuated. The sequence may be summarized as: PscanP−SgS−PgP−SgS−PgP−S, where Pscan in the preliminary PN scan, P is the PN field, S is the self-cal field, g denotes a change of grism, and the dash denotes a slew. The 5 grisms are RGS 000, RGS 180_rot, RGS 000_rot, RGS 180 and BGS.

OCF on-target times: PN scan = [1225s],14x[1073s],[1450s]. PN observations = [1310s],78x[1190s], [1370s]. Self-cal field observations = [715s], 6x[605s], [850s]. We note that the first and last observations always have increased durations.

Time allocation: The time allocation for the preliminary PN scan is 4.9 h. The time allocation for one PN procedure, including *#slewtime_field_min* field slews between the quincunx positions is 30.3 h. The time allocation for the self-cal procedure, including dither slews for off-sets and field slews to move between the grid positions is 1.6 h. The total time allocation for the NISP-S wavelength dispersion sequence, including five PN and self-cal procedures, the preliminary 2x2 grid and 30 minutes large slews between the P and S fields, is 166.9 h, or 7.0 days.

Field	R.A.	Dec	lon_ecl	lat_ecl	Comment
He2-436	19:32:06.69	-34:12:57.8	289.335	-12.309	
SMC-SMP-20	00:56:05.39	-70:19:24.7	317.466	-63.684	Preferred target
LMC-Sa-104a	04:25:32.18	-66:47:16.3	347.761	-80.702	

Table 4.7: Compact planetary nebulae, only one needs to be observed

4.2.11 CALBLOCK-F-011: NISP reciprocity failure

Procedure and Target: Perform the NISP reciprocity failure sequence in the SELFCAL-CENTER field.

Cadence: Perform this calblock yearly, beginning one year into the survey. For efficiency this calibration can be scheduled right after the biannual block F-009+F-016, in one of its two annual observations.

Sequence: The NISP reciprocity failure sequence consists in observing the selfcal field 9 times with one NISP-P filter, each visit making eight exposures on smeared pointings (using the spiral strategy) and additional 9 times of four exposures on smeared pointings, this time done with a LED turned on (each visit using a different LED). The latter take slightly longer to account for turn on/off time of the LED. Hence, the sequence consists of 9x8 exposures plus 9x4 illuminated exposures, a total of 108 pointings.

OCF on-target times: [500s], 106x[280s], [300s]

Time allocation: The time allocation for the NIPS reciprocity failure sequence is 8.5 h.

4.2.12 CALBLOCK-F-012: VIS flat-band voltage shift

Procedure and Target: Perform the VIS flat-band voltage-shift sequence off-sky, requiring no pointing.

The presented document is Proprietary information of the Euclid Consortium.
This document shall be used and disclosed by the receiving Party and its related entities (e.g. contractors and subcontractors) only for the purposes of fulfilling the receiving Party's responsibilities under the Euclid Project and that the identified and marked technical data shall not be disclosed or retransferred to any other entity without prior written permission of the document preparer.

Cadence: It must be scheduled as the first observation of a "PSF-block" consisting of the sequence F-012+F-015+F-013+F-008.

Sequence: The sequence is not relevant for the RSD computation, and can be summarized in 1 pointing only.

OCF on-target times: [2160s]

Time allocation: The time allocation for the VIS flat-band voltage shift sequence is 36 minutes

4.2.13 CALBLOCK-F-013: Phase diversity (photometric calibration component)

Procedure and Target: Perform the photometric classification part of the much larger phase diversity calibration sequence in a PSF field.

Cadence: It must be scheduled as part of the "PSF-block", always in a sequence F-012+F-015+F-013+F-008. Observations are done in the same PSF field used in F-008 and with the same spacecraft attitude angles.

Sequence: The PC-ROS variant of calblock-F-013 consists of 4 ROS_D1 pointings forming an S-dither pattern with ROS_D1

OCF on-target times: [1225s], 2x[1073s], [1450s]

Time allocation: The time allocation for the PC-ROS sequence is 1.35 h

4.2.14 CALBLOCK-F-014: Contamination scan

Part of PDCC, not included in the RSD.

4.2.15 CALBLOCK-F-015: VIS serial trap pumping

Procedure and Target: Perform the VIS serial trap pumping sequence in an available VIS PSF calibration field taken from the list shown in Table 4.6.

Cadence: It must be scheduled in a "PSF-block" consisting of the sequence F-012+F-015+F-013+F-008. The same PSF field and same spacecraft attitude angles must be observed for all the sequence.

Sequence: The sequence applies 12 variants of the serial trap pumping (STP) operations in three blocks with three in-between dither steps, making use of the smear spiral.

OCF on-target times: [2431s], [1714s], [2614s]

Time allocation: The time allocation for the VIS serial trap pumping sequence, including *#slewtime_dither* slews is 1.9 h.

4.2.16 CALBLOCK-F-016: VIS charge injection timing

Procedure and Target: Perform the VIS charge injection timing sequence in an unspecified target. It must be stray light free. If scheduled at the self-cal (SAA=90), then it must have AA > - 6. If not in self-cal then AA can have any value within the allowed range provided that SAA > 92 deg.

Cadence: Perform this calblock with a biannual cadence (five to seven months). Given the identical cadence, it can be scheduled together with CALBLOCK-F-009 at selfcal.

Sequence: Sequence of eight CI-timing pointings in one block with eight in-between dither steps.

OCF on-target times: [1557s], 6x[1107s], [1188s]

Time allocation: The time allocation for the VIS charge injection timing sequence, including *#slewtime_dither* slews is 2.7 h.

The presented document is Proprietary information of the Euclid Consortium.
This document shall be used and disclosed by the receiving Party and its related entities (e.g. contractors and subcontractors) only for the purposes of fulfilling the receiving Party's responsibilities under the Euclid Project and that the identified and marked technical data shall not be disclosed or retransferred to any other entity without prior written permission of the document preparer.

4.2.17 CALBLOCK-F-017: Grism sanity

For technical reasons, ROS Calblocks (i.e. F-002 to F-006) are required to start (end) with the red grism (RGS000) when executed immediately after (before) a non-ROS Calblock (F-007 to F-018), otherwise observations with the wrong grism may occur. This is not an issue for F-003 and F-006 that are always observed in red. F-004 and F-005 are observed with a sequence of red and blue ROS. The first and last ROS can be enforced to be red. The only issue is with F-002 that makes a full visit in a single ROS.

Procedure and Target: Add one additional ROS (red) at the center of the relevant Deep field before or after some of the F-002 visits, when needed to ensure grism sanity.

Cadence: This calblock is to be applied only to EDF blue visits that follow or precede a non-ROS observation.

Sequence: One ROS

Time allocation: The time allocation for one sequence, including *#slewtime_field* slew is 1.2 h.

4.2.18 CALBLOCK-F-018: NISP Persistence

Procedure and Target: Perform the sequence in an unspecified target.

Cadence: Perform this calblock monthly in between F-001 and F-007.

Sequence: Sequence of seven pointings with in-between slews.

OCF on-target times: [495s], [895s], 2x[1400s], [895s], [1400s], [1410s]

Time allocation: The time allocation for the NISP persistence sequence, including *#slewtime_dither* slews is 2.3 h.

4.3 Science optimization

A third class of inputs originates from guidelines for science optimization. The criteria used to make certain implementation choices and the models on which they are based are discussed in CRSDIV [AD01]. Some of the information presented here is described in more detail in the applicable version *#version_crsdiv* of CRSDIV.

4.3.1 EWS region of interest

The Euclid Wide Survey is implemented within a region of interest, defined by considering three sky backgrounds, namely zodiacal light, galactic extinction, and stellar density, as described in detail in [AD01]. In the broad RoI definition, strong zodiacal background is avoided by using an ecliptic latitude threshold of +/-10 deg. Stellar density, which affects the sky through both in-filed and out-of-field stray light, is controlled by using a Galactic latitude threshold of +/-23 deg. Finally, extinction is limited by imposing a maximum value of E(B-V) = 0.09. The intersection of the three threshold lines creates a RoI that is separated in four large areas that we will name northern mainland, southern mainland, northern island, and southern island.

#version_rsd uses an updated *#version_roi*, introduced in RSD_2023A. It keeps the ecliptic latitude threshold of +/-10 deg used in the previous RoI v2, but introduces a new Galactic latitude threshold with the goal of maximizing the overlap with the low-dust Wide-Fast-Deep (WFD)

The presented document is Proprietary information of the Euclid Consortium.
This document shall be used and disclosed by the receiving Party and its related entities (e.g. contractors and subcontractors) only for the purposes of fulfilling the receiving Party's responsibilities under the Euclid Project and that the identified and marked technical data shall not be disclosed or retransferred to any other entity without prior written permission of the document preparer.

component of the upcoming LSST survey of the Vera C. Rubin Observatory, as detailed in [RD03]. In summary, *#version_roi* gets closer to the galactic plane (changing the average threshold in galactic latitude from +/-23 deg to +/-20 deg on the galactic anticenter). This galactic latitude threshold is not a hard boundary, a detailed carved contour of extinction E(B-V) is performed, leaving out the galactic bulge, LMC, and the Taurus/Orion clouds, while keeping SMC. In addition, the area of the northern island above Dec = 3 deg, which was among the poorest areas of RoI v2, is not covered by LSST-WFD and is discarded, strongly reducing the northern island area.

#version_roi has a total area of *#roi_total* distributed in four separate regions: mainland-north *(#roi_mainlandnorth*), mainland-south *(#roi_mainlandsouth*), island-north *(#roi_islandnorth*), island-south *(#roi_islandsouth*). It is shown in Figure 4.6, overlaid with contours of the sky backgrounds. The median values of the sky backgrounds in the RoI quandrants are shown in Table 4.8. The mainlands, which contain the galactic poles, are less contaminated by the backgrounds than the islands.

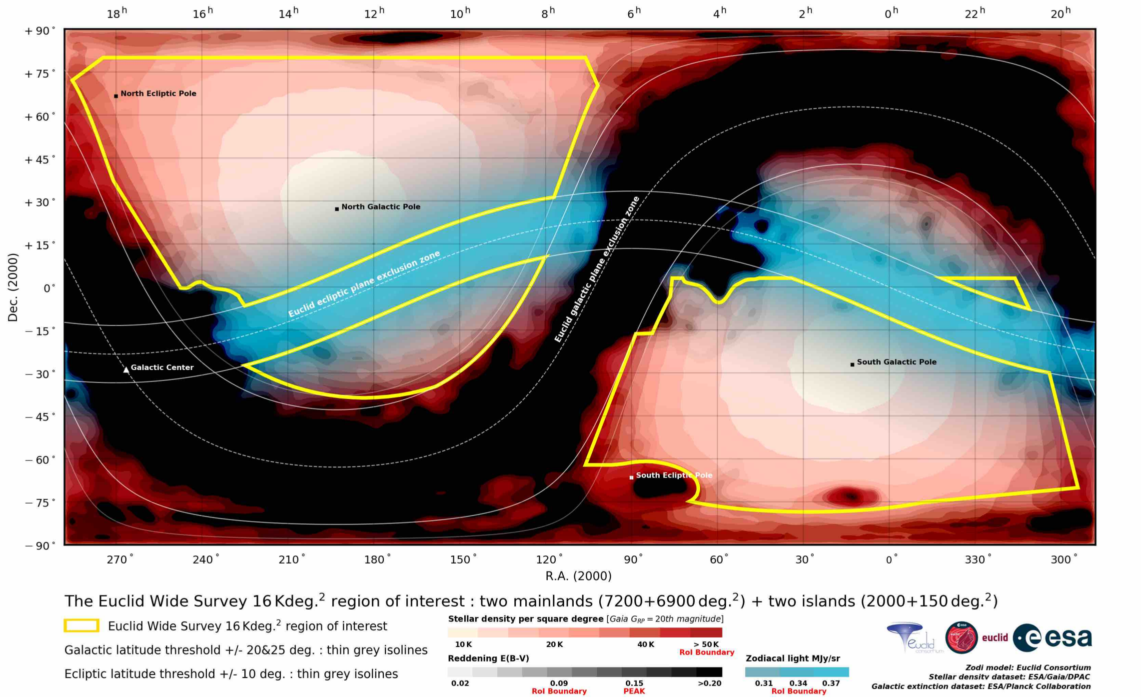

Figure 4.6: RoI in celestial coordinates. It is spread over the four regions within the yellow contours. The main contributions from sky background are shown: zodiacal light, reddening, and stellar density

	Area (deg^2)	**Stellar density** (deg^{-2})	**Reddening** E(B-V)	**Zodiacal light** (MJy/sr)
RoI	16 221	11 600	0.035	0.179
Northern Mainland	7142	9900	0.030	0.168
Northern Island	148	25 900	0.081	0.304
Southern Island	2053	21 900	0.070	0.247
Southern Mainland	6877	10 400	0.032	0.168

Table 4.8: Properties of the RoI and its four quadrants

4.3.2 Signal-to-Noise ratio

S/N 2D maps are computed in [AD01] for the five ROS bands: VIS (I_E band), NISP-Y-J-H (J_E, H_E, Y_E) and NISP-S (RG_E). The computation uses an all-sky map of Galactic dust measurements (Planck data), an all-sky map of the flux model from the Galaxy (Besançon model) to account for out-of-field stray light, and an all-sky map of zodiacal background (the simple model discussed in [AD01]). These maps are computed for the various Euclid bands. The S/N of an extended source (1.3 arc sec diameter aperture) with 24.5 mag observed with 3 stacked ROS VIS exposures is then computed considering all contributions of the instruments and telescope operations (constant across the sky) and the background maps. For NISP-Y-J-H the source used is a point source with 24 mag observed with 3 stacked ROS NISP-P exposures. For NISP-S the source is a H_α line of flux $5\text{x}10^{-16}$ cgs observed with 4 stacked ROS NISP-S exposures. Table 4.9 shows the median S/N for each of the five bands in the RoI and in each of its four regions. The S/N is clearly higher in the mainlands, and much higher in VIS than in NISP.

	RoI	**Northern Mainland**	**Northern Island**	**Southern Island**	**Southern Mainland**
I_E	16.14	16.63	12.47	13.68	16.50
Y_E	6.60	6.75	5.33	5.73	6.71
J_E	7.86	8.05	6.31	6.82	8.00
H_E	7.28	7.46	5.88	6.30	7.41
RG_E	4.53	4.66	3.58	3.88	4.62

Table 4.9: Median values of the S/N in *#version_roi* and its four quadrants, for each of the 5 Euclid bands of the nominal ROS

The S/N values can be used to define a merit function, a single value for each tile of the EWS indicative of the quality of the sky for each of the two core probes of Euclid. The merit function combines the S/N of I_E (VIS; characterizing the quality of the sky for the WL probe) and the S/N of RG_E (NISP-S; characterizing the quality of the sky for the GC probe), and is computed for each tile i as

$$Q\,(i) = \frac{1}{2}\left(\frac{\text{S/N\_VIS (i)} - \text{S/N\_VIS (min)}}{\text{S/N\_VIS (max)} - \text{S/N\_VIS (min)}} + \frac{\text{S/N\_NISPS (i)} - \text{S/N\_NISPS (min)}}{\text{S/N\_NISPS (max)} - \text{S/N\_NISPS (min)}}\right).$$

The two sets of S/N values are normalized by the full range of S/N values in the RoI for a better match of the internal variation wrt each other.

4.3.3 Tessellation

To construct the EWS, the RoI is first tessellated with Euclid tiles (cf. Sect. 4.1.2). In the pre-launch configuration, tiles are placed adjacently on the sky along parallels of latitude with no gaps between them and no overlap at the equator [AD01]. Due to the convergence towards the poles, the number of tiles per row decreases with latitude, and moreover they start to acquire some overlap. The natural overlap of the pre-launch tessellation is around 4%. One ROS observation of the EWS corresponds to placing the VIS and NISP FoVs on one tile of the tessellation.

The presented document is Proprietary information of the Euclid Consortium.
This document shall be used and disclosed by the receiving Party and its related entities (e.g. contractors and subcontractors) only for the purposes of fulfilling the receiving Party's responsibilities under the Euclid Project and that the identified and marked technical data shall not be disclosed or retransferred to any other entity without prior written permission of the document preparer.

The reduced AA range imposed by the stray light issue (cf. Sect. 4.1.1) forces us to observe with the telescope rotated from its natural position, allowing each pointing to place the FoV with a different orientation than the underlying tile. This is the tilting strategy described in Sect. 4.3.4. In *#version_rsd*, the maximum misalignment tolerated between tile and FoV position angles is *#fov_tolerance*.

The misalignment would in general create gaps between the observed FoVs. To avoid this, the tiles are placed closer together than they would be in the case of no tilt. The number of counts at pixel level is analyzed in a 3x3 grid of tiles. The analysis guides us in selecting the distance between the centers of the tiles, such as to be compliant with coverage requirements and avoid zero counts, i.e., gaps. This introduces overlaps between tiles, resulting in an effective reduction of 10% of the tile area to *#fov_tile_effective*. The resulting tessellation has a thus a mean overlap of 14%, which translates in a decrease of survey efficiency.

4.3.4 Visibility windows and tilting strategy

The pre-launch strategy for EWS construction was to observe the Euclid tiles close to transit, applying an AA rotation to off-transit observations in order to always observe aligned with the tessellation tiles. The pre-launch window of visibility available at a given time around the transit meridian is enclosed by the dashed lines in Figure 4.7. The window of visibility informs us of the reach in longitude as function of latitude. The reach corresponds to the longitude range where the range of AA can be used to rotate the FoVs to align them with the tiles. It is not symmetric around the transit meridian because the SAA range is not symmetric around 90 deg. It is wider at low latitudes, where off-transit observations do not rotate much the FoV with respect to the meridians, and hence AA is kept close to zero and the reach is determined by the SAA range. It is narrower at high latitudes, where off-transit observations strongly rotate the FoV, that has to be aligned applying an AA rotation; the reach being thus determined by the narrow AA range.

The reduction and off-setting of the AA range had the double effect of thinning and skewing the window of visibility. The resulting window of visibility no longer contains the transit meridian and has a strongly reduced longitude reach at all latitudes (grey regions in Figure 4.7), including zero reach at the lowest latitudes, where FoVs naturally have AA close to zero and are thus always out of reach. With this reduced reach, it would be impossible to complete the survey.

This critical problem is solved with a tilting strategy. In this strategy, FOVs are allowed to rotate by up to ± *#fov_tolerance* with respect to the tessellation tiles. This means that the reach is no longer determined solely by the AA and SAA ranges, but also by the tilt tolerance. Indeed, as the observing meridian crosses a patch, tiles remain visible for a longer time by applying a combination of AA variation and tilt. This strategy partly recovers the tiles' original visibility (blue regions in Figure 4.7).

Even though the visibility is partially recovered, it has two new features: it barely includes the transit meridian (and hence observations are no longer peaked at SAA = 90 deg), and introduces a leading/trailing asymmetry, in which visibility is longer in one hemisphere and shorter in the other. For observations in the leading side, the visibility is longer in the southern hemisphere (dubbed the *summer season*) and shorter in the northern hemisphere (the *winter season*). For observations in the trailing side the situation is reversed. Let us consider the RoI, containing two mainlands in opposite quadrants of the sky (so in different north-south and east-west hemispheres), and two islands likewise in opposite quadrants. This implies that at any given time there are regions of one of the mainlands and of one of the islands within reach in the leading side, while the other mainland and

The presented document is Proprietary information of the Euclid Consortium.
This document shall be used and disclosed by the receiving Party and its related entities (e.g. contractors and subcontractors) only for the purposes of fulfilling the receiving Party's responsibilities under the Euclid Project and that the identified and marked technical data shall not be disclosed or retransferred to any other entity without prior written permission of the document preparer.

island are reachable in the trailing side. This implies that in a first half of the year the two mainlands are simultaneously in summer season and the two islands are simultaneously in winter season, while in a second half of the year it is winter in the mainlands and summer in the islands.

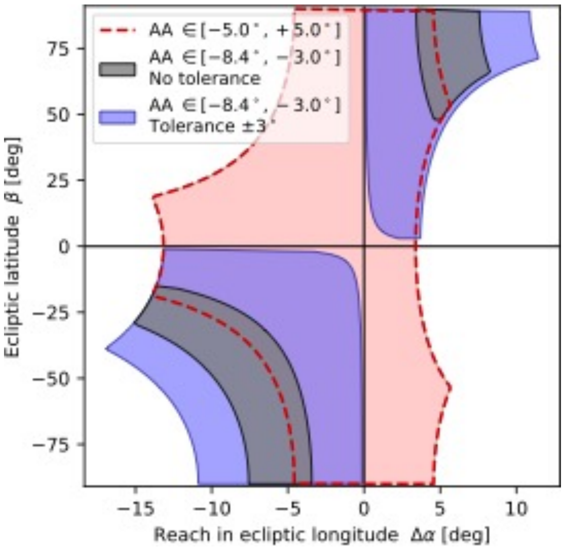

Figure 4.7: Reach in ecliptic longitude around transit for the leading side of the survey, for SAA in [87, 104] deg. The red dashed lines enclose the reach for the originally planned symmetric AA range. The grey regions are the skewed and thinned visibility windows corresponding to the new AA limitations. By allowing the fields to tilt by up to *#fov_tolerance* with respect to the tessellation, a much larger area of the sky becomes accessible (blue regions). For observations in the trailing side, the areas must be rotated by 180 deg around the origin

4.3.5 Bright stars

The basic tessellation of contiguous tiles is modified to deal with bright stars. Stars brighter than 4 AB magnitude in any of the Euclid photometric bands, named *blinding* stars, are damaging to the Euclid detectors. We introduce lateral off-sets in the tiling of latitude rows, opening a gap in the row as described in [AD01], such that no blinding star falls onto the Euclid FoV. In practice, a separation of at least 0.6 deg is left between the star and the center of the neighboring tiles. Since the stars are not necessarily at the same latitude as the center of the rows, the shift usually needs to be applied to more than one row, creating narrow vertical gaps in the tessellation near each star. There are *#stars_allsky* blinding stars in the sky, of which *#stars_roi* are located within the RoI.

Blinding stars brighter than 0 AB magnitude for VIS and -1 AB magnitude for NISP have a strong out-field stray light and may render a full FoV useless if observed to close to it [RD04]. Out of the *#stars_allsky* blinding stars, there are 12 in these conditions, with only 5 of them lying inside the RoI (R Doradus, Arcturus, Tiaki, Canopus, and W Hydrae). We apply larger avoidance radii around these stars, up to 1.7 deg, creating larger gaps in the tessellation. The assigned avoidance radii take into account not only the stars magnitudes but also their proper motions during the survey period, as described in [AD01].

Within the RoI boundaries there are *#starsholes_roi* small holes, corresponding to avoidance areas around the *#stars_roi* blinding stars that occur within the RoI. The number of holes is smaller than the number of stars, since neighboring stars define a single contiguous hole. The full set of holes is shown in Figure 4.8.

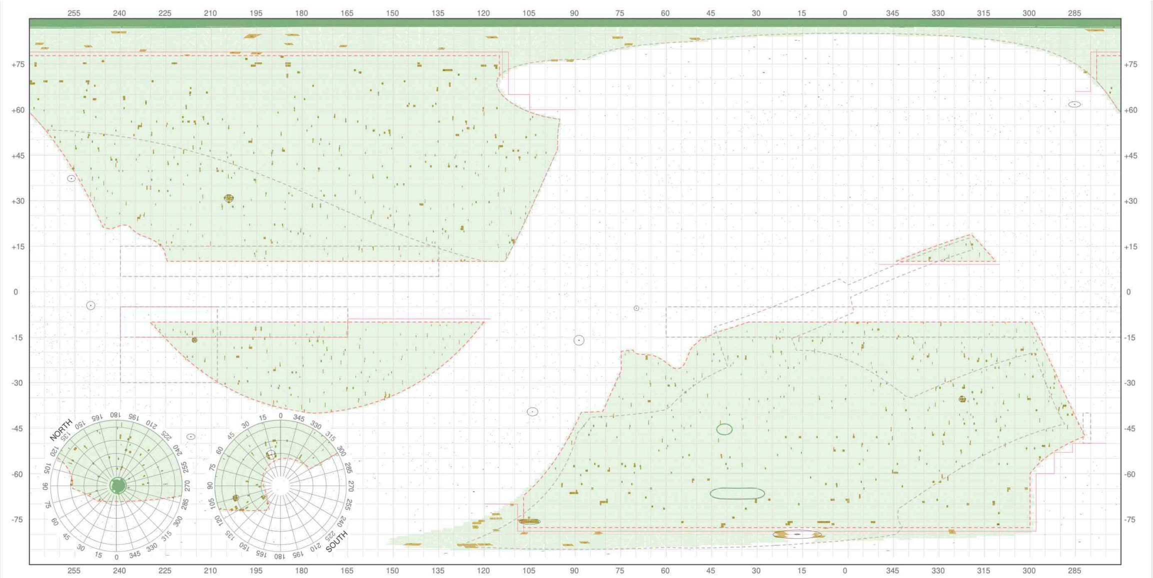

Figure 4.8: RoI in ecliptic coordinates, showing all the blinding stars tessellation gaps (brown areas) and also circular avoidance radius around the brightest stars. DES and UNIONS footprints, respectively in the southern and northern hemisphere are also shown, as are four rectangular masks (cf. Sect. 4.3.7)

4.3.6 Polar caps

At high latitudes, observations on the tessellation have very short visibilities. This was the case even in the pre-launch configuration. Indeed, due to the tessellation convergence at the ecliptic poles, a small depointing from transit would induce a large variation in position angle of the Euclid FoV that could not be compensated by rolling, given the limited AA ranges.

The solution implemented, as described in [AD01], was to introduce local tessellations above and below the latitude of ±*#threshold_polarcap,* i.e. covering the polar caps of the EWS with a certain number of patches. Creating a local tessellation for each patch solved the problem, at the expense of introducing larger overlap between fields on the borders of adjacent patches, which are not aligned. The width of the patches in longitude is determined by the largest size that can hold a fixed tessellation that can be connected with field slews. Moreover, the patches were designed to take up to 5 days to observe, such that each patch can be observed with its fields aligned with the local tiles by using an up to 5 deg variation in AA. Given these considerations, the northern cap was divided in 13 patches and the southern cap in 8 patches; being fewer since most of the area near the SEP is occupied by LMC and is thus outside of the Euclid RoI.

The border longitudes between patches are unconstrained. We choose to center the northern cap patches on longitudes linked to the position angles of CPC-N. In this way it is possible to schedule a polar cap patch back-to-back with a CPC-N observation, thus optimizing the observing plan. The footprints of the polar caps are shown in Figure 4.9, where it is also clear in the southern polar cap that patch tessellations are tailor made to avoid the many blinding stars of the southern cap.

The introduction of the reduced AA range does not allow to compensate the orbital movement during 5-day long observations. One possible solution to the new problem could be to redesign the set of patches, introducing smaller ones. However, introducing more targets would fragment EWS windows, interfering with the EWS scheduling. The alternative was to apply the tilting strategy

The presented document is Proprietary information of the Euclid Consortium.
This document shall be used and disclosed by the receiving Party and its related entities (e.g. contractors and subcontractors) only for the purposes of fulfilling the receiving Party's responsibilities under the Euclid Project and that the identified and marked technical data shall not be disclosed or retransferred to any other entity without prior written permission of the document preparer.

(Sect. 4.3.4) to the polar patches, thus increase their visibilities. By using the same tilting tolerance of *#fov_tolerance*, the visibility increases to 6.5 deg (trailing side), which is enough to schedule them. There are however fewer scheduling opportunities since the visibility on the leading side is only of 1.5 deg, due to the asymmetry of the AA range. With this strategy the set of 21 polar patches shown in Figure 4.9, can still be used. However, this implies that the orientation of each field in a patch is chosen independently and they are no longer aligned.

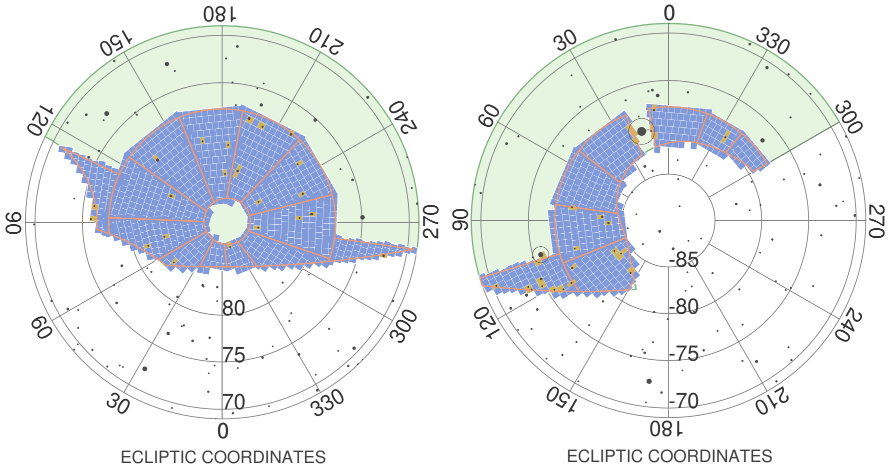

Figure 4.9: Footprint of the EWS northern (left panel) and southern (right panel) polar caps

4.3.7 Masking

The EWS is constructed by observing patches chronologically. Progression is made longitude-wise as the satellite moves in the orbit, and on average from the poles to the ecliptic, such that the higher quality sky is observed first. At a given time step there are several candidate patches, within the trailing and leading visibility regions, competing for the same time slot, and priorities must be set. Some of the priorities are enforced by masking out lower priority regions. The masked regions used in the computation of *#version_rsd* are shown in Figure 4.8.

The DES footprint, (occupying a large part of the southern mainland and the northern island) and the UNIONS footprint (on the northern mainland) are used to prioritize the coverage of areas already known to have ground-based observations available to Euclid. A large, coordinated campaign of ground-based observations with different observatories is in place to provide g-r-i-z photometry to matching depths across the EWS and EDS areas. The progression of the southern hemisphere ground-based coverage is more advanced with the completion of the DES survey (which will be superseded by deeper LSST data from the Rubin Observatory). The northern hemisphere requires dedicated observations provided by the UNIONS survey (including observations with CFHT, Pan-STARRS, Subaru and Javalambre telescopes). During the first #threshold_ext of the mission, EWS gives priority to the DES footprint, creating a north-south asymmetry to ensure sufficient overlap with ground-based coverage for DR1. Later on, priority shifts to the north to achieve an area equilibrium between the two hemispheres.

Later in the scheduling, when lower latitudes are reached, the four rectangular masks visible in in Figure 4.8 start to play a role. The two masks on the southern island favor the selection of mainland versus island patches, avoiding the creation of a disconnected footprint on the southern island and thus promoting a more compact EWS coverage. The rectangular mask below the ecliptic in the southern mainland prevents the creation of an irregular top border in the last patches, easing the scheduling of a potential extension of the mission. Finally, the horizontal mask above the ecliptic in the northern mainland is a planets' avoidance strip. Indeed, during the final year of the mission, when observations reach low latitudes, the longitude range of Mars and Jupiter is masked out to avoid stray light from those planets.

4.3.8 Stress longitudes and unallocated time

Not all longitudes have the same available area for EWS scheduling. This is a combination of two factors. Naturally, some longitudes have more area in the RoI than others by design, but in addition to this, the EDFs, EAFs, and periodic calibrations schedule after stage-one is not uniformly distributed across longitudes. The two effects are shown Figure 4.10, where the time left for EWS scheduling after stage-one is converted into equivalent area at the exchange rate of 10 deg^2 per day.

This results in different levels of EWS scheduling "stress" as function of longitude. We define *high-stress* longitudes as the ones where the blue line is above the red line and *low-stress* longitudes as the ones where the red line is above the blue line.

Ecliptic longitude 220 deg (and its anti-meridian at 40 deg) is a notable high-stress longitude, that not only has a large area in the RoI, but it also contains EDF-F and EDF-S, and also the SXDS and VVDS EAFs. The dip of the red line at those longitudes, seen in Figure 4.10, is an indication that there is not enough time to observe all the RoI for the EWS in these longitudes. In the final year of the survey a choice must be made between the low ecliptic region of the southern mainland (around 40 deg, where VVDS and SXDS are located) and the northern mainland (around 220 deg).

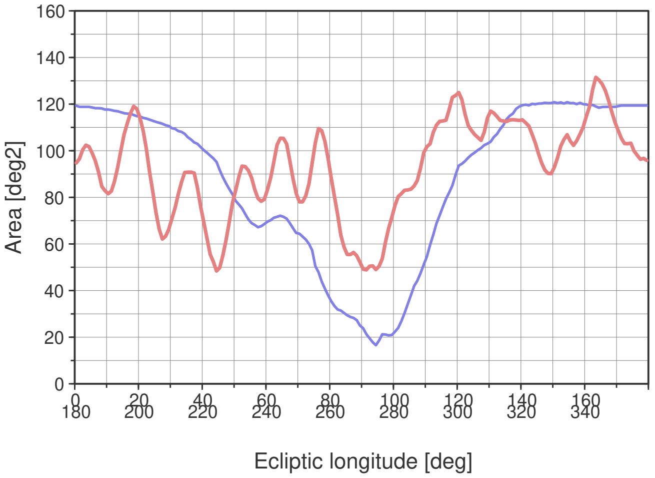

Figure 4.10: Area per longitude (valid for the pre-launch windows of visibility), showing the RoI area per bin of ecliptic longitude (blue line) and the available time for EWS scheduling per bin of ecliptic longitude converted to equivalent area (red line).

Conversely, the dip of the blue line around longitudes 90 and 270 deg is a notable low-stress longitude. It corresponds to the large area of the sky where the Galactic and ecliptic exclusion zones intersect and the RoI area is small. This area is fully scheduled by the EWS in less than the 6 orbits of the nominal mission duration. When the area is exhausted, *#version_rsd* does not reobserve it in subsequent orbits, and since all other non-observed areas are out of reach, no scheduled is done. This leads to the appearance of *unallocated time* in the schedule.

4.3.9 Thermal stability

PSF variations arise from change in focus caused by temperature changes in the PLM due to AA and SAA variations between pointings. The results of a STOP analysis initially showed that the main contributors to temperature changes are variations in AA [RD08]. It is thus important to design the survey to limit the AA variation when filling a patch, and to avoid large jumps in AA when moving from EWS fields to calibration fields.

The strategy of placing tilted FoVs, introduced in ECTile 2.0 to cope with the new AA operational range, is an extra degree of freedom that eased the possibility of observing a whole patch with a constant AA, which was difficult to achieve with ECTile 1.0. The target value of *#solar_aatarget* was chosen in *#version_rsd*.

This is a major change from the pre-launch strategy where AA swept the AA range during an EWS patch observation. Figure 4.11 compares the two strategies by looking at the variation of AA during the scheduling of a patch. In the pre-launch configuration [RD09], FoVs are placed with a steady increase of AA in order to remain aligned with the tessellation as the transit meridian traverses the patch. Point-to-point AA variations can be in excess of 2 deg. In contrast, with the tilting strategy, FoVs are placed with a constant AA value and the FoVs are allowed to tilt within the specified limiting tolerance. If the limit is approached, which may happen at the beginning or end of a patch, the FoVs cannot be further tilted, and AA starts to change. AA point-to-point variations are mostly kept under 1 deg.

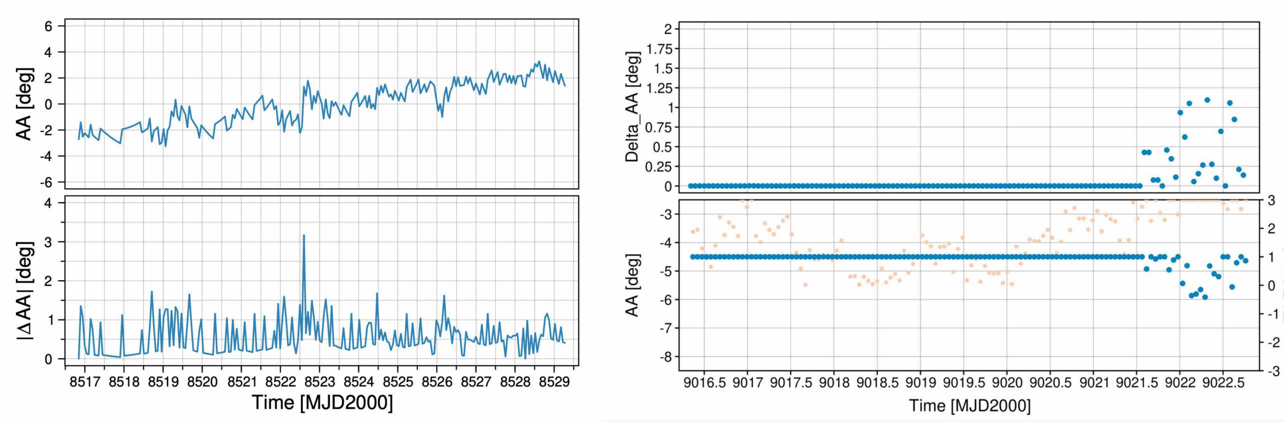

Figure 4.11: AA progression during the observation of a patch. Left panel: Pre-launch configuration. AA (top) and AA field-to-field variation (bottom) Right panel: In-flight configuration. AA field-to-field variation (top) and AA (bottom), also showing the tilt progression (pink dots with corresponding scale on the right side of the bottom righ panel)

However, PDCC data have shown that the PLM temperature has a stronger dependence on SAA than on AA [RD15]; in the new operational AA range, rotated away from the Sun, the impact of SAA gets higher. The computation of an RSD needs to take this into account. When observing the tiles of a typical EWS patch, SAA can remain approximately constant if the patch is traversed at the same speed of the orbital movement. This is possible for patches with a height of approximately 20 tiles. The movement between tiles is also primarily done “upwards/downwards” than “laterally or zigzagging”, which would create jumps in SAA. A typical EWS patch is shown in Figure 4.12, with the angular distance between the transit lines at the start and end of the patch scheduling being close to the width of the patch. This keeps the SAA field-to-field variations typically under 0.5 deg.

We note that even though the field-to-field variations may be limited by design, the new visibility windows (cf. Sect. 4.3.4) force the telescope to operate for longer in a “hot” regime, i.e, there will be a longer tail in the SAA distribution than in pre-launch RSDs.

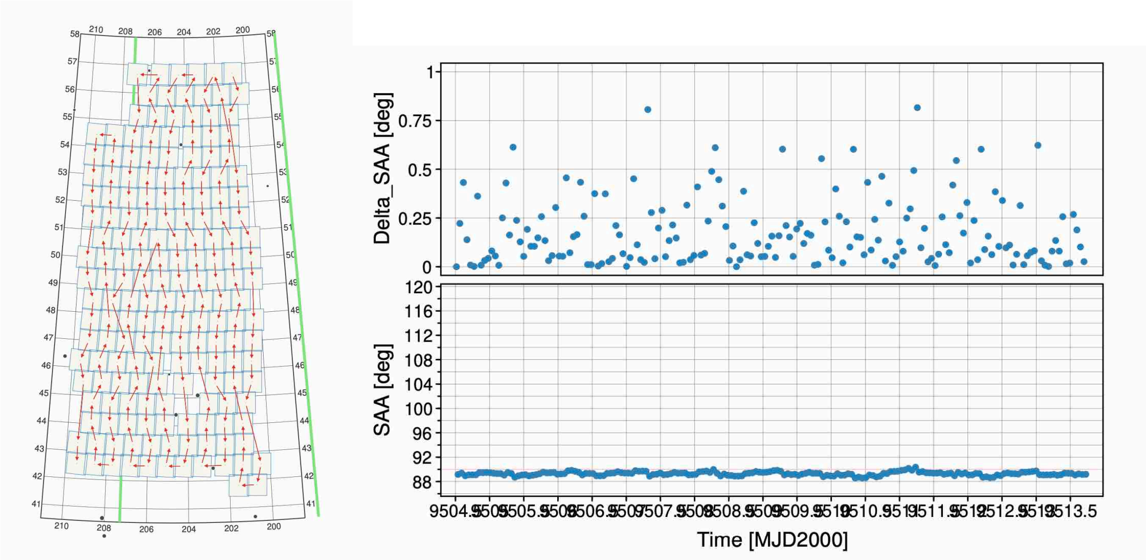

Figure 4.12: SAA progression in a typical EWS patch in the in-flight configuration. Left panel: the vertical green lines show the transit meridians at the beginning and at the end of the observation. Right panel: Progression of SAA field-to-field variation (top) and SAA (bottom)

4.3.10 Smearing pattern

Observations of the deep fields as well as several calibration observations require repeated observations of the same target, either consecutively or over different visits. The centers of the consecutive pointings are slightly offset to improve the quality of stacked images. To avoid clustering of random offsets, we use a set of pointings lying on a spiral computed around a central location, as described in [AD01]. These produce a non-regular, yet fairly uniform distribution. In summary, the pointing in visit i is given in polar coordinates by ($i^{1/2}$ *s, i*g), where g is the golden angle, g = 180 ($3-5^{1/2}$) deg, and s is the scale of the spiral. A spiral of diameter d containing n points has scale s = d / (2 $n^{1/2}$).

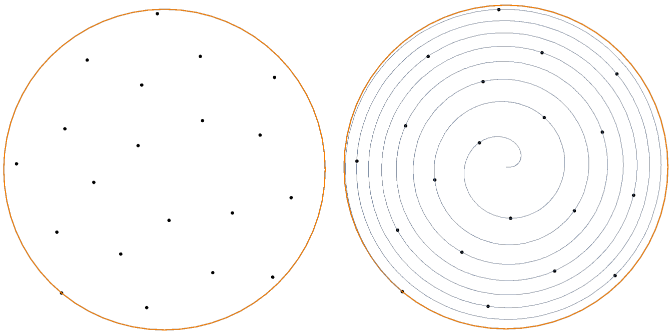

Figure 4.13: Smearing pattern with 20 pointings. The spiral used for the determination of the points is shown in the right panel

The presented document is Proprietary information of the Euclid Consortium.
This document shall be used and disclosed by the receiving Party and its related entities (e.g. contractors and subcontractors) only for the purposes of fulfilling the receiving Party's responsibilities under the Euclid Project and that the identified and marked technical data shall not be disclosed or retransferred to any other entity without prior written permission of the document preparer.

The observations that make use of the smear spiral are F-002, F-004, F-005, F-008, F-009, and F-015, implementing a scale of 6 arcmin. For non-ROS calibrations, the pointings of a given sequence are re-ordered such that the distance between two consecutive pointings is in most cases larger than 73 arcsec. This avoids having long sequences of dither slews, which are forbidden [AD02].

4.3.11 Effective number of visits and zodiacal background

The EDFs and EAFs are observed multiple time to reach the required depths. However, we need to consider that the number of visits needed to reach a certain depth depends on the sky background. In particular, the zodiacal background that in the Euclid wavelength range is caused by scattered sunlight from particles in the zodiacal dust cloud. [AD01] considers several zodiacal light models according to which the background on a given sky position depends on the ecliptic latitude, wavelength, and observing SAA. The background is in general symmetric in ecliptic latitude, increasing by a factor g (|β|) as the latitude decreases.

To compensate for this increase, we consider that the number of ROS visits needed to reach a given S/N value is given by $(S/N)^2$ g(|β|). We use the values from Table 4.10 to determine the number of visits for the EDFs and EAFs observations, regardless of the SAA of the observation.

|β| (deg)	10	15	20	25	30	45	60	75	NEP
g (|β|)	2.92	2.51	2.16	1.91	1.71	1.35	1.12	1.03	1.00

Table 4.10: Zodiacal background amplitude relative to the value at NEP, g, as function of ecliptic latitude β, and for SAA = 90 deg [AD01]

4.3.12 Additional Euclid surveys

It is expected that the Euclid mission will include additional surveys beyond EWS, EDS and the calibration program, in particular making use of any time left unallocated.

RSD_2025A is required to include a reserved timeslot of 28h for the implementation of the first approved additional survey, namely the "Euclid Galactic Bulge Survey" (EGBS) (we note that the reserved timeslot in *#version_rsd* will be given in Table 5.2) The detailed implementation is to be made by SOC in that reserved time. The EGBS is a survey for the purpose of microlensing, and executed with VIS-only. It is a science program driven by the Euclid Consortium scientists although it was motivated by a request of the Roman mission community aimed at obtaining data in advance of Roman's Galactic Bulge Time Domain survey.

4.3.13 Reobservation of lost or skipped fields

A *reobservation* is a new instance of a previously *skipped* or *lost* observation.

Early in the survey the mission executed two decontamination campaigns. Decontamination campaign #1, targeted to folding mirror 3 and mirror 3, lasted 8.3 days. Decontamination campaign #2, around 3 months later, and targeted to folding mirror 3 lasted 5.5 days. All observations scheduled for those periods were skipped. However, as seen in Figure 4.14, the observations skipped for the first

The presented document is Proprietary information of the Euclid Consortium.
This document shall be used and disclosed by the receiving Party and its related entities (e.g. contractors and subcontractors) only for the purposes of fulfilling the receiving Party's responsibilities under the Euclid Project and that the identified and marked technical data shall not be disclosed or retransferred to any other entity without prior written permission of the document preparer.

decontamination campaign were periodic calibrations hence not requiring rescheduling. On the contrary, the observations skipped for decontamination campaign #2 are rescheduled in *#version_rsd*, and consist of the North-cap-06 and eight tiles of the EWS. We note that North-cap-06 had already been rescheduled in *#replan_basis*, hence the new rescheduling does not take additional time with respect to the previous survey. Besides these, *#version_rsd* also reschedules the first six tiles of EWS, which had been skipped at the beginning of the survey, unrelated to the decontaminations.

In the period in-between the two decontaminations the conditions of the system experienced rapid changes and the observations executed in that period were declared lost. It was decided at mission level to repeat them in a major reobservation campaign. The intra-decontamination period lasted for 77 days in the first year of the survey, between MJD2000 8846 and 8923 and #version_rsd schedules the reobservation campaign in the corresponding dates of the second year. The schedule of the intra-decontamination period in the first year of the survey, as well as the original schedule in *#replan_basis* for the equivalent period of the second year, are shown in Figure 4.14. The picture gives an overview of the observations to be rescheduled and of what needs to be displaced to create space for the rescheduling. The monthly block and PSF observations do not need to be repeated, since new executions will be naturally scheduled in the second year. COSMOS and CPC-N-06 were already scheduled for reobservation in *#replan_basis* hence their new rescheduling does not take additional time with respect to the previous survey. We note that COSMOS was rescheduled according to its new strategy (cf. Sect. 4.2.5) with the new observation taking one day less than in #replan_basis. The other reobservations, naturally, take additional time. Besides the reobservation campaign, #rsd_version reschedules other lost observations, as well as the new EGBS.

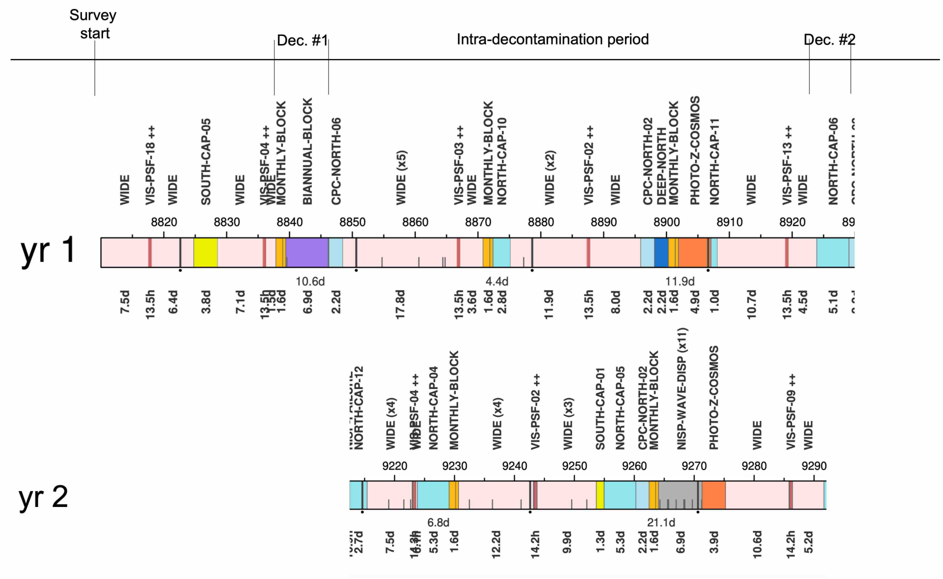

Figure 4.14: #replan-basis schedule. The early part of the first survey year contains the decontamination campaigns and the intra-decontamination period. The second year plan shows the observations to be displaced by the reobservation campaign

Table 4.11 details the EWS area to be reobserved. For non-EWS observations, an EWS equivalent area is computed for the reobservation duration assuming that in *#ros_total* of time, an area of #fov_tile_effective could be covered. We note that for polar caps the equivalent area is larger than the actual area because of the large overlaps. In total, the reobservations produce a potential EWS area loss in *#version_rsd* of around 700 deg^2 with respect to the area quoted in *#replan_basis*.

Campaign	Label	Area (deg^2)	Duration (days)	Equivalent area variation (deg^2)
Reobservation campaign	Survey Window 3	145.0	-	145.0
	Survey Window 4	242.9	-	242.9
	Survey Window 5	139.1	-	139.1
	North-cap-10, 11	28.2	3.8	36.4
	CPC-N-02		2.2	21.2
	EDF-N		2.2	21.2
Reobservations of other lost observations	CPC-N-06		2.2	0
	COSMOS		3.9	-9.8
	CPC-N-01, 07		4.4	42.4
	EDF-N x 2		2.2	42.4
	EWS 13 tiles	8.3	-	8.3
Reobservations of skipped observations	EWS 6 tiles	3.0	-	3.0
	North-cap-06		5.1	0
New observations	EGBS		1.2	11.5
Total EWS Area				**692.1**

Table 4.11: List of reobservations to be scheduled in *#version_rsd*. For each observation it is indicated the EWS equivalent area that it consumes. The total area corresponds to the maximum decrease of EWS area caused by the reobservations, in the extreme case that none of the displaced observations can be rescheduled within the time limit of the survey.

5 Implementation

As described in Sect.3, after defining the inputs the ECTile construction of an RSD starts with the scheduling of the various calibrations and EDFs in stage-one and ends with the computation of the EWS in stage-two.

5.1 Stage-one

Stage-one of the ECTile RSD generation is to schedule the observations of the specific targets. These are the observations defined in the calibration blocks described in Sect. 4.2 (except the VIS PSF calibrations that are scheduled in stage-two together with the EWS) plus the polar caps of the EWS. Most observations are strongly constrained by their limited visibility windows (the exception being the high latitude ones) and by their required cadences. A compliant plan of observations needs to be devised at this stage. This problem does not have a unique solution; indeed, several observing plans can be constructed, all compliant with the requirements. A set of priorities is defined, providing guidelines for an optimal construction. An illustrative strategy is detailed in Sect. 3.2.2. In summary it consists in distributing the observations by their visibility windows, fulfilling targets cadences and priorities, in a sequence as compact as possible. A compact sequence uses fewer large slews and leaves larger contiguous slots of time to be used in stage-two, helping in achieving a spatially compact EWS footprint with a faster progression of EWS area coverage.

The result of stage-one is the intermediate schedule, shown in Figure 5.1. The schedule is presented as a timeline with the duration of *#time_duration* separated in one-year rows, with the MJD2000 date running above the rows. The nominal duration of the RSD is less than the initially planned 6 years, since the first two months of ESOP (the PDCC phase) were removed from the survey duration. The assumed starting date is *#time_startingdate_mjd*, occurring on *#time_startingdate*, and the RSD covers *#time_duration_days* days. The replanned part of the RSD starts on *#replan_restart* with patch *#replan_patch* that occurs in the first planning cycle after *#time_breakpoint.* We note that the breakpoint is always defined by a SOPS, but the first actual restarting date must wait for the completion of the patch contemporary to the SOPS. Before the restart *#version_rsd* is identical to *#replan_basis*, including the original observation IDs and the observations known to have failed.

The times implemented for on-target observations are the precise times specified in the OCF files and not the allocated times defined in [AD03]. The implemented slew times are the precise times computed from the slew time estimator [RD02]. In Figure 5.1 each box of a unique color represents an observing sequence on a target. The labels above the boxes indicate when more than one visit is made consecutively to the same target, while below the boxes the duration of each observation is given. F-017 observations are too short to allow to draw a box and are instead indicated by a red dot. White rectangles show the periods available to observe the EWS after the stage-one observations are scheduled and are known as *survey windows*. Adjacent boxes show that some sequences are scheduled back-to-back, which allows to leave larger contiguous areas for the EWS scheduling, while also saving large slews. The vertical alignment of identical boxes across the years shows that some observations are scheduled at the same time on the various years. When scheduling the targets, enough time must be left for EWS in each year to ensure the fulfilment of the planned data releases. Differently from the other target observations, PSF calibrations are not scheduled at this stage, but on stage-two together with the EWS. This strategy allows for them to be observed with SAA and AA values matching the ones of the contemporary EWS observations, thus optimizing thermal stability, as required. The pink horizontal bars inside the white rectangles mark an interval of time starting *#threshold_thermalization* (the assumed thermal stabilization time) into each wide block, showing the periods when visits to a PSF target can be made. The dots under the rows indicate SOPS windows. Finally, the rulers at the top and bottom of the figure show the ecliptic longitude of the leading and trailing transit meridians (the meridians of SAA=90 deg) as function of time, also indicating the longitude and anti-longitude of the 20 PSF fields. The schedule of each type of targets is detailed in the next sub-sections.

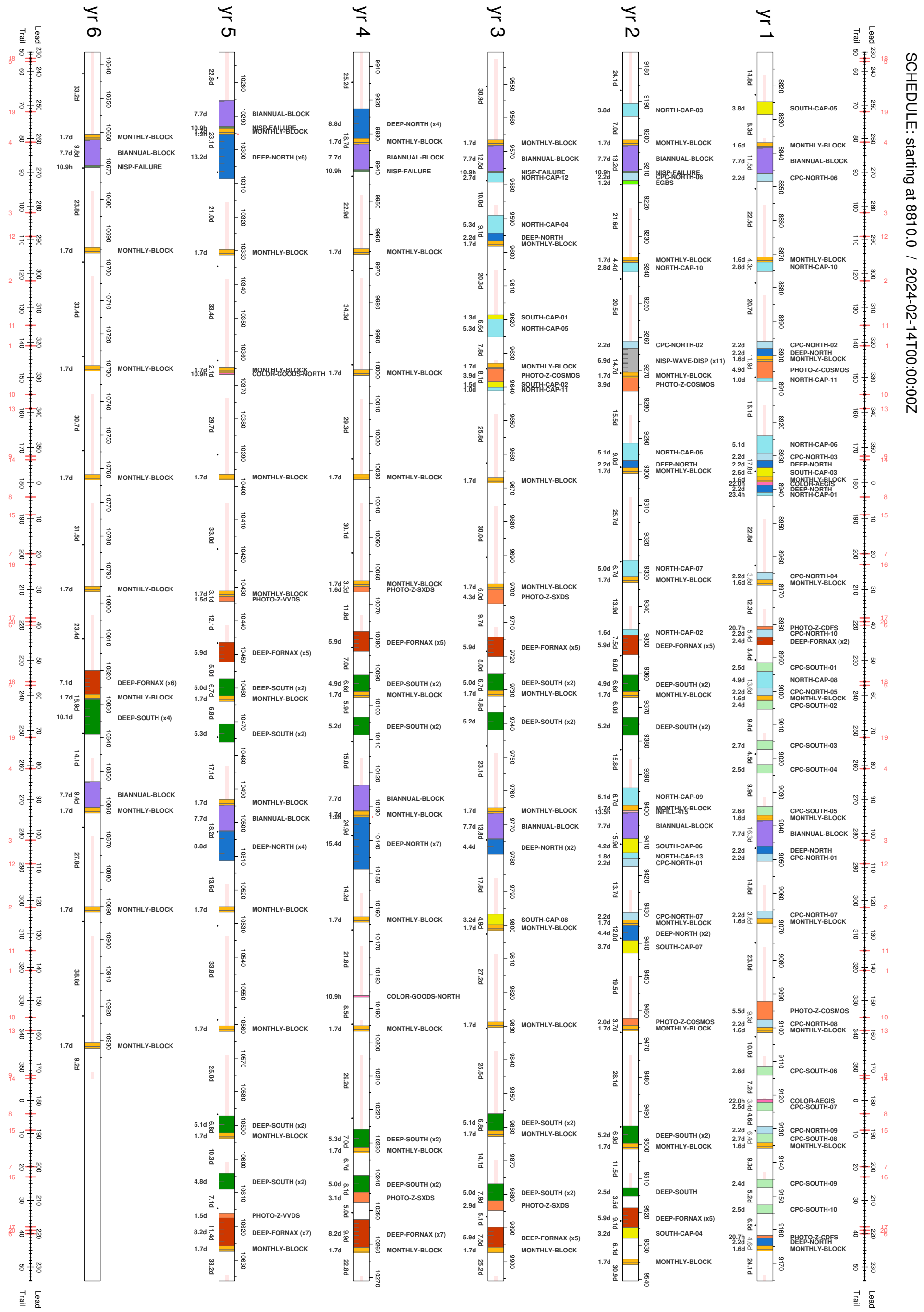

Figure 5.1: Calibration and Deep Fields schedule at the end of stage-one. Each row is one survey year

The presented document is Proprietary information of the Euclid Consortium.
This document shall be used and disclosed by the receiving Party and its related entities (e.g. contractors and subcontractors) only for the purposes of fulfilling the receiving Party's responsibilities under the Euclid Project and that the identified and marked technical data shall not be disclosed or retransferred to any other entity without prior written permission of the document preparer.

5.1.1 Instrument calibrations

A fraction of the observations scheduled in stage-one has the goal of obtaining data for calibration products. They implement the sequences defined in the calibration blocks F-001 (selfcal-variant), F-007 (VIS-non-lin), F-009 (NISP-non-lin), F-010 (NISP-wave-disp), F-011 (NISP-failure), F-012 (VIS-flatband), F-016 (VIS-charge-injection) and F-018 (NISP-persistence). The schedule of these observations in *#version_rsd* is given in Table 5.1.

Calblock	Label	Start (MJD 2000)	Duration (days)	Year
[1]CALBLOCK-F-001	SELFCAL-v1	8837.825	1.091308	0.0762
[1]CALBLOCK-F-007	VIS-NON-LIN	8838.919	0.493056	0.0792
[1]CALBLOCK-F-009	NISP-NON-LIN	8839.414	0.166088	0.0805
[1]CALBLOCK-F-009	NISP-NON-LIN	8839.582	6.568692	0.0810
[1]CALBLOCK-F-016	VIS-CHARGE-INJECTION	8846.154	0.117211	0.0990
[2]CALBLOCK-F-001	SELFCAL-v2	8870.803	1.090729	0.1665
CALBLOCK-F-007	VIS-NON-LIN	8871.897	0.493056	0.1695
[3]CALBLOCK-F-001	SELFCAL-v3	8900.307	1.090231	0.2472
CALBLOCK-F-007	VIS-NON-LIN	8901.400	0.493056	0.2502
CALBLOCK-F-001	SELFCAL-v4	8936.391	1.090694	0.3460
CALBLOCK-F-007	VIS-NON-LIN	8937.484	0.493056	0.3490
CALBLOCK-F-001	SELFCAL-v1	8966.879	1.091505	0.4295
CALBLOCK-F-007	VIS-NON-LIN	8967.974	0.486690	0.4325
CALBLOCK-F-001	SELFCAL-v2	9001.206	1.090914	0.5235
CALBLOCK-F-007	VIS-NON-LIN	9002.300	0.486690	0.5265
CALBLOCK-F-001	SELFCAL-v3	9037.575	1.090382	0.6231
CALBLOCK-F-007	VIS-NON-LIN	9038.668	0.487847	0.6261
CALBLOCK-F-009	NISP-NON-LIN	9039.158	0.166088	0.6274
CALBLOCK-F-009	NISP-NON-LIN	9039.326	6.568692	0.6279
CALBLOCK-F-016	VIS-CHARGE-INJECTION	9045.898	0.122419	0.6459
CALBLOCK-F-001	SELFCAL-v4	9067.470	1.090868	0.7049
CALBLOCK-F-007	VIS-NON-LIN	9068.563	0.487847	0.7079
CALBLOCK-F-001	SELFCAL-v1	9100.287	1.091481	0.7948
CALBLOCK-F-007	VIS-NON-LIN	9101.381	0.466262	0.7978
CALBLOCK-F-001	SELFCAL-v2	9134.363	1.090880	0.8881
CALBLOCK-F-007	VIS-NON-LIN	9135.457	0.467419	0.8911

The presented document is Proprietary information of the Euclid Consortium.
This document shall be used and disclosed by the receiving Party and its related entities (e.g. contractors and subcontractors) only for the purposes of fulfilling the receiving Party's responsibilities under the Euclid Project and that the identified and marked technical data shall not be disclosed or retransferred to any other entity without prior written permission of the document preparer.

CALBLOCK-F-001	SELFCAL-v3	9164.401	1.090382	0.9703
CALBLOCK-F-007	VIS-NON-LIN	9165.495	0.467419	0.9733
CALBLOCK-F-001	SELFCAL-v4	9201.268	1.090868	1.0712
CALBLOCK-F-018	NISP-PERSISTENCE	9202.362	0.098553	1.0742
CALBLOCK-F-007	VIS-NON-LIN	9202.462	0.467419	1.0745
CALBLOCK-F-009	NISP-NON-LIN	9202.932	0.166088	1.0758
CALBLOCK-F-009	NISP-NON-LIN	9203.100	7.433275	1.0762
CALBLOCK-F-016	VIS-CHARGE-INJECTION	9210.536	0.122419	1.0966
CALBLOCK-F-011	NISP-FAILURE	9210.661	0.455671	1.0969
CALBLOCK-F-001	SELFCAL-v1	9236.365	1.091481	1.1673
CALBLOCK-F-018	NISP-PERSISTENCE	9237.460	0.098553	1.1703
CALBLOCK-F-007	VIS-NON-LIN	9237.560	0.466262	1.1706
CALBLOCK-F-010	NISP-WAVE-DISP	9263.843	0.221516	1.2426
CALBLOCK-F-010	NISP-WAVE-DISP	9264.066	1.266227	1.2432
CALBLOCK-F-010	NISP-WAVE-DISP	9265.354	0.070613	1.2467
CALBLOCK-F-010	NISP-WAVE-DISP	9265.427	0.070613	1.2469
CALBLOCK-F-010	NISP-WAVE-DISP	9265.519	1.266227	1.2471
CALBLOCK-F-010	NISP-WAVE-DISP	9266.788	1.266227	1.2506
CALBLOCK-F-010	NISP-WAVE-DISP	9268.075	0.070613	1.2541
CALBLOCK-F-010	NISP-WAVE-DISP	9268.148	0.070613	1.2543
CALBLOCK-F-010	NISP-WAVE-DISP	9268.240	1.266227	1.2546
CALBLOCK-F-010	NISP-WAVE-DISP	9269.509	1.266273	1.2581
CALBLOCK-F-010	NISP-WAVE-DISP	9270.797	0.073171	1.2616
CALBLOCK-F-001	SELFCAL-v2	9271.125	1.090914	1.2625
CALBLOCK-F-018	NISP-PERSISTENCE	9272.218	0.098553	1.2655
CALBLOCK-F-007	VIS-NON-LIN	9272.319	0.466262	1.2658
CALBLOCK-F-001	SELFCAL-v3	9299.120	1.090394	1.3391
CALBLOCK-F-018	NISP-PERSISTENCE	9300.214	0.098553	1.3421
CALBLOCK-F-007	VIS-NON-LIN	9300.314	0.465104	1.3424
CALBLOCK-F-001	SELFCAL-v4	9332.112	1.090891	1.4295
CALBLOCK-F-018	NISP-PERSISTENCE	9333.206	0.098553	1.4325
CALBLOCK-F-007	VIS-NON-LIN	9333.306	0.465104	1.4327
CALBLOCK-F-001	SELFCAL-v1	9365.315	1.091493	1.5204

CALBLOCK-F-018	NISP-PERSISTENCE	9366.409	0.098553	1.5234
CALBLOCK-F-007	VIS-NON-LIN	9366.510	0.465104	1.5236
CALBLOCK-F-001	SELFCAL-v2	9398.742	1.090903	1.6119
CALBLOCK-F-018	NISP-PERSISTENCE	9399.835	0.098553	1.6149
CALBLOCK-F-007	VIS-NON-LIN	9399.936	0.466262	1.6152
CALBLOCK-F-009	NISP-NON-LIN	9401.011	0.166088	1.6181
CALBLOCK-F-009	NISP-NON-LIN	9401.179	7.433275	1.6186
CALBLOCK-F-016	VIS-CHARGE-INJECTION	9408.616	0.122419	1.6389
CALBLOCK-F-001	SELFCAL-v3	9433.245	1.090382	1.7063
CALBLOCK-F-018	NISP-PERSISTENCE	9434.338	0.098553	1.7093
CALBLOCK-F-007	VIS-NON-LIN	9434.438	0.467419	1.7096
CALBLOCK-F-001	SELFCAL-v4	9464.644	1.090856	1.7923
CALBLOCK-F-018	NISP-PERSISTENCE	9465.738	0.098553	1.7953
CALBLOCK-F-007	VIS-NON-LIN	9465.839	0.466262	1.7956
CALBLOCK-F-001	SELFCAL-v1	9499.791	1.091470	1.8885
CALBLOCK-F-018	NISP-PERSISTENCE	9500.885	0.098553	1.8915
CALBLOCK-F-007	VIS-NON-LIN	9500.986	0.467419	1.8918
CALBLOCK-F-001	SELFCAL-v2	9533.886	1.090880	1.9819
CALBLOCK-F-018	NISP-PERSISTENCE	9534.980	0.098553	1.9849
CALBLOCK-F-007	VIS-NON-LIN	9535.080	0.467419	1.9852
CALBLOCK-F-001	SELFCAL-v3	9566.573	1.090382	2.0714
CALBLOCK-F-018	NISP-PERSISTENCE	9567.666	0.098553	2.0744
CALBLOCK-F-007	VIS-NON-LIN	9567.767	0.467419	2.0747
CALBLOCK-F-009	NISP-NON-LIN	9568.236	0.166088	2.0759
CALBLOCK-F-009	NISP-NON-LIN	9568.404	7.433275	2.0764
CALBLOCK-F-016	VIS-CHARGE-INJECTION	9575.840	0.122419	2.0968
CALBLOCK-F-011	NISP-FAILURE	9575.966	0.455671	2.0971
CALBLOCK-F-001	SELFCAL-v4	9596.628	1.090868	2.1537
CALBLOCK-F-018	NISP-PERSISTENCE	9597.722	0.098553	2.1567
CALBLOCK-F-007	VIS-NON-LIN	9597.822	0.467419	2.1569
CALBLOCK-F-001	SELFCAL-v1	9632.670	1.091493	2.2523
CALBLOCK-F-018	NISP-PERSISTENCE	9633.765	0.098553	2.2553
CALBLOCK-F-007	VIS-NON-LIN	9633.865	0.465104	2.2556

The presented document is Proprietary information of the Euclid Consortium.
This document shall be used and disclosed by the receiving Party and its related entities (e.g. contractors and subcontractors) only for the purposes of fulfilling the receiving Party's responsibilities under the Euclid Project and that the identified and marked technical data shall not be disclosed or retransferred to any other entity without prior written permission of the document preparer.

CALBLOCK-F-001	SELFCAL-v2	9667.001	1.090903	2.3463
CALBLOCK-F-018	NISP-PERSISTENCE	9668.095	0.098553	2.3493
CALBLOCK-F-007	VIS-NON-LIN	9668.195	0.465104	2.3496
CALBLOCK-F-001	SELFCAL-v3	9698.642	1.090394	2.4330
CALBLOCK-F-018	NISP-PERSISTENCE	9699.736	0.098553	2.4360
CALBLOCK-F-007	VIS-NON-LIN	9699.836	0.465104	2.4362
CALBLOCK-F-001	SELFCAL-v4	9730.153	1.090880	2.5192
CALBLOCK-F-018	NISP-PERSISTENCE	9731.246	0.098553	2.5222
CALBLOCK-F-007	VIS-NON-LIN	9731.347	0.465104	2.5225
CALBLOCK-F-001	SELFCAL-v1	9765.142	1.091481	2.6150
CALBLOCK-F-018	NISP-PERSISTENCE	9766.237	0.098553	2.6180
CALBLOCK-F-007	VIS-NON-LIN	9766.337	0.465104	2.6183
CALBLOCK-F-009	NISP-NON-LIN	9766.804	0.166088	2.6196
CALBLOCK-F-009	NISP-NON-LIN	9766.972	7.433275	2.6200
CALBLOCK-F-016	VIS-CHARGE-INJECTION	9774.409	0.125428	2.6404
CALBLOCK-F-001	SELFCAL-v2	9800.006	1.090880	2.7105
CALBLOCK-F-018	NISP-PERSISTENCE	9801.100	0.098553	2.7135
CALBLOCK-F-007	VIS-NON-LIN	9801.200	0.467419	2.7138
CALBLOCK-F-001	SELFCAL-v3	9828.835	1.090359	2.7894
CALBLOCK-F-018	NISP-PERSISTENCE	9829.928	0.098553	2.7924
CALBLOCK-F-007	VIS-NON-LIN	9830.029	0.468854	2.7927
CALBLOCK-F-001	SELFCAL-v4	9860.991	1.090856	2.8775
CALBLOCK-F-018	NISP-PERSISTENCE	9862.084	0.098553	2.8804
CALBLOCK-F-007	VIS-NON-LIN	9862.185	0.466262	2.8807
CALBLOCK-F-001	SELFCAL-v1	9895.661	1.091481	2.9724
CALBLOCK-F-018	NISP-PERSISTENCE	9896.755	0.098553	2.9754
CALBLOCK-F-007	VIS-NON-LIN	9896.856	0.467419	2.9756
CALBLOCK-F-001	SELFCAL-v2	9931.433	1.090891	3.0703
CALBLOCK-F-018	NISP-PERSISTENCE	9932.526	0.098553	3.0733
CALBLOCK-F-007	VIS-NON-LIN	9932.627	0.467419	3.0736
CALBLOCK-F-009	NISP-NON-LIN	9933.096	0.166088	3.0749
CALBLOCK-F-009	NISP-NON-LIN	9933.264	7.433275	3.0753
CALBLOCK-F-016	VIS-CHARGE-INJECTION	9940.701	0.122419	3.0957

CALBLOCK-F-011	NISP-FAILURE	9940.826	0.455671	3.0960
CALBLOCK-F-001	SELFCAL-v3	9964.239	1.090382	3.1601
CALBLOCK-F-018	NISP-PERSISTENCE	9965.332	0.098553	3.1631
CALBLOCK-F-007	VIS-NON-LIN	9965.433	0.466262	3.1634
CALBLOCK-F-001	SELFCAL-v4	10000.290	1.090891	3.2588
CALBLOCK-F-018	NISP-PERSISTENCE	10001.384	0.098553	3.2618
CALBLOCK-F-007	VIS-NON-LIN	10001.485	0.465104	3.2621
CALBLOCK-F-001	SELFCAL-v1	10031.231	1.091505	3.3435
CALBLOCK-F-018	NISP-PERSISTENCE	10032.325	0.098553	3.3465
CALBLOCK-F-007	VIS-NON-LIN	10032.426	0.465104	3.3468
CALBLOCK-F-001	SELFCAL-v2	10062.999	1.090914	3.4305
CALBLOCK-F-018	NISP-PERSISTENCE	10064.093	0.098553	3.4335
CALBLOCK-F-007	VIS-NON-LIN	10064.193	0.465104	3.4338
CALBLOCK-F-001	SELFCAL-v3	10095.749	1.090382	3.5202
CALBLOCK-F-018	NISP-PERSISTENCE	10096.842	0.098553	3.5232
CALBLOCK-F-007	VIS-NON-LIN	10096.943	0.465104	3.5235
CALBLOCK-F-009	NISP-NON-LIN	10122.336	0.166088	3.5930
CALBLOCK-F-009	NISP-NON-LIN	10122.504	7.433275	3.5934
CALBLOCK-F-016	VIS-CHARGE-INJECTION	10129.941	0.122419	3.6138
CALBLOCK-F-001	SELFCAL-v4	10130.066	1.090868	3.6141
CALBLOCK-F-018	NISP-PERSISTENCE	10131.160	0.098553	3.6171
CALBLOCK-F-007	VIS-NON-LIN	10131.260	0.466262	3.6174
CALBLOCK-F-001	SELFCAL-v1	10162.749	1.091481	3.7036
CALBLOCK-F-018	NISP-PERSISTENCE	10163.843	0.098553	3.7066
CALBLOCK-F-007	VIS-NON-LIN	10163.944	0.466262	3.7069
CALBLOCK-F-001	SELFCAL-v2	10195.498	1.090880	3.7933
CALBLOCK-F-018	NISP-PERSISTENCE	10196.592	0.098553	3.7963
CALBLOCK-F-007	VIS-NON-LIN	10196.692	0.467419	3.7966
CALBLOCK-F-001	SELFCAL-v3	10231.316	1.090359	3.8913
CALBLOCK-F-018	NISP-PERSISTENCE	10232.409	0.098553	3.8943
CALBLOCK-F-007	VIS-NON-LIN	10232.510	0.466262	3.8946
CALBLOCK-F-001	SELFCAL-v4	10260.797	1.090856	3.9721
CALBLOCK-F-018	NISP-PERSISTENCE	10261.891	0.098553	3.9751

The presented document is Proprietary information of the Euclid Consortium.
This document shall be used and disclosed by the receiving Party and its related entities (e.g. contractors and subcontractors) only for the purposes of fulfilling the receiving Party's responsibilities under the Euclid Project and that the identified and marked technical data shall not be disclosed or retransferred to any other entity without prior written permission of the document preparer.

CALBLOCK-F-007	VIS-NON-LIN	10261.992	0.467419	3.9753
CALBLOCK-F-009	NISP-NON-LIN	10283.728	0.166088	4.0348
CALBLOCK-F-009	NISP-NON-LIN	10283.896	7.433275	4.0353
CALBLOCK-F-016	VIS-CHARGE-INJECTION	10291.332	0.122419	4.0557
CALBLOCK-F-011	NISP-FAILURE	10291.458	0.455671	4.0560
CALBLOCK-F-001	SELFCAL-v1	10291.916	1.091481	4.0573
CALBLOCK-F-018	NISP-PERSISTENCE	10293.010	0.098553	4.0603
CALBLOCK-F-007	VIS-NON-LIN	10293.111	0.467419	4.0605
CALBLOCK-F-001	SELFCAL-v2	10329.702	1.090903	4.1607
CALBLOCK-F-018	NISP-PERSISTENCE	10330.795	0.098553	4.1637
CALBLOCK-F-007	VIS-NON-LIN	10330.896	0.465104	4.1640
CALBLOCK-F-001	SELFCAL-v3	10364.756	1.090394	4.2567
CALBLOCK-F-018	NISP-PERSISTENCE	10365.849	0.098553	4.2597
CALBLOCK-F-007	VIS-NON-LIN	10365.950	0.466262	4.2600
CALBLOCK-F-001	SELFCAL-v4	10396.560	1.090891	4.3438
CALBLOCK-F-018	NISP-PERSISTENCE	10397.653	0.098553	4.3468
CALBLOCK-F-007	VIS-NON-LIN	10397.754	0.465104	4.3470
CALBLOCK-F-001	SELFCAL-v1	10431.224	1.091505	4.4387
CALBLOCK-F-018	NISP-PERSISTENCE	10432.318	0.098553	4.4417
CALBLOCK-F-007	VIS-NON-LIN	10432.419	0.465104	4.4419
CALBLOCK-F-001	SELFCAL-v2	10462.267	1.090903	4.5237
CALBLOCK-F-018	NISP-PERSISTENCE	10463.361	0.098553	4.5267
CALBLOCK-F-007	VIS-NON-LIN	10463.461	0.465104	4.5269
CALBLOCK-F-001	SELFCAL-v3	10493.107	1.090394	4.6081
CALBLOCK-F-018	NISP-PERSISTENCE	10494.200	0.098553	4.6111
CALBLOCK-F-007	VIS-NON-LIN	10494.300	0.465104	4.6114
CALBLOCK-F-009	NISP-NON-LIN	10494.768	0.166088	4.6126
CALBLOCK-F-009	NISP-NON-LIN	10494.936	7.433275	4.6131
CALBLOCK-F-016	VIS-CHARGE-INJECTION	10502.372	0.125428	4.6335
CALBLOCK-F-001	SELFCAL-v4	10524.926	1.090868	4.6952
CALBLOCK-F-018	NISP-PERSISTENCE	10526.020	0.098553	4.6982
CALBLOCK-F-007	VIS-NON-LIN	10526.120	0.466262	4.6985
CALBLOCK-F-001	SELFCAL-v1	10560.481	1.091481	4.7926

CALBLOCK-F-018	NISP-PERSISTENCE	10561.575	0.098553	4.7956
CALBLOCK-F-007	VIS-NON-LIN	10561.676	0.466262	4.7958
CALBLOCK-F-001	SELFCAL-v2	10592.634	1.090880	4.8806
CALBLOCK-F-018	NISP-PERSISTENCE	10593.728	0.098553	4.8836
CALBLOCK-F-007	VIS-NON-LIN	10593.828	0.466262	4.8839
CALBLOCK-F-001	SELFCAL-v3	10625.713	1.090359	4.9711
CALBLOCK-F-018	NISP-PERSISTENCE	10626.806	0.098553	4.9741
CALBLOCK-F-007	VIS-NON-LIN	10626.906	0.467419	4.9744
CALBLOCK-F-001	SELFCAL-v4	10660.617	1.090868	5.0667
CALBLOCK-F-018	NISP-PERSISTENCE	10661.710	0.098553	5.0697
CALBLOCK-F-007	VIS-NON-LIN	10661.811	0.467419	5.0700
CALBLOCK-F-009	NISP-NON-LIN	10662.281	0.166088	5.0713
CALBLOCK-F-009	NISP-NON-LIN	10662.449	7.433275	5.0717
CALBLOCK-F-016	VIS-CHARGE-INJECTION	10669.885	0.122419	5.0921
CALBLOCK-F-011	NISP-FAILURE	10670.010	0.458252	5.0924
CALBLOCK-F-001	SELFCAL-v1	10694.269	1.091493	5.1588
CALBLOCK-F-018	NISP-PERSISTENCE	10695.363	0.098553	5.1618
CALBLOCK-F-007	VIS-NON-LIN	10695.463	0.466262	5.1621
CALBLOCK-F-001	SELFCAL-v2	10729.476	1.090903	5.2552
CALBLOCK-F-018	NISP-PERSISTENCE	10730.570	0.098553	5.2582
CALBLOCK-F-007	VIS-NON-LIN	10730.670	0.465104	5.2585
CALBLOCK-F-001	SELFCAL-v3	10761.843	1.090394	5.3439
CALBLOCK-F-018	NISP-PERSISTENCE	10762.936	0.098553	5.3468
CALBLOCK-F-007	VIS-NON-LIN	10763.036	0.465104	5.3471
CALBLOCK-F-001	SELFCAL-v4	10794.981	1.090891	5.4346
CALBLOCK-F-018	NISP-PERSISTENCE	10796.075	0.098553	5.4376
CALBLOCK-F-007	VIS-NON-LIN	10796.175	0.465104	5.4379
CALBLOCK-F-001	SELFCAL-v1	10827.144	1.091493	5.5226
CALBLOCK-F-018	NISP-PERSISTENCE	10828.238	0.098553	5.5256
CALBLOCK-F-007	VIS-NON-LIN	10828.338	0.465104	5.5259
CALBLOCK-F-009	NISP-NON-LIN	10853.012	0.166088	5.5935
CALBLOCK-F-009	NISP-NON-LIN	10853.180	7.433275	5.5939
CALBLOCK-F-016	VIS-CHARGE-INJECTION	10860.616	0.122419	5.6143

The presented document is Proprietary information of the Euclid Consortium.
This document shall be used and disclosed by the receiving Party and its related entities (e.g. contractors and subcontractors) only for the purposes of fulfilling the receiving Party's responsibilities under the Euclid Project and that the identified and marked technical data shall not be disclosed or retransferred to any other entity without prior written permission of the document preparer.

CALBLOCK-F-001	SELFCAL-v2	10860.742	1.090903	5.6146
CALBLOCK-F-018	NISP-PERSISTENCE	10861.836	0.098553	5.6176
CALBLOCK-F-007	VIS-NON-LIN	10861.936	0.465104	5.6179
CALBLOCK-F-001	SELFCAL-v3	10890.167	1.090382	5.6952
CALBLOCK-F-018	NISP-PERSISTENCE	10891.260	0.098553	5.6982
CALBLOCK-F-007	VIS-NON-LIN	10891.360	0.467419	5.6985
CALBLOCK-F-001	SELFCAL-v4	10930.730	1.090856	5.8062
CALBLOCK-F-018	NISP-PERSISTENCE	10931.823	0.098553	5.8092
CALBLOCK-F-007	VIS-NON-LIN	10931.924	0.466262	5.8095

Table 5.1: Schedule of the instrument calibrations, with the period prior to the restart date shaded in grey. Notes on faulty observations: 1. cancelled by the first decontamination campaign; 2. scheduled with a wrong BGS separation; 3. unusable. The faulty instances do not need to be compensated by additional visits, since they are part of periodic observations and will be revisited anyway [AD03].

F-001, F-018 and F-007 are always scheduled back-to-back, in the same order, forming a monthly block; there are 64 monthly blocks scheduled, keeping an average cadence of 11 visits per year. F-018 was introduced in *#version_rsd* and is thus only part of the schedule after *#replan_restart,* being present in the last 53 monthly blocks. Figure 5.2 shows the histogram of the cadence of monthly blocks, which is within the required range of [25, 40] days, with one outlier at 40.5 days.

The two sequences of F-009 are scheduled together with F-016 twice a year, forming a biannual block. This block is always scheduled immediately after or before a monthly block; they are scheduled 12 times.

F-011, with a yearly cadence, is always scheduled back-to-back with the first biannual block of the year; it is scheduled 5 times, starting in the second year.

F-010 is scheduled on the preferred target (SMC-SMP-20) three months into the second year.

Finally, non-ROS observations are never interrupted by a SOPS. SOPS windows always occur during ROS observations or at the end of a non-ROS sequence.

All these considerations produce a compact schedule of the instrument calibrations that is compliant with CalF specifications, as detailed in Sect. 7.3.

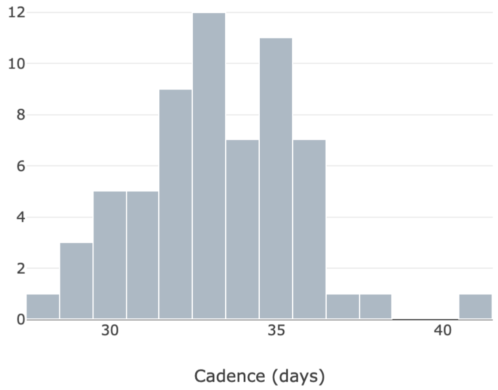

Figure 5.2: Histogram of the cadence of the monthly calibrations

The presented document is Proprietary information of the Euclid Consortium.
This document shall be used and disclosed by the receiving Party and its related entities (e.g. contractors and subcontractors) only for the purposes of fulfilling the receiving Party's responsibilities under the Euclid Project and that the identified and marked technical data shall not be disclosed or retransferred to any other entity without prior written permission of the document preparer.

5.1.2 Auxiliary fields

Another fraction of the observations scheduled in stage-one has the goal of obtaining data for sample characterization. The observations required by F-004 (color gradients) and F-005 (photo-z) are acquired in the Euclid Auxiliary fields, while the observations required by F-002 (noise bias) and F-003 (CPC) are acquired in the Euclid Deep fields.

The schedule of the EAFs observations in *#version_rsd* is given in Table 5.2. The EGBS is also included in the EAFs table (cf. Sect. 4.3.12). We note there is a visit to COSMOS that ends with a blue grism pointing and is immediately followed by an F-001 observation (cf. discussion in Sect. 5.1.3).

Calblock	Label	Start (MJD2000)	Duration (days)	Year
[1]CALBLOCK-F-005	PHOTO-Z-COSMOS	8901.909	4.909641	0.2516
CALBLOCK-F-004	COLOR-AEGIS	8937.984	0.917373	0.3504
CALBLOCK-F-005	PHOTO-Z-CDFS	8980.766	0.862396	0.4675
CALBLOCK-F-005	PHOTO-Z-COSMOS	9092.526	5.537095	0.7735
CALBLOCK-F-004	COLOR-AEGIS	9121.089	0.917245	0.8517
CALBLOCK-F-005	PHOTO-Z-CDFS	9161.312	0.862384	0.9618
RESERVED	EGBS	9213.328	1.169259	1.1043
[2]CALBLOCK-F-005	PHOTO-Z-COSMOS	9272.801	3.895671	1.2671
[3]CALBLOCK-F-005	PHOTO-Z-COSMOS	9462.580	2.049178	1.7867
CALBLOCK-F-005	PHOTO-Z-COSMOS	9634.346	3.903461	2.2569
CALBLOCK-F-005	PHOTO-Z-SXDS	9700.318	4.306042	2.4376
CALBLOCK-F-005	PHOTO-Z-SXDS	9881.949	2.869792	2.9348
CALBLOCK-F-005	PHOTO-Z-SXDS	10064.675	1.638819	3.4351
CALBLOCK-F-004	COLOR-GOODS-NORTH	10185.892	0.455521	3.7670
CALBLOCK-F-005	PHOTO-Z-SXDS	10244.451	3.075012	3.9273
CALBLOCK-F-004	COLOR-GOODS-NORTH	10366.424	0.455544	4.2613
CALBLOCK-F-005	PHOTO-Z-VVDS	10432.900	1.472650	4.4433
CALBLOCK-F-005	PHOTO-Z-VVDS	10615.952	1.472650	4.9444

Table 5.2: Schedule of the observations of the Auxiliary Fields, with the period prior to the restart date shaded in grey. Notes on faulty observations: 1. unusable, required to be repeated; 2. repetition of the lost visit; 3. Visit ending with the blue grism and followed by a monthly block

The visits to the smallest fields (of sizes 1x1 or 2x1 FoV) are spread in two sets, observed 6 months apart, with equal number of visits on each. One of the visits is made with the FoV upside down with respect to the other, and hence at the end of the second visit, we obtain two blue grism spectral directions of equal depth separated by approximately 180 deg. The blue to red grism

The presented document is Proprietary information of the Euclid Consortium.
This document shall be used and disclosed by the receiving Party and its related entities (e.g. contractors and subcontractors) only for the purposes of fulfilling the receiving Party's responsibilities under the Euclid Project and that the identified and marked technical data shall not be disclosed or retransferred to any other entity without prior written permission of the document preparer.

#bgs_brratio ratio is implemented as close as possible (within discretization error) in each visit, thus being fulfilled at every moment throughout the survey.

The largest fields are observed in 4 visits. In the first visit the full area is observed to 3x the EWS S/N (i.e., with 27 passes), and the following three visits gradually increase the depth to the required 5x EWS S/N (with 19, 10 and 19 passes, respectively). The visits are spaced 6 months apart. Even visits and odd visits are rotated by 180 deg, like for the small fields. The chosen number of passes per visit ensures equal depth of both spectra directions when an odd-even pair of visits is completed. Like for the small fields, the blue to red grism *#bgs_brratio* ratio is implemented in each visit. There are four visits to COSMOS after the breakpoint because the first planned visit (at MJD2000 = 8901.909) was lost. We note that the reobservation made at MJD2000 = 9272.801 takes less time than the lost visit because the observing strategy for COSMOS changed in the meantime [AD03].

The highest priority fields, AEGIS, CDFS and COSMOS, are observed first, with COSMOS being completed in the first semester of the third survey year. The SXDS is observed in the third and fourth years, and finally GOODS-N and VVDS are completed in the fifth year.

5.1.3 Euclid Deep fields and CPC

The visits to the Deep fields form a large part of the observations scheduled in stage-one. They are not part of the tessellation and can thus have a free orientation. Hence their scheduling only requires a span in AA large enough to keep their tiles aligned as the orbit moves during their observation. Given their dimensions the required range is at most 3 deg, and so their scheduling is not impacted by the reduced AA range, and has remained stable since the latest pre-launch configuration. Moreover, the visibility of EDF-S is enlarged by the post-launch increase of the SAA range.

We note that all of the three deep fields happen to have one blinding star close to their borders. For certain orientations of the covering pattern, the star's exclusion radius intersects one or two of the FoVs of the pattern. In order to avoid this, when necessary, the patterns are adjusted by shifting the impacted FoVs inwards, such as to exclude the star and its avoidance radius. The covering of the target deep-field area was not compromised by this strategy.

The majority of the visits to EDF-S and EDF-N in the first year are the CPC observations. The set of 10 visits is required to be made at orientations compliant with the requirement on a minimum separation. The decrease in the AA range compared with the pre-launch configuration reduces the range of EDF possible orientations at a given epoch. It tuns out to be impossible to find a set of 10 orientations compliant with the minimum separation requirement during the visibility windows available in the year. The problem is solved by allowing a patch-level tilt on the orientation of the CPC with tolerance 1 deg. This means that the CPC patch may be observed with an orientation rotated by up to 1 deg with respect to the natural orientation of the patch in that observation epoch. In contrast to the tilting strategy at tile level, which would produce effectively smaller tiles and a reduced EDF area on the CPC visits, when tilting at patch level the tiles within the patch are aligned to each other. This strategy is applied to both CPC-N and CPC-S.

In the case of CPC-N, with long visibility, this strategy allows us to keep the uniform distribution of spectra directions with a 32.727 deg cadence of position angles. This cadence, which is 360/11, was chosen to mimic the "monthly" cadence of the self-cal field, to allow for back-to-back scheduling if needed in an optimization of the observing plan. We note that, since there are only 10 and not 11 CPC visits, this introduces a larger step of 2 x 32.727 deg in the otherwise uniform cadence. However, since associated to each reference direction there are other three, forming a K-pattern of 4 directions, the maximum gap between neighboring directions is much smaller than this gap, as seen in the distribution of directions shown in Figure 5.3 (left panel). The minimum separation between spectra directions in this solution is 6.36 deg.

In the case of CPC-S, its shorter visibility imposes a set of more clustered visits. CPC-S is scheduled in two sets of 5 visits, with a position angle of 10 deg apart between visits of the same set. The two sets are separated by 84 deg, which results in the spectral directions shown in Figure 5.3 (right panel). The minimum separation between spectra directions in this solution is 4 deg, which is exactly the minimum allowed separation *#threshold_cpcmin.*

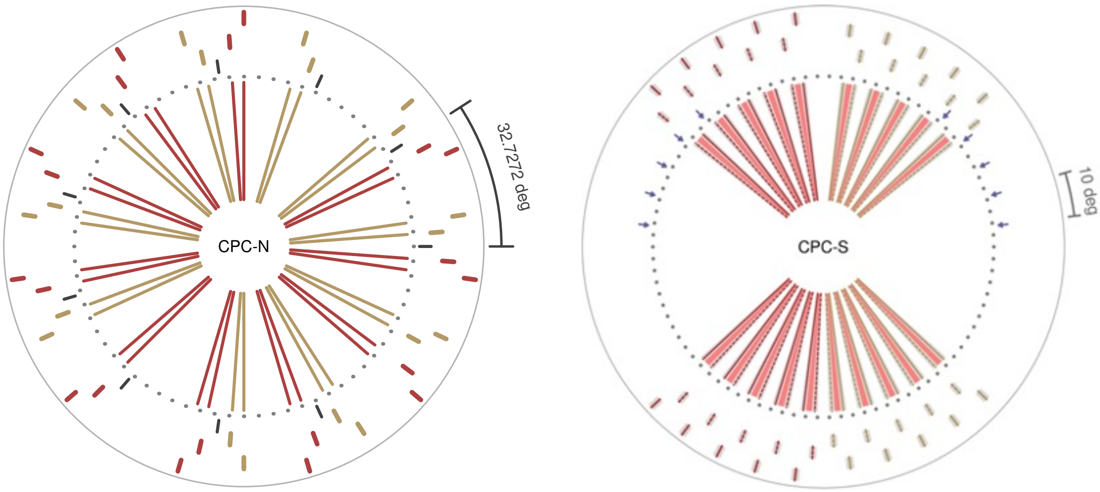

Figure 5.3: Each CPC visit to the CPC-N field (left panel) and to the CPC-S field (right panel) defines 4 spectral directions, according to the K-pattern: 0 and 0_rot (red), and 180 and 180_rot (brown). Inner circles dots are 5 deg apart, and the ticks show the position angle cadence

The detailed schedule of the EDFs observations in *#version_rsd* is given in Table 5.3. The first part of the table, prior to the breakpoint, contains the intra-decontamination period to be reobserved, which contains two CPC-N visits and one EDF-N visit. There are two other CPC-N visits and two more visits to EDF-N that failed. The four CPC-N visits are reobserved in the second year of the survey, meaning that only16 of the 20 CPC visits can be completed in the first year. We note that a cadence in CPC position angles does not translate directly into a time cadence, as can be inferred in Table 5.3, since the observations can be made in leading or trailing directions, and also can be off-set from the natural timing by using the SAA and AA range.

The non-CPC observations of the EDFs are scheduled with no angle constraints. In particular the three lost EDF-N visits, giving its perennial visibility, can be reobserved anytime, and two additional EDF-N visits are scheduled, without any of the visits being linked to a particular lost visit. (We note that a third additional visit remains to be rescheduled in a future revision of the RSD). In contrast EDF-F has a short visibility, forcing us to schedule several visits in sequence.

Table 5.3 also scheduled F-017 (grism sanity), which is a ROS pointing (RGS) that is placed in-between a non-ROS observation and a BGS Deep field visit to ensure a correct grism switch to blue. We note there are 12 instances where a BGS Deep field is followed by F-001 (which also starts with BGS) where an F-017 could have been scheduled as an extra safety measure. However, it was assumed that SOC deals with this type of transitions and an F-017 was not scheduled.

The presented document is Proprietary information of the Euclid Consortium.
This document shall be used and disclosed by the receiving Party and its related entities (e.g. contractors and subcontractors) only for the purposes of fulfilling the receiving Party's responsibilities under the Euclid Project and that the identified and marked technical data shall not be disclosed or retransferred to any other entity without prior written permission of the document preparer.

Field	MJD2000	Duration (days)	Year	Grism
[1]CPC-NORTH-06	8846.274	2.204826	0.0993	(Red)
[1]CPC-NORTH-02	8895.891	2.204213	0.2352	(Red)
[1]DEEP-NORTH	8898.099	2.204745	0.2412	(Blue)
CPC-NORTH-03	8929.059	2.204329	0.3260	Red
DEEP-NORTH	8931.267	2.204664	0.3320	Blue
[2]DEEP-NORTH	8938.909	2.204317	0.3529	(Blue)
CPC-NORTH-04	8964.672	2.203692	0.4235	Red
CPC-NORTH-10	8981.648	2.204826	0.4699	Red
DEEP-FORNAX	8983.873	1.177685	0.4760	Blue
DEEP-FORNAX	8985.053	1.177836	0.4793	Blue
CPC-SOUTH-01	8991.531	2.511505	0.4970	Red
CPC-NORTH-05	8998.997	2.204329	0.5174	Red
CPC-SOUTH-02	9002.809	2.409259	0.5279	Red
CPC-SOUTH-03	9014.578	2.666111	0.5601	Red
CPC-SOUTH-04	9021.770	2.512245	0.5798	Red
CPC-SOUTH-05	9034.987	2.564560	0.6160	Red
[2]DEEP-NORTH	9046.025	2.211782	0.6462	(Blue)
[2]CPC-NORTH-01	9048.487	2.204491	0.6529	(Red)
[2]CPC-NORTH-07	9065.261	2.204329	0.6989	(Red)
CPC-NORTH-08	9098.079	2.204259	0.7887	Red
CPC-SOUTH-06	9111.813	2.563669	0.8263	Red
CPC-SOUTH-07	9122.029	2.511829	0.8543	Red
CPC-NORTH-09	9129.194	2.211933	0.8739	Red
CPC-SOUTH-08	9131.675	2.665833	0.8807	Red
CPC-SOUTH-09	9145.131	2.409074	0.9175	Red
CPC-SOUTH-10	9152.533	2.511343	0.9378	Red
[4]DEEP-NORTH	9162.194	2.204491	0.9643	Blue
[3]CPC-NORTH-06	9211.120	2.204826	1.0982	Red
[3]CPC-NORTH-02	9261.617	2.204213	1.2365	Red
[4]DEEP-NORTH	9296.657	2.212176	1.3324	Blue
DEEP-FORNAX	9348.571	1.177685	1.4745	Red
DEEP-FORNAX	9349.751	1.177836	1.4778	Blue

DEEP-FORNAX	9350.932	1.177685	1.4810	Blue
DEEP-FORNAX	9352.112	1.177836	1.4842	Red
DEEP-FORNAX	9353.293	1.179884	1.4875	Blue
DEEP-SOUTH	9360.369	2.511273	1.5068	Blue
[4]DEEP-SOUTH	9362.883	2.409236	1.5137	Blue
DEEP-SOUTH	9372.896	2.562720	1.5411	Blue
DEEP-SOUTH	9375.462	2.666030	1.5482	Blue
[3]CPC-NORTH-01	9414.995	2.204826	1.6564	Red
[3]CPC-NORTH-07	9431.036	2.204271	1.7003	Red
DEEP-NORTH	9434.909	2.204329	1.7109	Red
DEEP-NORTH	9437.117	2.212188	1.7170	Blue
DEEP-SOUTH	9494.384	2.571586	1.8737	Red
[4]DEEP-SOUTH	9497.206	2.562951	1.8815	Blue
DEEP-SOUTH	9512.860	2.511204	1.9243	Blue
DEEP-FORNAX	9518.704	1.177836	1.9403	Red
DEEP-FORNAX	9519.885	1.177685	1.9436	Blue
DEEP-FORNAX	9521.065	1.177836	1.9468	Blue
DEEP-FORNAX	9522.246	1.185116	1.9500	Red
DEEP-FORNAX	9523.681	1.177836	1.9540	Blue
[4]DEEP-NORTH	9594.419	2.204491	2.1476	Blue
DEEP-FORNAX	9714.318	1.177685	2.4759	Red
DEEP-FORNAX	9715.499	1.177836	2.4791	Blue
DEEP-FORNAX	9716.679	1.177685	2.4824	Blue
DEEP-FORNAX	9717.860	1.185266	2.4856	Red
DEEP-FORNAX	9719.295	1.177685	2.4895	Blue
DEEP-SOUTH	9725.105	2.511088	2.5054	Blue
[4]DEEP-SOUTH	9727.619	2.511748	2.5123	Blue
DEEP-SOUTH	9736.663	2.562755	2.5371	Red
DEEP-SOUTH	9739.229	2.666030	2.5441	Blue
DEEP-NORTH	9774.789	2.204664	2.6414	Red
DEEP-NORTH	9776.997	2.204491	2.6475	Blue
DEEP-SOUTH	9855.583	2.563773	2.8626	Blue
[4]DEEP-SOUTH	9858.150	2.571273	2.8697	Blue

The presented document is Proprietary information of the Euclid Consortium.
This document shall be used and disclosed by the receiving Party and its related entities (e.g. contractors and subcontractors) only for the purposes of fulfilling the receiving Party's responsibilities under the Euclid Project and that the identified and marked technical data shall not be disclosed or retransferred to any other entity without prior written permission of the document preparer.

DEEP-SOUTH	9876.914	2.511389	2.9210	Blue
DEEP-SOUTH	9879.428	2.511389	2.9279	Red
DEEP-FORNAX	9889.742	1.177569	2.9562	Blue
DEEP-FORNAX	9890.922	1.177951	2.9594	Red
DEEP-FORNAX	9892.103	1.177569	2.9626	Blue
DEEP-FORNAX	9893.284	1.177951	2.9659	Red
[4]DEEP-FORNAX	9894.464	1.177569	2.9691	Blue
DEEP-NORTH	9922.601	2.204826	3.0461	Blue
DEEP-NORTH	9924.809	2.204329	3.0522	Blue
DEEP-NORTH	9927.017	2.204826	3.0582	Blue
[4]DEEP-NORTH	9929.225	2.204329	3.0643	Blue
DEEP-FORNAX	10078.067	1.177951	3.4718	Blue
DEEP-FORNAX	10079.247	1.177569	3.4750	Red
DEEP-FORNAX	10080.428	1.177951	3.4782	Blue
DEEP-FORNAX	10081.609	1.184803	3.4815	Red
DEEP-FORNAX	10083.044	1.177951	3.4854	Blue
DEEP-SOUTH	10090.803	2.511111	3.5066	Blue
DEEP-SOUTH	10093.318	2.409248	3.5135	Blue
DEEP-SOUTH	10103.337	2.563021	3.5410	Blue
DEEP-SOUTH	10105.904	2.665891	3.5480	Blue
CALBLOCK-F-017	10131.729	0.048657	3.6187	Red
DEEP-NORTH	10131.781	2.204664	3.6188	Blue
DEEP-NORTH	10133.989	2.204491	3.6249	Blue
DEEP-NORTH	10136.197	2.204664	3.6309	Blue
DEEP-NORTH	10138.405	2.211470	3.6370	Blue
DEEP-NORTH	10140.868	2.204664	3.6437	Blue
DEEP-NORTH	10143.076	2.204491	3.6498	Blue
DEEP-NORTH	10145.284	2.204664	3.6558	Blue
DEEP-SOUTH	10225.959	2.665787	3.8767	Red
[4]DEEP-SOUTH	10228.628	2.665625	3.8840	Blue
DEEP-SOUTH	10239.518	2.409120	3.9138	Blue
DEEP-SOUTH	10241.931	2.511250	3.9204	Blue
DEEP-FORNAX	10252.517	1.177569	3.9494	Blue

The presented document is Proprietary information of the Euclid Consortium.
This document shall be used and disclosed by the receiving Party and its related entities (e.g. contractors and subcontractors) only for the purposes of fulfilling the receiving Party's responsibilities under the Euclid Project and that the identified and marked technical data shall not be disclosed or retransferred to any other entity without prior written permission of the document preparer.

DEEP-FORNAX	10253.697	1.177951	3.9526	Red
DEEP-FORNAX	10254.878	1.177569	3.9559	Blue
DEEP-FORNAX	10256.059	1.177951	3.9591	Blue
DEEP-FORNAX	10257.239	1.177569	3.9623	Red
DEEP-FORNAX	10258.420	1.177951	3.9656	Blue
DEEP-FORNAX	10259.601	1.177569	3.9688	Red
CALBLOCK-F-017	10293.581	0.048657	4.0618	Red
DEEP-NORTH	10293.633	2.204826	4.0620	Red
DEEP-NORTH	10295.841	2.204329	4.0680	Blue
DEEP-NORTH	10298.049	2.204826	4.0741	Blue
DEEP-NORTH	10300.257	2.204329	4.0801	Blue
DEEP-NORTH	10302.465	2.204826	4.0861	Blue
DEEP-NORTH	10304.673	2.212176	4.0922	Blue
DEEP-FORNAX	10447.275	1.177685	4.4826	Blue
DEEP-FORNAX	10448.455	1.177836	4.4858	Blue
DEEP-FORNAX	10449.636	1.177685	4.4891	Red
DEEP-FORNAX	10450.816	1.177836	4.4923	Blue
DEEP-FORNAX	10451.997	1.177685	4.4955	Red
DEEP-SOUTH	10457.219	2.511273	4.5098	Blue
DEEP-SOUTH	10459.734	2.511551	4.5167	Red
DEEP-SOUTH	10468.163	2.562743	4.5398	Blue
DEEP-SOUTH	10470.729	2.666007	4.5468	Blue
DEEP-NORTH	10502.752	2.204664	4.6345	Red
DEEP-NORTH	10504.960	2.204491	4.6405	Blue
DEEP-NORTH	10507.168	2.204664	4.6466	Blue
DEEP-NORTH	10509.376	2.204491	4.6526	Blue
DEEP-SOUTH	10587.481	2.563854	4.8665	Blue
[4]DEEP-SOUTH	10590.048	2.563715	4.8735	Blue
DEEP-SOUTH	10604.243	2.409097	4.9124	Red
DEEP-SOUTH	10606.656	2.511424	4.9190	Blue
DEEP-FORNAX	10617.432	1.177836	4.9485	Blue
DEEP-FORNAX	10618.612	1.177685	4.9517	Blue
DEEP-FORNAX	10619.793	1.177836	4.9549	Red

The presented document is Proprietary information of the Euclid Consortium.
This document shall be used and disclosed by the receiving Party and its related entities (e.g. contractors and subcontractors) only for the purposes of fulfilling the receiving Party's responsibilities under the Euclid Project and that the identified and marked technical data shall not be disclosed or retransferred to any other entity without prior written permission of the document preparer.

DEEP-FORNAX	10620.973	1.177685	4.9582	Blue
DEEP-FORNAX	10622.154	1.177836	4.9614	Blue
DEEP-FORNAX	10623.335	1.177685	4.9646	Red
[4]DEEP-FORNAX	10624.515	1.177836	4.9679	Blue
DEEP-FORNAX	10820.043	1.177685	5.5032	Red
DEEP-FORNAX	10821.224	1.177836	5.5064	Blue
DEEP-FORNAX	10822.404	1.177685	5.5097	Blue
DEEP-FORNAX	10823.585	1.177836	5.5129	Red
DEEP-FORNAX	10824.766	1.177685	5.5161	Blue
DEEP-FORNAX	10825.946	1.177836	5.5194	Red
DEEP-SOUTH	10828.826	2.408796	5.5272	Red
DEEP-SOUTH	10831.238	2.511806	5.5338	Blue
DEEP-SOUTH	10833.753	2.562720	5.5407	Blue
DEEP-SOUTH	10836.319	2.672998	5.5478	Blue

Table 5.3: Schedule of the observations of the Deep Fields. The period prior to the restart date is shaded in grey, with a darker tone showing the intra-decontamination period to be reobserved. Light grey in the early post-restart period indicates the epoch used for the reobservations. Notes: 1. observations from the intra-decontamination period to be reobserved; 2. unusable, required to be repeated; 3. repetition of lost visits; 4. blue visit followed by a monthly block

The progression of the EDFs and CPCs observations is shown in Figure 5.4. The lost visits that had taken place prior to the restart date are not counted. EDF-S and EDF-F follow roughly a 6-month cadence from the start of the second year onwards, being completed towards the end of the nominal mission, following an identical strategy to the one of *#replan_basis*. Comparing with *#replan_basis*, *#version_rsd* has less visits to EDF-N in the first year because several visits had failed. They are compensated by an increase in the second year. Using the long visibility of the high-latitude sky, a large number of consecutive visits to the extended EDF-N is distributed among the fourth and fifth years during the two low-stress periods that would remain otherwise unallocated. This deviates slightly from *#replan_basis* where the later visits were mostly concentrated in the fourth year. In both cases, this strategy allows for the earlier completion of EDF-N.

Year	**Cumulated observed fraction of the EDS (%)**
1	17.9%
2	34.9%
3	49.0%
4	71.5%
5	93.0%

The presented document is Proprietary information of the Euclid Consortium.
This document shall be used and disclosed by the receiving Party and its related entities (e.g. contractors and subcontractors) only for the purposes of fulfilling the receiving Party's responsibilities under the Euclid Project and that the identified and marked technical data shall not be disclosed or retransferred to any other entity without prior written permission of the document preparer.

6	99.1 %

Table 5.4: The cumulated observed fraction of the Euclid Deep Survey at the end of each year of the mission, using observing time as a proxy for the EDS area and depth completion

The progression of the EDFs is also shown in table format in Table 5.4, where the cumulated completed fraction of the total Euclid Deep Survey at the end of each year is given. The effect of the lost visits is seen as a relatively lower fraction in the first year, which is compensated by additional visits in the second year. In general, the number of visits is more evenly distributed by the years with respect to *#replan_basis*. The EDS does not reach 100% due to the lack of one visit to the EDF-N that will need to be included in a future RSD release.

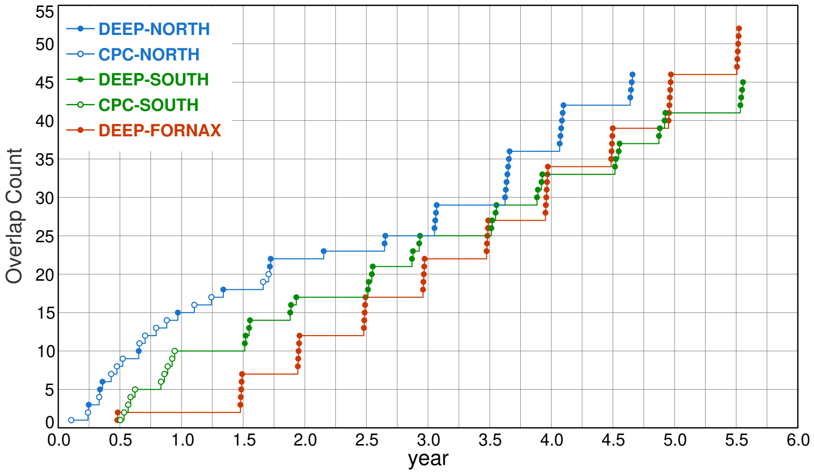

Figure 5.4: Progression of the CPC and Deep fields during the mission

In each visit to a EDF all exposures are taken with the same ROS variant (red or blue), the one indicated in Table 5.3. Figure 5.5 shows, for each of the 3EDFs, the progression of the cumulated fraction of BLUE visits, i.e, the current total number of BLUE visits normalized by the current total number of BLUE+RED visits. Naturally, the rescheduled visits are not double counted.

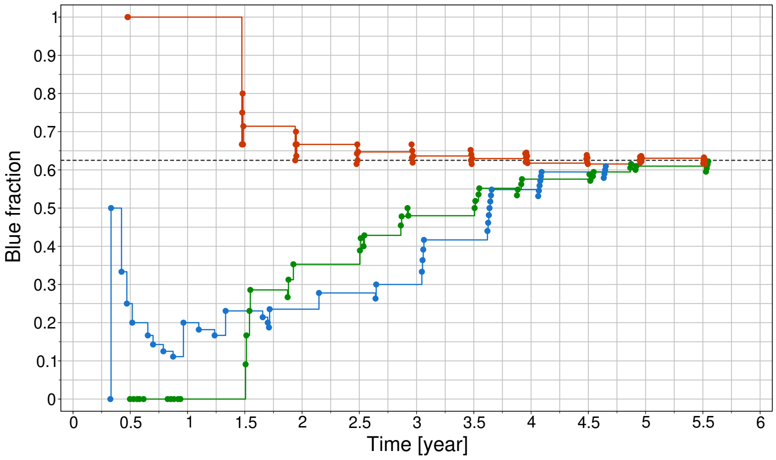

Figure 5.5: Progression of the fraction of the BLUE grism visits for EDF-N (blue), EDF-S (green) and EDF-F (red), including the CPC visits. The dashed line indicates the target fraction of 25/40=0.625

EDF-N and EDF-S start with a low fraction because they start with the CPC visits, which are all RED. Afterwards, most of the visits to EDF-N and EDF-S are BLUE, to compensate the RED start and increase the B/R ratio. Non-CPC EDF-S visits only start in the second year, which explains why the fraction remains at zero during the first year. EDF-F is mostly scheduled with 5 consecutive visits to optimize visibility, and they are always 3 BLUE and 2 RED. EDF-F is the only field that keeps the target *#bgs_brratio* ratio throughout the mission, with the the other fields only approaching the goal at the middle of the fourth year.

5.1.4 Polar caps

At high ecliptic latitudes (above *#threshold_polarcap*) the two polar caps are covered with a pre-determined number of patches. Even though part of the EWS, these latitudes are not included in the global tessellation but are instead scheduled in stage-one. In this way, each patch of the polar caps is a stage-one target. As discussed in Sect. 4.3.6, the reason is that the convergence of the ecliptic meridians at the poles would make the eigen-slews between neighboring tiles of the global tessellation too large and non-compliant with requirements.

The detailed schedule of the EDFs observations in *#version_rsd* is given in Table 5.5. The first part of the table, prior to the breakpoint, contains the intra-decontamination period to be reobserved and Northcap-06 that had been replaced by decontamination activities. After the restart, the reobservation of Northcap-10 takes place in the similar epoch than the original observation, while Northcap-11 is scheduled later. One third of the patches had to be delayed for the third year, pushed by the large reobservation period. Indeed, due to the strong asymmetry of the visibility window most of the polar patches have only one visibility window per year.

Field	MJD2000	Duration (days)	Year
SOUTH-CAP-05	8824.763	3.797894	0.0404
[1]NORTH-CAP-10	8872.395	2.768241	0.1708
[1]NORTH-CAP-11	8907.082	1.024421	0.2658
[2]NORTH-CAP-06	8923.922	5.131817	0.3119
SOUTH-CAP-03	8933.496	2.624190	0.3381
NORTH-CAP-01	8941.117	0.973125	0.3590
NORTH-CAP-08	8994.066	4.927130	0.5039
NORTH-CAP-03	9190.469	3.848785	1.0417
[3]NORTH-CAP-10	9238.032	2.768206	1.1719
[3]NORTH-CAP-06	9291.522	5.130139	1.3183
NORTH-CAP-07	9327.078	5.030475	1.4157
NORTH-CAP-02	9346.912	1.639606	1.4700
NORTH-CAP-09	9393.656	5.081678	1.5980
SOUTH-CAP-06	9408.762	4.162998	1.6393
NORTH-CAP-13	9413.195	1.794282	1.6515

SOUTH-CAP-07	9439.600	3.745104	1.7237
SOUTH-CAP-04	9524.867	3.180625	1.9572
NORTH-CAP-12	9576.427	2.673750	2.0984
NORTH-CAP-04	9589.131	5.284780	2.1331
SOUTH-CAP-01	9618.694	1.279861	2.2141
NORTH-CAP-05	9619.998	5.286377	2.2177
SOUTH-CAP-02	9638.511	1.537014	2.2683
[3]NORTH-CAP-11	9640.071	1.024514	2.2726
SOUTH-CAP-08	9796.752	3.230845	2.7016

Table 5.5: Schedule of the observations of the polar caps. The period prior to the restart date is shaded in grey, with a darker tone showing the intra-decontamination period to be reobserved. Light grey in the early post-restart period indicates the epoch used for the reobservations. Notes: 1. observations from the intra-decontamination period to be reobserved; 2. skipped for decontamination campaign; 3. rescheduled lost visits

5.2 Stage-two

The second stage of an ECTile RSD generation is the scheduling of the EWS observations on a global tessellation on the sphere using the time periods defined by the *survey windows*, i.e. the time periods that remained free after the first stage implementation (cf. Figure 5.1). After the preparatory step of computing the tessellated RoI, the building of the EWS starts chronologically, one survey window at a time.

For the first survey window, its *visibility window* is computed, i.e., a spatial region (including leading and trailing sides) within reach during the survey window given the pointing constraints and the tilting tolerance. In general, a visibility window contains four separate regions (one per quadrant of the RoI). During a survey window there is only time to observe part of the visibility window. Several *patches*, i.e., compact sets of tiles, are proposed by ECTile in the four quadrants of the visibility window. One of the quadrants, containing one or more patches, is selected according to optimization strategies. If the visibility window contains a patch of tiles for reobservation (i.e. failed tiles from a previous RSD) then the *large infill* mechanism presents that patch among the patches proposed in that survey window.

Once the selection is made, a tile-to-tile observing sequence is computed within each patch of the survey window, using the *diffusion algorithm*. We note that the tolerance on the position angle of the FoVs introduces the possibility of keeping AA approximately constant during the observation of a patch. Sometimes, ECTile does not find a valid observing sequence for a patch, or patches have irregular shapes of are placed in locations that will be difficult to connect with future patches. In all these cases, the user has the option to adjust *time margin parameters* and try a different scheduling of the survey window.

After all patches are scheduled, a search is done to find PSF calibration fields within reach in the *PSF survey window*. A PSF survey window is the survey window excluding its first *#threshold_thermalization* days, and smaller survey windows do not contain a PSF survey window. If the search is successful, the *PSF block* (consisting of the sequence F-012+F-015+F-013+F-008) is scheduled with SAA and AA values matching the ones of the contemporary EWS patch. When the time reserved for SOPS also falls in the survey window, a SOPS is scheduled. If the visibility

The presented document is Proprietary information of the Euclid Consortium.
This document shall be used and disclosed by the receiving Party and its related entities (e.g. contractors and subcontractors) only for the purposes of fulfilling the receiving Party's responsibilities under the Euclid Project and that the identified and marked technical data shall not be disclosed or retransferred to any other entity without prior written permission of the document preparer.

window contains individual tiles selected for reobservation, they can be scheduled at this stage with the *small infill* mechanism. To create space for the insertion of a PSF block, a SOPS window, or small infills in the survey window, ECTile removes some of the scheduled tiles, hence slightly shortening the patches of that survey window.

Once the survey window is finalized, ECTile moves to the next one. The RoI is progressively covered from survey window to survey window, aiming for perfect fit of patches, with no holes in between. Survey windows for which no new patches can be generated remain unallocated.

5.2.1 Schedule

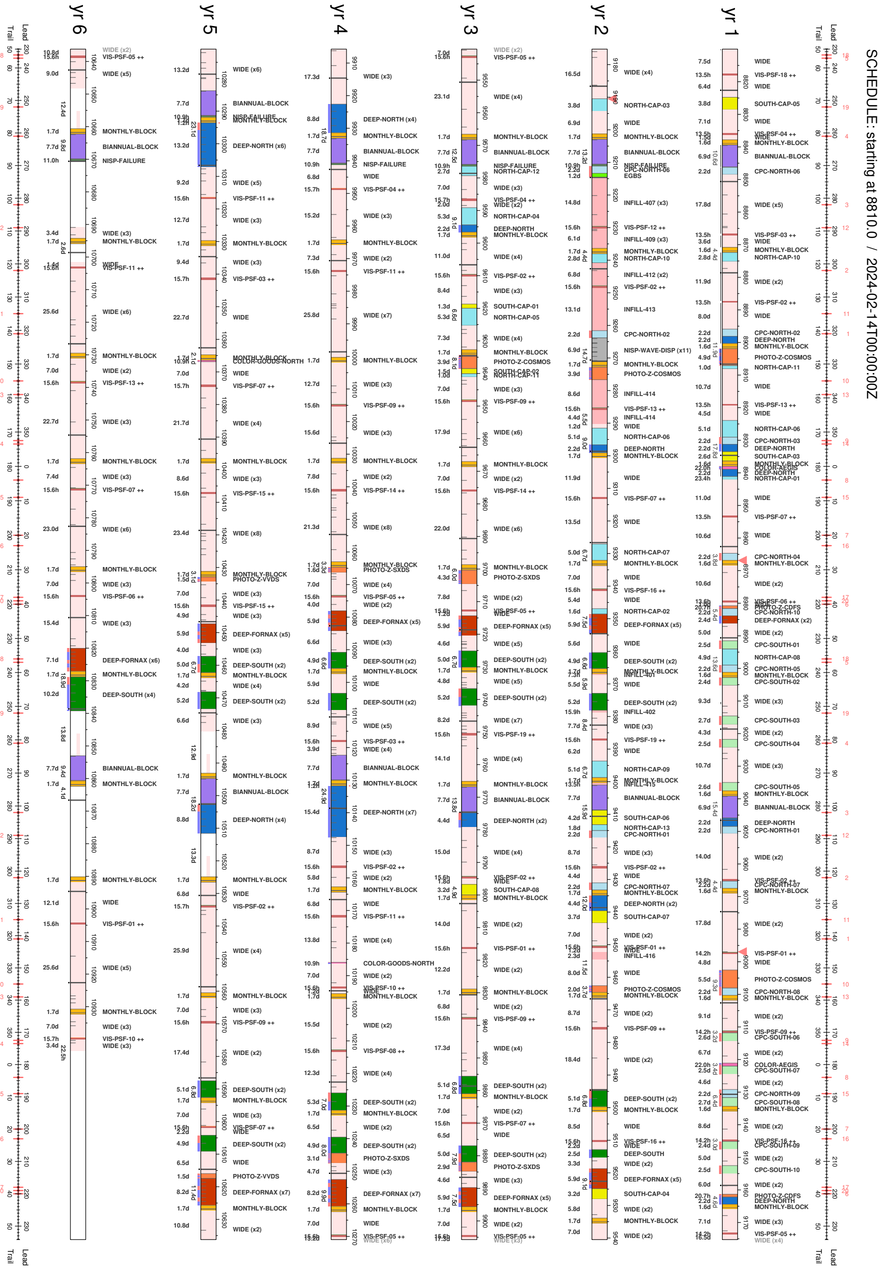

Figure 5.6: Complete *#version_rsd* schedule at the end of stage-two, including EWS, EDS, EAFs, calibrations, EWS infills, SOPS windows, and the EGBS. Each row is one survey year

The presented document is Proprietary information of the Euclid Consortium.
This document shall be used and disclosed by the receiving Party and its related entities (e.g. contractors and subcontractors) only for the purposes of fulfilling the receiving Party's responsibilities under the Euclid Project and that the identified and marked technical data shall not be disclosed or retransferred to any other entity without prior written permission of the document preparer.

The stage-two process results in the final schedule, shown in Figure 5.6. Pink boxes are scheduled survey windows, while dark pink boxes are infills, i.e. reobservations. Wide infills may take a full survey window, while small infills share a survey window with other observations. “Wide x n” indicates the survey window contain n patches, the ones indicated by short tickmarks. The duration of the survey windows is given below the boxes. White boxes are unallocated survey windows, corresponding to low-stress periods (Sect. 4.3.8). The observations of the PSF fields occur at the red lines. There are no PSF calibration observations scheduled in the unallocated survey windows. The black lines indicate SOPS windows. The color bars below the F-002 to F-005 observations to the EAFs and EDFs indicate the grism (red or blue) used in each of the visits to those fields. The thin lines under some of the observations indicate observations to be rescheduled, corresponding to the ones shown in Table 4.11. They occupy the full length of the intra-decontamination period survey, but a few other short lines can be seen under other survey windows or calibration blocks. There are three restart dates marked by red triangles: close to MJD2000 = 8970 is the RSD_2024B restarting point; close to 9090 is the restarting point of RSD_2024C; and close to 9190 at *#replan_restart_mjd* is the restarting point of the current *#version_rsd.*

5.2.2 PSF fields and SOPS windows

Table 5.6 shows when and which of the F-008 PSF fields are scheduled. We note they are always scheduled together with other calibration sequences (see caption). There are 60 visits to PSF calibration fields, of which 12 visits in year 1, followed by 10 visits in year 2, 12 in year 3, 11 in year 4, 8 in year 5 and 7 in year 6. Their cadences are shown in Figure 5.7 are mostly determined by the availability of survey windows. After the breakpoint, there is a large gap before the first PSF visit. This is due to the presence of a short window survey that does not allow stabilization time, followed by the long bi-annual calibration and the new EGBS. Afterwards, the cadence remains within limits or close to the upper limit, until unallocated the appearance of unallocated survey windows where the lack of reference SAA and AA values prevent the scheduling of a PSF visit.

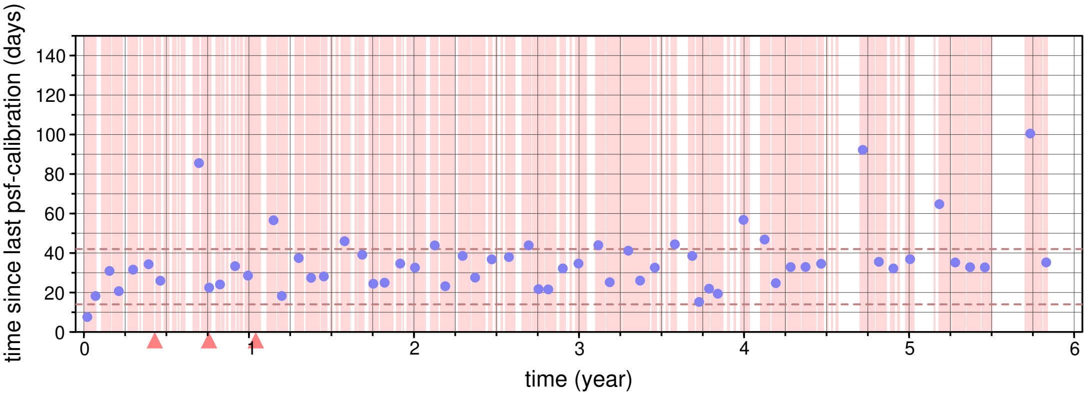

Figure 5.7: Histogram of the cadence of the PSF calibration observations. The three restart dates of RSD_2024B, RSD_2024C and *#version_rsd* are indicated by the triangles. The cadence is required to stay between the two dashed lines

The fields PSF-17 and PSF-20 are never observed. They are close together in the southern sky at the anti-meridian of field PSF-06 of the northern sky. The three fields are always visible simultaneously and the ECTile choice always fall on PSF-06.

The starting time of the period reserved for SOPS is also shown in Table 5.6. SOPS is scheduled every Monday always very close to noon UTC with one exception at MJD2000 = 9270 for which a valid solution was not found and MOC awarded a 8h waiver. The table also shows that no PSF sequence starts less than 3 days after the start of the previous SOPS window, even though two instances start just under 3 days after the end of the previous SOPS.

Field	MJD2000	UTC	Difference (days)
VIS-PSF-18	8817.592	2024-02-21T14:12:24Z	---
SOPS	8822.504	2024-02-26T12:04:58Z	---
VIS-PSF-04	8835.801	2024-03-10T19:13:31Z	13.3
SOPS	8850.505	2024-03-25T12:06:50Z	---
VIS-PSF-03	8866.704	2024-04-10T16:52:54Z	16.2
SOPS	8878.512	2024-04-22T12:16:47Z	---
VIS-PSF-02	8887.372	2024-05-01T08:54:30Z	8.9
SOPS	8906.507	2024-05-20T12:09:03Z	---
VIS-PSF-13	8918.942	2024-06-01T22:36:32Z	12.4
SOPS	8934.522	2024-06-17T12:30:48Z	---
VIS-PSF-07	8953.256	2024-07-06T06:07:49Z	18.7
SOPS	8962.495	2024-07-15T11:52:34Z	---
VIS-PSF-06	8979.222	2024-08-01T05:18:39Z	16.7
SOPS	8990.502	2024-08-12T12:03:38Z	---
SOPS	9018.482	2024-09-09T11:33:23Z	---
SOPS	9046.486	2024-10-07T11:39:39Z	---
VIS-PSF-02	9064.768	2024-10-25T18:24:36Z	18.3
SOPS	9074.515	2024-11-04T12:21:13Z	---
VIS-PSF-01	9087.227	2024-11-17T05:26:10Z	12.7
SOPS	9102.484	2024-12-02T11:36:38Z	---
VIS-PSF-09	9111.301	2024-12-11T07:13:28Z	8.8
SOPS	9130.529	2024-12-30T12:40:27Z	---
VIS-PSF-16	9144.639	2025-01-13T15:19:15Z	14.1
SOPS	9158.490	2025-01-27T11:44:32Z	---
VIS-PSF-05	9173.198	2025-02-11T04:44:39Z	14.7
SOPS	9186.504	2025-02-24T12:04:36Z	---
SOPS	9214.497	2025-03-24T11:55:14Z	---

The presented document is Proprietary information of the Euclid Consortium.
This document shall be used and disclosed by the receiving Party and its related entities (e.g. contractors and subcontractors) only for the purposes of fulfilling the receiving Party's responsibilities under the Euclid Project and that the identified and marked technical data shall not be disclosed or retransferred to any other entity without prior written permission of the document preparer.

VIS-PSF-12	9229.768	2025-04-08T18:25:18Z	15.3
SOPS	9242.502	2025-04-21T12:02:01Z	---
VIS-PSF-02	9248.019	2025-04-27T00:26:59Z	5.5
[1]SOPS	9270.870	2025-05-19T20:52:03Z	---
VIS-PSF-13	9285.461	2025-06-03T11:03:44Z	14.6
SOPS	9298.505	2025-06-16T12:06:49Z	---
VIS-PSF-07	9312.867	2025-06-30T20:48:10Z	14.4
SOPS	9326.511	2025-07-14T12:15:07Z	---
VIS-PSF-16	9341.002	2025-07-29T00:02:31Z	14.5
SOPS	9354.473	2025-08-11T11:20:11Z	---
SOPS	9382.519	2025-09-08T12:27:15Z	---
VIS-PSF-19	9386.974	2025-09-12T23:21:35Z	4.5
SOPS	9410.506	2025-10-06T12:08:34Z	---
VIS-PSF-02	9426.089	2025-10-22T02:07:11Z	15.6
SOPS	9438.503	2025-11-03T12:03:01Z	---
VIS-PSF-01	9450.527	2025-11-15T12:37:35Z	12.0
SOPS	9466.518	2025-12-01T12:25:35Z	---
VIS-PSF-09	9475.482	2025-12-10T11:33:59Z	9.0
SOPS	9494.487	2025-12-29T11:40:00Z	---
VIS-PSF-16	9510.119	2026-01-14T02:51:25Z	15.6
SOPS	9522.503	2026-01-26T12:03:01Z	---
VIS-PSF-05	9542.723	2026-02-15T17:19:52Z	20.2
SOPS	9550.510	2026-02-23T12:14:30Z	---
SOPS	9578.479	2026-03-23T11:29:24Z	---
VIS-PSF-04	9586.568	2026-03-31T13:37:28Z	8.1
SOPS	9606.528	2026-04-20T12:39:38Z	---
[2]VIS-PSF-02	9609.750	2026-04-23T17:59:59Z	3.222
SOPS	9634.500	2026-05-18T11:59:14Z	---
VIS-PSF-09	9648.289	2026-06-01T06:54:52Z	13.8
SOPS	9662.516	2026-06-15T12:22:38Z	---
VIS-PSF-14	9675.837	2026-06-28T20:04:35Z	13.3
SOPS	9690.515	2026-07-13T12:20:30Z	---
VIS-PSF-05	9712.622	2026-08-04T14:55:46Z	22.1

The presented document is Proprietary information of the Euclid Consortium.
This document shall be used and disclosed by the receiving Party and its related entities (e.g. contractors and subcontractors) only for the purposes of fulfilling the receiving Party's responsibilities under the Euclid Project and that the identified and marked technical data shall not be disclosed or retransferred to any other entity without prior written permission of the document preparer.

SOPS	9718.527	2026-08-10T12:38:18Z	---
SOPS	9746.527	2026-09-07T12:38:42Z	---
VIS-PSF-19	9750.555	2026-09-11T13:18:15Z	4.0
SOPS	9774.534	2026-10-05T12:48:47Z	---
VIS-PSF-02	9794.441	2026-10-25T10:34:49Z	19.9
SOPS	9802.509	2026-11-02T12:12:21Z	---
VIS-PSF-01	9816.143	2026-11-16T03:25:20Z	13.6
SOPS	9830.498	2026-11-30T11:55:52Z	---
VIS-PSF-09	9837.710	2026-12-07T17:02:29Z	7.2
SOPS	9858.509	2026-12-28T12:12:20Z	---
VIS-PSF-07	9869.878	2027-01-08T21:04:23Z	11.4
SOPS	9886.485	2027-01-25T11:38:18Z	---
VIS-PSF-05	9904.541	2027-02-12T12:58:54Z	18.1
SOPS	9914.487	2027-02-22T11:40:25Z	---
SOPS	9942.529	2027-03-22T12:40:44Z	---
VIS-PSF-04	9948.506	2027-03-28T12:08:11Z	6.0
SOPS	9970.483	2027-04-19T11:35:21Z	---
[2]VIS-PSF-11	9973.687	2027-04-22T16:28:10Z	3.204
SOPS	9998.489	2027-05-17T11:43:26Z	---
VIS-PSF-09	10014.869	2027-06-02T20:50:34Z	16.4
SOPS	10026.502	2027-06-14T12:02:22Z	---
VIS-PSF-14	10040.897	2027-06-28T21:30:23Z	14.4
SOPS	10054.518	2027-07-12T12:24:43Z	---
VIS-PSF-05	10073.495	2027-07-31T11:52:25Z	19.0
SOPS	10082.481	2027-08-09T11:31:42Z	---
SOPS	10110.480	2027-09-06T11:31:09Z	---
VIS-PSF-03	10117.907	2027-09-13T21:45:52Z	7.4
SOPS	10138.507	2027-10-04T12:09:49Z	---
VIS-PSF-02	10156.417	2027-10-22T09:59:49Z	17.9
SOPS	10166.526	2027-11-01T12:36:08Z	---
VIS-PSF-11	10171.627	2027-11-06T15:02:10Z	5.1
VIS-PSF-10	10193.540	2027-11-28T12:56:48Z	---
SOPS	10194.511	2027-11-29T12:15:35Z	---

The presented document is Proprietary information of the Euclid Consortium.
This document shall be used and disclosed by the receiving Party and its related entities (e.g. contractors and subcontractors) only for the purposes of fulfilling the receiving Party's responsibilities under the Euclid Project and that the identified and marked technical data shall not be disclosed or retransferred to any other entity without prior written permission of the document preparer.

VIS-PSF-08	10212.916	2027-12-17T21:59:04Z	18.4
SOPS	10222.513	2027-12-27T12:19:00Z	---
SOPS	10250.515	2028-01-24T12:20:59Z	---
VIS-PSF-05	10269.692	2028-02-12T16:36:13Z	19.2
SOPS	10278.527	2028-02-21T12:37:36Z	---
SOPS	10306.521	2028-03-20T12:29:28Z	---
VIS-PSF-11	10316.517	2028-03-30T12:23:10Z	10.0
SOPS	10334.507	2028-04-17T12:09:39Z	---
VIS-PSF-03	10341.253	2028-04-24T06:03:54Z	6.7
SOPS	10362.490	2028-05-15T11:45:01Z	---
VIS-PSF-07	10374.117	2028-05-27T02:48:12Z	11.6
SOPS	10390.487	2028-06-12T11:40:20Z	---
VIS-PSF-15	10407.036	2028-06-29T00:50:34Z	16.5
SOPS	10418.486	2028-07-10T11:39:20Z	---
VIS-PSF-15	10441.592	2028-08-02T14:11:42Z	23.1
SOPS	10474.482	2028-09-04T11:33:34Z	---
SOPS	10502.498	2028-10-02T11:55:50Z	---
SOPS	10530.505	2028-10-30T12:06:33Z	---
[2]VIS-PSF-02	10533.817	2028-11-02T19:35:54Z	3.312
SOPS	10558.519	2028-11-27T12:26:16Z	---
VIS-PSF-09	10569.361	2028-12-08T08:39:05Z	10.8
SOPS	10586.492	2028-12-25T11:47:43Z	---
VIS-PSF-07	10601.520	2029-01-09T12:28:45Z	15.0
SOPS	10614.515	2029-01-22T12:20:38Z	---
VIS-PSF-05	10638.393	2029-02-15T09:25:23Z	23.9
SOPS	10642.484	2029-02-19T11:36:12Z	---
SOPS	10670.468	2029-03-19T11:13:35Z	---
SOPS	10698.500	2029-04-16T12:00:00Z	---
VIS-PSF-11	10703.135	2029-04-21T03:13:23Z	4.6
SOPS	10726.488	2029-05-14T11:42:25Z	---
VIS-PSF-13	10738.330	2029-05-26T07:54:51Z	11.8
SOPS	10754.491	2029-06-11T11:46:18Z	---
VIS-PSF-07	10771.146	2029-06-28T03:30:05Z	16.7

The presented document is Proprietary information of the Euclid Consortium.
This document shall be used and disclosed by the receiving Party and its related entities (e.g. contractors and subcontractors) only for the purposes of fulfilling the receiving Party's responsibilities under the Euclid Project and that the identified and marked technical data shall not be disclosed or retransferred to any other entity without prior written permission of the document preparer.

SOPS	10782.483	2029-07-09T11:34:59Z	---
VIS-PSF-06	10803.876	2029-07-30T21:00:35Z	21.4
SOPS	10810.4901	2029-08-06T11:45:49Z	---
SOPS	10838.525	2029-09-03T12:35:21Z	---
SOPS	10866.500	2029-10-01T12:00:00Z	---
SOPS	10894.510	2029-10-29T12:13:16Z	---
VIS-PSF-01	10904.389	2029-11-08T09:20:13Z	9.9
SOPS	10922.501	2029-11-26T12:01:28Z	---
VIS-PSF-10	10939.623	2029-12-13T14:56:30Z	17.1

Table 5.6: Schedule of the SOPS and of the visits to the PSF calibration fields. The period prior to the restart date is shaded in grey, with a lighter tone indicating the epoch where the PSF block consisted of F-012+F008 and a darker tone showing the period where the PSF block consisted of F-012+F015+F008. No shade indicates the period after the restart date, where the PSF blocks consist of F-012+F-015+F-013+F-008. Notes: 1. SOPS outside the required period; 2. PSF shortly after SOPS

5.2.3 EWS Patches

The schedule of the EWS, included in the full schedule of Figure 5.6, is shown in map format in Figure 5.8 in ecliptic coordinates (cylindrical projection).

The EWS patches are shown in six shades of blue, from dark to pale, each shade representing the year of observation of the patch. In the two mainlands, the observations start from the ecliptic poles progressing towards the equator. Poorer quality areas, such as the islands and the low latitudes of the mainlands are observed last. The outlines of the three EDFs, which are also covered by the EWS, are shown in green. The two polar caps are shown in two insets for a better view of the 21 polar cap patches and the EDF-N. The two dashed contours show the UNIONS and DES footprints, respectively in the northern and southern hemispheres, that provide ground-based data for Euclid. It is clear that a higher priority is given to the southern hemisphere in the first year. The small red circles indicate the six EAFs, with CDFS being enclosed by EDF-F; they are all inside the Euclid RoI except for COSMOS at the edge of the southern island. SXDS and VVDS, even though inside the RoI are just outside the footprint of the EWS in *#version_rsd*, which is justified by being in a high-stress longitude. The brown rectangles are regions skipped due to the presence of blinding stars. There are *#starsholes_enclosed* avoidance regions of different sizes and shapes. The five circles on the ecliptic plane are the avoidance zones around Mars, Jupiter, Saturn, Neptune and Uranus at the end of the survey. The largest ones, Mars and Jupiter intersect the RoI on the left side of the map, and a low latitude strip at those longitudes is masked out of the RoI.

There is also a small number of burgundy patches. These are sets of tiles that had been observed in the first year of the survey (scheduled in RSD_2024A/B/C), and are rescheduled in *#version_rsd* for reobservation. The schedule of the reobservations is detailed in Table 5.7. The majority of them, infills 407 to 416 are part of the reobservation campaign that reschedules the full set of tiles previously observed during the three survey windows of the inter-decontamination period (cf. Sect. 4.3.13). They are scheduled during the survey windows that take place exactly one year after the original observations. Although the orbital movement introduces a one-year symmetry, the schedule plan is not identical in the first two years of the survey; in particular the

The presented document is Proprietary information of the Euclid Consortium.
This document shall be used and disclosed by the receiving Party and its related entities (e.g. contractors and subcontractors) only for the purposes of fulfilling the receiving Party's responsibilities under the Euclid Project and that the identified and marked technical data shall not be disclosed or retransferred to any other entity without prior written permission of the document preparer.

second year has the new EGBS and the large F-010 observation. Thus, the survey windows are not identical in the two years and there is no time to observe all tiles of the patches to be repeated in the three equivalent survey windows of the second year. For that reason, part of the observations is scheduled later in infills 415 and 416. Moreover, we note the same areas are not necessarily observed with identical patches as in the first observation, or even with the same number of patches as before. In addition, there are two sets of tiles, infills 401 and 402, that are not part of the reobservation campaign, but are a repetition of failed or skipped observations, and are implemented with the small infill mechanism. The total area reobserved with infills amounts to 534.9 deg^2 that replace observations previously planned to take place during those times.

ID	MJD2000	Duration (days)	Year	Type	Original ID	Area (deg^2)
INFILL-407	9214.770	5.395	1.1082	large	Patches 14-18	48.2
INFILL-408	9220.172	5.859	1.1230	large	Patches 14-18	56.5
INFILL-409	9226.037	3.797	1.1390	large	Patches 14-18	35.6
INFILL-410	9230.551	0.357	1.1514	large	Patches 24-25	4.4
INFILL-411	9230.911	5.449	1.1524	large	Patches 24-25	51.1
INFILL-412	9240.808	2.110	1.1795	large	Patches 24-25	19.2
INFILL-413	9243.171	17.763	1.1860	large	Patches 24-25	167.8
INFILL-414	9276.713	12.937	1.2778	large	Patch 34	119.4
INFILL-401	9366.996	0.305	1.5250	small	Obs 1-6	2.6
INFILL-402	9378.134	0.664	1.5555	small	Obs 3496-3508	5.7
INFILL-415	9400.426	0.564	1.6165	small	Patches 14-18	4.7
INFILL-416	9452.274	2.255	1.7584	small	Patch 34	19.7

Table 5.7: Schedule of the EWS reobservations implemented in *#version_rsd*, with an indication of their area. Observations scheduled in the reobservation campaign period are shaded in light grey. The original patches or observation IDs used in *#plan_basis* are also given

The bottom part of Figure 5.8 contains two sets of six lines, each line corresponding to a year. They contain all survey windows vertically aligned with the longitude where they may be scheduled. Each window is schedulable in two orbital positions (with the telescope pointing in the leading or in the trailing direction). The one actually observed is filled in a shade of blue, while the other is left in grey. In one of the two scheduling opportunities it is summer season while in the other it is winter season, where the scheduling is more difficult. The summer/winter season in the North/South is indicated by the two sets of long/short arrows in the header.

At the end of the nominal mission, the EWS footprint is very compact, with no gaps between patches. However, there is not enough time to cover the full RoI. The region left uncovered, shown in light green in Figure 5.8, contains the lowest S/N areas of the RoI. It is located at lower ecliptic latitudes, both in the mainland and in the islands. In contrast with previous RSDs, the small northern island is not covered at all, trading-off with a more compact covering of the southern island.

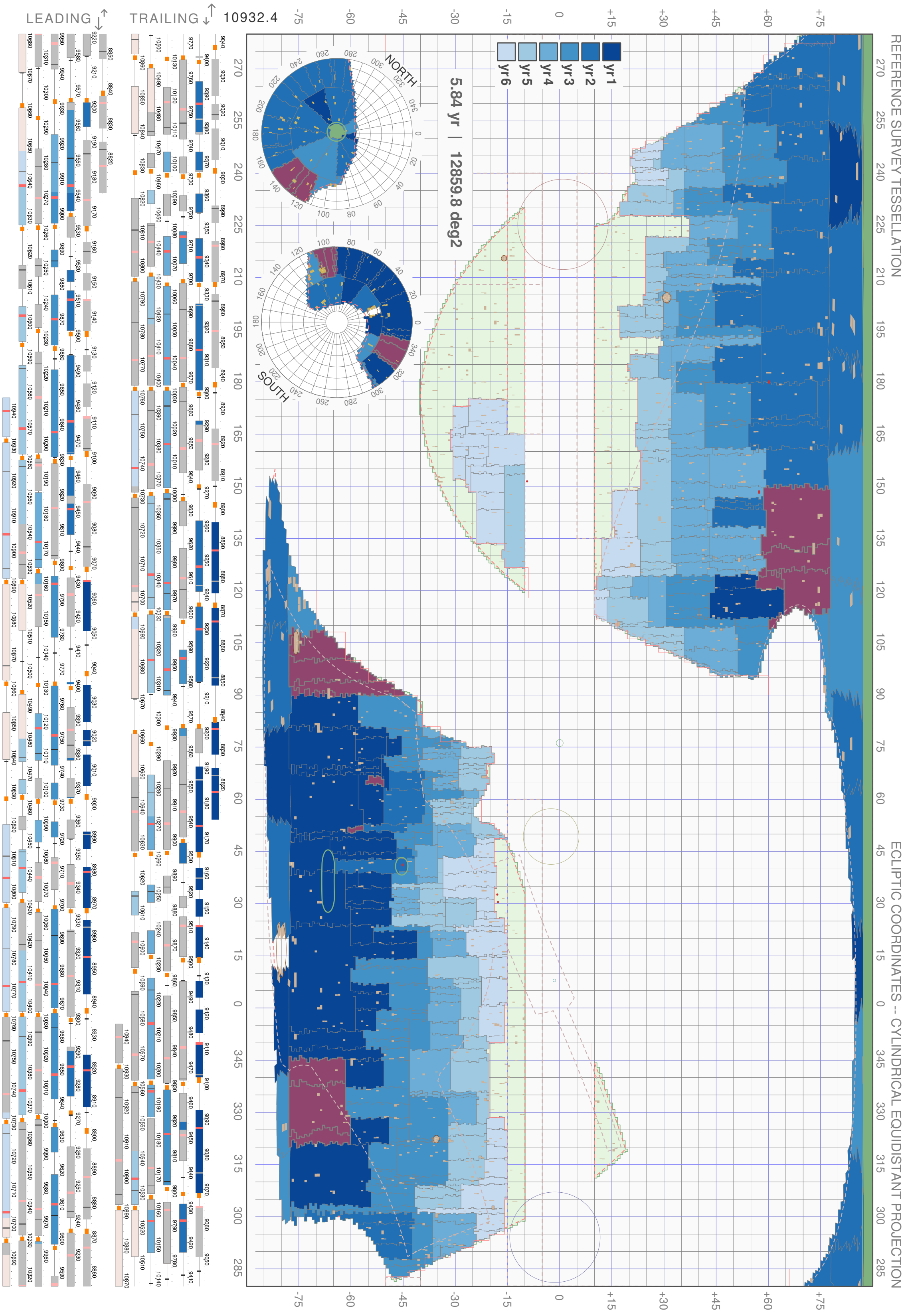

Figure 5.8: Euclid footprint in ecliptic coordinates, showing the time progression of the sky coverage

The presented document is Proprietary information of the Euclid Consortium.
This document shall be used and disclosed by the receiving Party and its related entities (e.g. contractors and subcontractors) only for the purposes of fulfilling the receiving Party's responsibilities under the Euclid Project and that the identified and marked technical data shall not be disclosed or retransferred to any other entity without prior written permission of the document preparer.

6 Analysis

6.1 Euclid footprint

6.1.1 Area

The final observed area reached by the EWS is *#ews_area_observed*. The reobserved EWS tiles are only counted once, their pre-restart observations being discarded from the calculation. Within the compact EWS enclosed areas there is an additional fragmented area of *#starsholes_enclosed_area* that is not observed due to the presence of blinding stars. Hence, the EWS footprint encloses a larger area of *#ews_area_enclosed*, on which the area lost for blinding stars is *#starsholes_enclosed_areafrac*. The observed EWS area is distributed by the four RoI regions as follows:

- Northern mainland observed area = 6015.3 deg^2 (82.5% complete)
- Southern mainland observed area = 6156.2 deg^2 (88.1% complete)
- Northern island observed area = 0 deg^2 (0 % complete)
- Southern mainland observed area = 686.9 deg^2 (32.6% complete)

Figure 6.1 shows the progress of the EWS observed area with time, also showing that the required EWS area of 14,000 deg^2 is not reached within the nominal mission duration of *#time_duration*.

In the first semester of the survey there is a long period without progression. During this time there were observations made but they were rescheduled for reobservation in the second year, hence do not contribute to the total area. In the final years, the EWS progression is stalled during the low-pressure periods, giving rise to unallocated time, amounting to *#unallocated_time*. The unallocated time is converted into an effective area of *#unallocated_area* by considering that an average ROS observation, including a typical field slew, has a duration of *#ros_total* and that the Euclid FoV is placed on a tile of *#fov_tile_effective*. The effective unallocated area corresponds to the area that could be observed by non-overlapping ROS observations during the unallocated time.

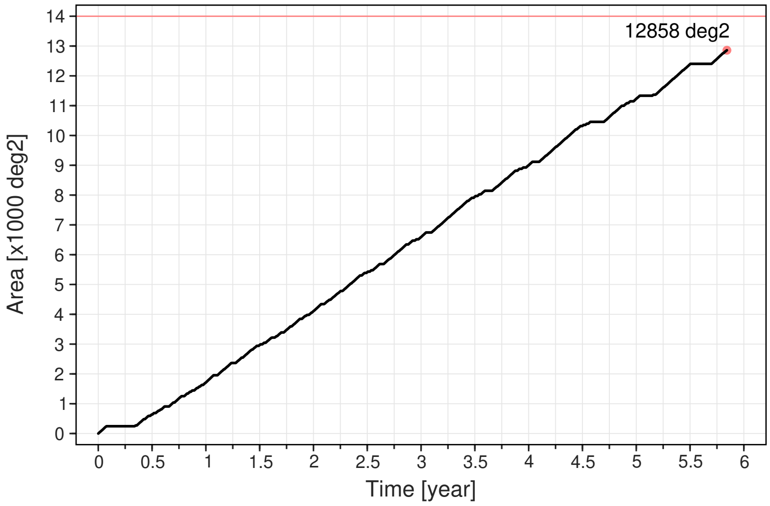

Figure 6.1: Area progression of the EWS

The presented document is Proprietary information of the Euclid Consortium.
This document shall be used and disclosed by the receiving Party and its related entities (e.g. contractors and subcontractors) only for the purposes of fulfilling the receiving Party's responsibilities under the Euclid Project and that the identified and marked technical data shall not be disclosed or retransferred to any other entity without prior written permission of the document preparer.

Table 6.1 reports the EWS area observed per year. The survey has a slow start in the first year, not only because of the many calibrations that take place then but mainly due to the lost observations. The area of 2500 deg^2 is only reached #time_2500_ews years into the survey. In the next years the area progression is kept at around 18% per year, including in the 5th year, meaning unallocated time only appears later, compared to previous RSD versions. The drop in the final year is always less severe than in previous versions.

Comparing with the progression of the EDS, cf. Table 5.4, we note that the EDS generally builds up at a faster pace than the EWS, only slowing down in the third year. This is due to the relatively lower number of EDF-N observations in the third year, when the time is needed to finish the observations that were displaced from the second year by the reobservation campaign. During the 4th year the EDS grows again faster, with EDF-N using the low-stress longitudes to delay the start of unallocated time. This comparison is relevant for the usage of the EDS as a WL noise bias field, which requires the EDS must grow at a faster rate than the EWS.

Year	Area per year (deg^2)	Fractional Area per year	Cumulated Area (deg^2)	Cumulated Fractional Area
1	1718.1	13.4 %	1718.1	13.4 %
2	2392.5	18.6 %	4110.6	32.0 %
3	2481.5	19.3 %	6592.1	51.3 %
4	2407.7	18.7 %	8999.8	70.0 %
5	2238.0	17.4 %	11237.8	87.4 %
6	1620.6	12.6 %	12858.4	100.0 %

Table 6.1: EWS area observed per year, and its cumulated progression

Table 6.2 shows the EWS cumulated area observed in each ecliptic hemisphere at the end of each year. The percentages shown refer to the final observed area of the Euclid footprint in each hemisphere, which is larger in the southern hemisphere. The north/south ratio takes into account the different total areas of the two hemispheres.

Year	North (deg^2)	South (deg^2)	N:S ratio	North fraction in UNIONS	South fraction in DES
1	190.4 (3.2%)	1527.8 (22.3%)	12:88	99.0%	88.6%
2	1884.4 (31.3%)	2226.1 (32.5%)	49:51	97.9%	79.1%
3	2999.4 (49.9%)	3592.8 (52.5%)	49:51	89.3%	80.6%
4	4584.2 (76.2%)	4415.6 (64.5%)	54:46	74.9%	77.6%
5	5679.6 (94.4%)	5558.0 (81.2%)	54:46	75.4%	70.9%
6	6015.3 (100%)	6843.2 (100%)	50:50	74.6%	63.0%

Table 6.2: Cumulated EWS area observed per hemisphere at the end of each survey year

During the first year there is a very strong north-south asymmetry. This is the outcome of the strategy of prioritizing the coverage of the DES footprint where there is ground-based data

The presented document is Proprietary information of the Euclid Consortium.
This document shall be used and disclosed by the receiving Party and its related entities (e.g. contractors and subcontractors) only for the purposes of fulfilling the receiving Party's responsibilities under the Euclid Project and that the identified and marked technical data shall not be disclosed or retransferred to any other entity without prior written permission of the document preparer.

available, in detriment of the north hemisphere covered by the ground-based UNIONS. The north-south equilibrium is reached in the second year. Also shown is the fraction of the observed area in the northern (southern) hemisphere at the end of each year that is within the UNIONS (DES) footprint. The detailed progression of the Euclid coverage of the UNIONS and DES areas is shown in Figure 6.2. At #time_2500_ext years into the survey, EWS reaches 2500 deg^2 of the DES and UNION footprints.

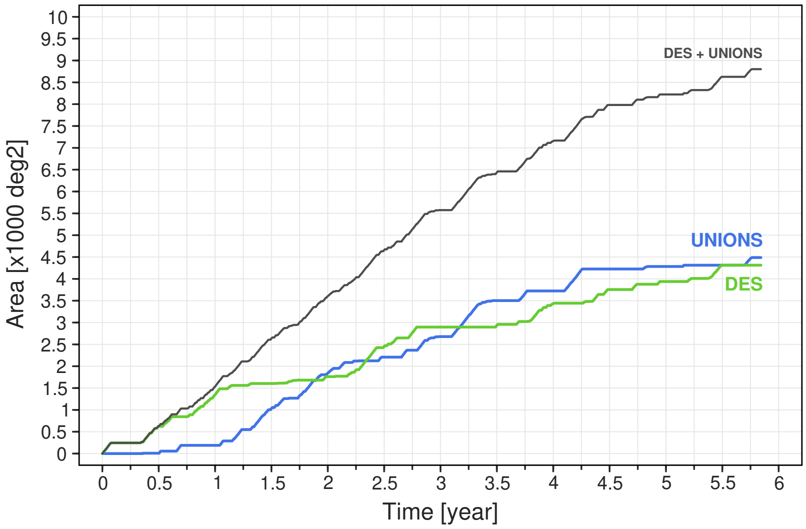

Figure 6.2: Area progression of the EWS coverage of the UNIONS and DES footprints

Finally, the progression of unallocated time is given in Table 6.3. The unallocated time takes place mostly in the final two years of the survey.

Year	Time (days)	Cumulated time (days)	Cumulated Fractional time (%)
1	0	0	0
2	0	0	0
3	0	0	0
4	0	0	0
5	26.2	26.2	24.6%
6	80.1	106.3	100.0%

Table 6.3: Unallocated time at the end of each survey year

6.1.2 Overlap

The global overlap is computed by measuring and summing up the areas of all overlapping polygonal fragments in the EWS. The total overlapping area amounts to *#overlap_global_area*, in agreement with the estimate given in Sect. 4.3.3. This is a fraction of *#overlap_global* of the EWS area, resulting in a total non-overlapped area in the EWS of *#ews_area_overlapfree*.

We can alternatively estimate the overlap by considering the number of observations used to observe the total area. We start by estimating in a mean effective area covered by one EWS observation, knowing that the EWS footprint is covered with 26778 fields, of which *#count_fields_polar* are in the polar caps. This effective area of the observed field can be used to estimate the mean field overlap in the Euclid footprint as (tile_area - field_eff_area)/tile_area. The results are given in Table 6.4. As expected, the opverlap is much larger in the polar caps. However, this method seems to underestimate the direct computation of the overlapping area of *#overlap_global* quoted above. We note the estimate does not include the areas in star holes since they are avoided by construction.

	#Fields	Area (deg^2)	Field effective area (deg^2)	Tile area (deg^2)	Field overlap in area
Polar caps	1345	587.1	0.4365	0.5508	20.8%
Global tessellation EWS	25 433	12 271.3	0.4825	0.5508	12.4%
Total EWS	26 778	12 858.4	0.4802	0.5508	12.8%

Table 6.4: Breakdown of the EWS footprint area. The effective unique area surveyed by the Euclid field is smaller in the polar caps than in the global tessellation region. In both cases it is smaller than *#fov_tile_ effective* that only accounts for the overlap due to the tilting strategy (10%) but not for the natural overlap due to the convergence of the meridians (4%)

Another relevant quantity is the field-to-field overlap, defined as the overlapping area of each FoV. The distribution of the field-to-field overlap is shown in Figure 6.3. We note that the sum of the values of the histogram is much larger than *#overlap_global_area*, since adjacent FoVs share overlapped regions that are accounted multiple times in the histogram. The values range from a minimum of 57.5 $arcmin^2$ to a maximum of 0.552 deg^2 (cases where the full tile is overlapped), with a mean of *#overlap_f2f_mean*. On the minimum end, there are only four cases with overlap below 100 $arcmin^2$. Assuming an average overlap of 100/4 $arcmin^2$ per side of the FoV, of rectangular shape and with length given by the longest side of the FoV (0.778 deg), the width of a 25 $arcmin^2$ rectangle is 32 arcsec. There are thus four cases with a linear overlap potentially below 32 arcsec.

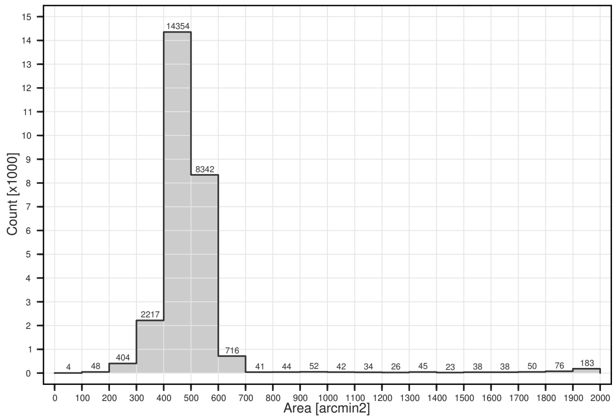

Figure 6.3: Distribution of field-to-field overlaps over the EWS

6.1.3 S/N properties

The S/N of ROS observations over the whole RoI was discussed in Sect. 4.3.2. Here, we consider the S/N in the EWS footprint of *#version_rsd*. Figure 6.4 to Figure 6.6 show the distributions of the S/N in the EWS footprint for I_E (most relevant for WL), Y_E, H_E, J_E and RG_E (most relevant for GC), respectively. Table 6.5 gives the median S/N values over the EWS footprint for the five bands in each of the quadrants of the footprint.

The values are larger in the footprint than in the RoI in both mainlands, showing that the best areas of the RoI are observed. Concerning the islands, the northern island is not observed in *#version_rsd*, and the southern island have a poorer coverage than the mainlands but still manages to get its best areas observed.

For VIS (I_E), a S/N above 10 is achieved over the whole RoI, with an average above 16, a significant gain over the requirement. The NISP spectroscopy (RG_E) has a negligible area below S/N = 3.5. The S/N of NISP photometry (J_E, H_E, Y_E) is always above 5.

	Northern Mainland	**Northern Island**	**Southern Island**	**Southern Mainland**
I_E	16.73	-	13.85	17.04
Y_E	6.80	-	5.77	6.88
J_E	8.11	-	6.81	8.21
H_E	7.51	-	6.29	7.60
RG_E	4.69	-	3.86	4.76

Table 6.5: Median values of the S/N for each of the 5 Euclid EWS bands in each of the three regions of the *#version_rsd* footprint

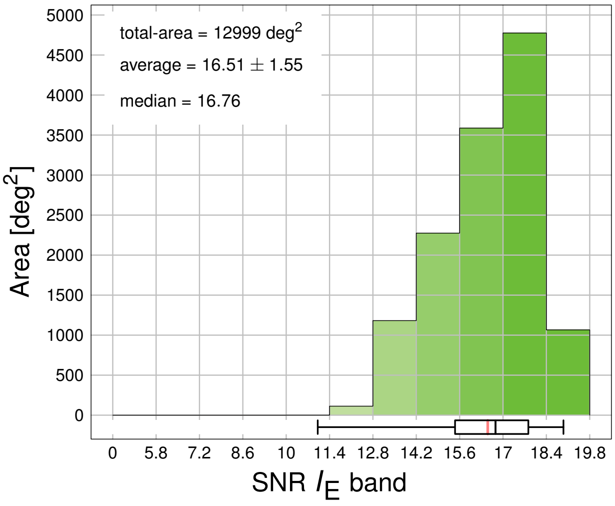

Figure 6.4: Distribution of VIS S/N on the *#version_rsd* footprint

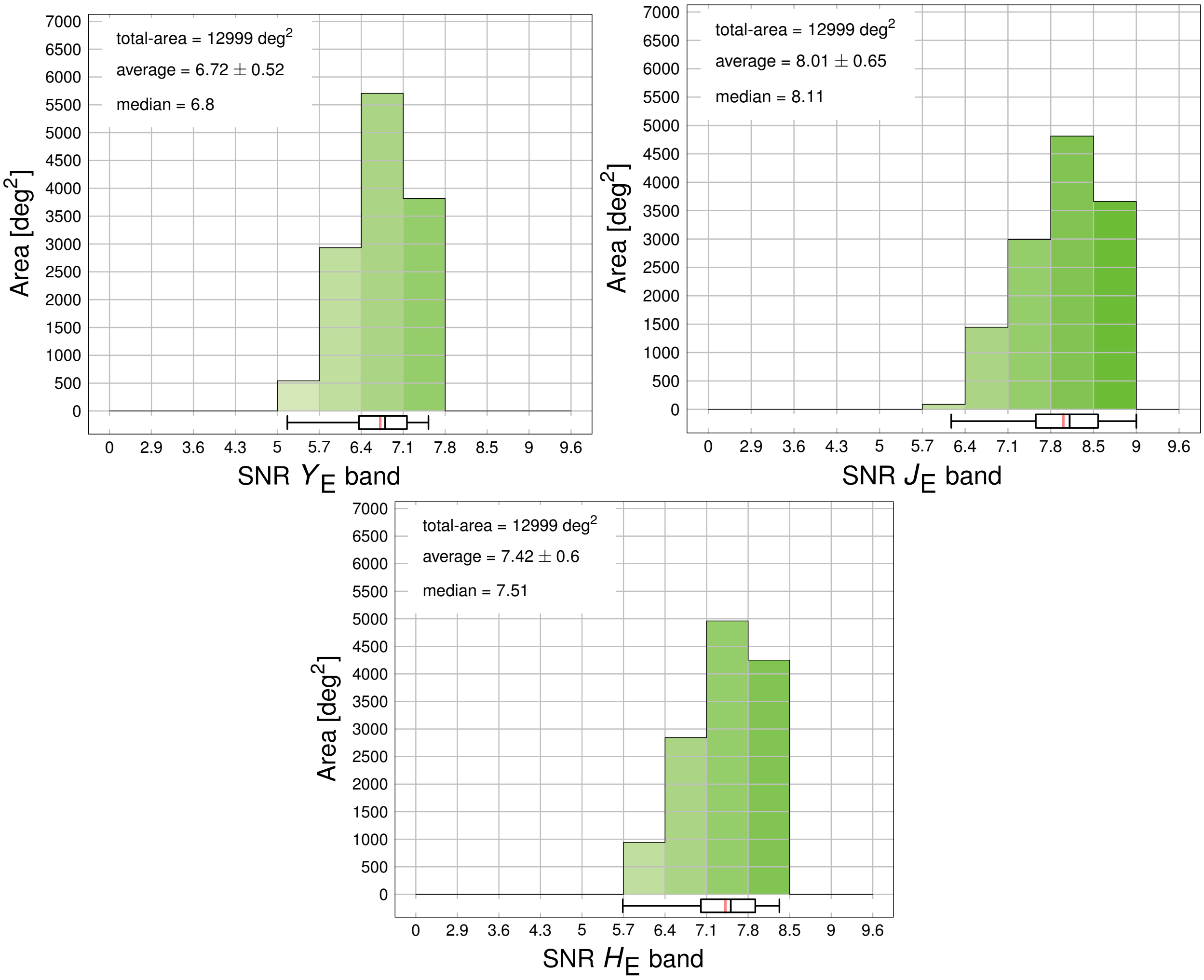

Figure 6.5: Distribution of NISP-P S/N on the #*version_rsd* footprint

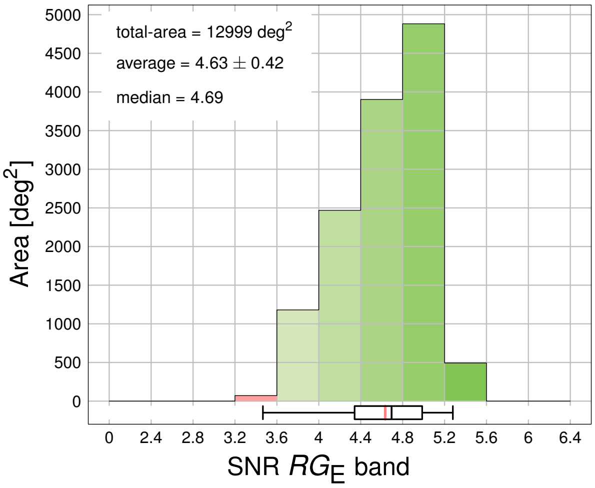

Figure 6.6: Distribution of NISP-S (red grism) S/N on the #*version_rsd* footprint

The presented document is Proprietary information of the Euclid Consortium.
This document shall be used and disclosed by the receiving Party and its related entities (e.g. contractors and subcontractors) only for the purposes of fulfilling the receiving Party's responsibilities under the Euclid Project and that the identified and marked technical data shall not be disclosed or retransferred to any other entity without prior written permission of the document preparer.

The merit function Q is computed from the S/N values normalized by the full range of S/N in the footprint, as defined in Sect. 4.3.2. The histogram of the Q values in the Euclid footprint is shown in Figure 6.7 (left panel). We note the parameter is always above *#quality_q_min*. For comparison, in a previous weight parameter (given by the number of GC galaxies obtained from simulations) the lowest value was less than half of the highest value. This shows that the worst quality areas for GC and WL do not coincide; the minimum in I_E S/N is not at the same location as the minimum in RG_E.

The right panel of Figure 6.7 shows the time evolution of the merit function as the EWS progresses. The behavior on large timescales is indicated by the red line that depicts the time-averaged Q. Its amplitude decreases with time due to the strategy of observing from high to low ecliptic latitudes, which leads to an increase of the zodiacal background on large timescales, showing the observations go from the best to the worst areas. On small timescales the instantaneous Q values oscillate as the observations move along ecliptic longitude. Indeed, the background increases along longitude as the observations cross the galactic plane that traverses the ecliptic meridians.

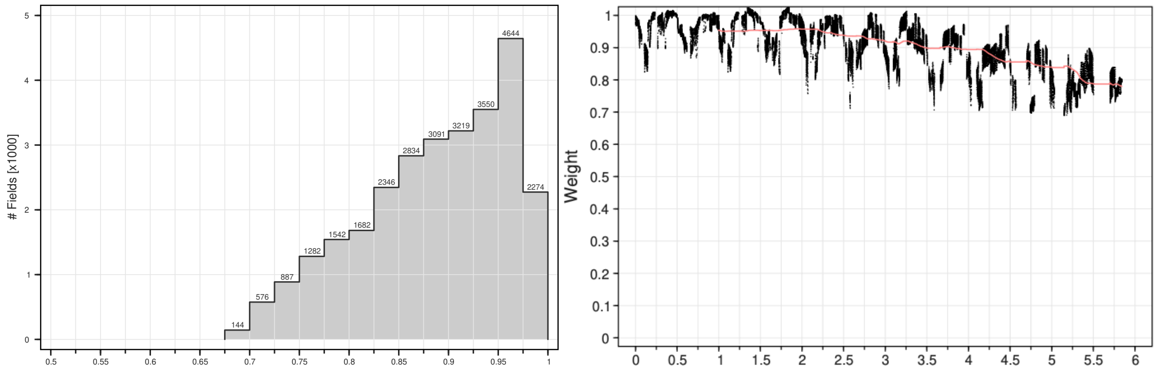

Figure 6.7: The merit function of the observed EWS fields: distribution (left panel) and time evolution (right panel)

6.1.4 The Euclid fields

The Euclid footprint defined by the EWS also contains the EDS and other fields useful for science. The repeated visits to the Deep fields and to some of the calibration fields that use the ROS (or ROS_D1), form a set of 10 fields observed in all channels that are deeper than the EWS and in some cases even deeper than the EDS.

Table 6.6 shows some properties of these “Euclid Fields”. The fields consist of the Deep fields, the Auxiliary fields for sample characterization and the Self-calibration field. They are listed in the table in decreasing order of depth. The depth is given by the difference in magnitude with respect to the depth of EWS and is computed as

$$\Delta m = 2.5\log(\sqrt{N\_visits\_eff})$$

where the effective number of visits is used in the estimate (and not the actual number of visits performed to compensate the background).

The presented document is Proprietary information of the Euclid Consortium.
This document shall be used and disclosed by the receiving Party and its related entities (e.g. contractors and subcontractors) only for the purposes of fulfilling the receiving Party's responsibilities under the Euclid Project and that the identified and marked technical data shall not be disclosed or retransferred to any other entity without prior written permission of the document preparer.

The depth of CFDS includes the overlapping EDF-F visits. Each visit to the self-cal makes 76 ROS_D1 pointings, equivalent to 76/4 ROS visits, with the pointings spread out on an area of roughly 4 FoVs; hence the effective number of visits per month to a FoV-equivalent area is 4.75 to which the EDF-N visits must be added. The resulting depth is a mean value over the self-cal field (depth is not homogeneous across the field). Other properties given in Table 6.6 are the approximate area of the field, the semester of completion, and the indication whether the field is contained within the EWS footprint. COSMOS is just outside the southern island of the RoI. The SXDS and VVDS fields are close to the edge of the southern mainland in a high-stress region of the RoI, hence due to stochasticity they may end up either being inside or outside in different RSD versions.

Field	**Completion** (semester)	**Area** (deg^2)	**Visits (effective)**	**Δm**	**EWS Footprint**
Self-Cal	12	2.5	304 + 40	3.17	in
CDFS	2	0.5	25 + 40	2.27	in
EDF-N	10	20	40	2.00	in
EDF-F	12	10	40	2.00	in
EDF-S	12	23	40	2.00	in
COSMOS	5	2	25	1.75	out
SXDS	8	2	25	1.75	out
VVDS	10	0.5	25	1.75	out
CANDELS/AEGIS	2	1	16	1.50	in
CANDELS/GOODS-N	9	0.5	16	1.50	in

Table 6.6: Properties of the Euclid Fields

6.2 RSD time budget

This section presents, in two sub-sections, the distribution of the time allocated in *#version_rsd* per observation type. The first sub-section details the time allocated for target observations, while the second one includes all components of the RSD. The replanning introduces the possibility of scheduling the same observation twice (or multiple times, which does not occur in *#version_rsd*). This brings an ambiguity in the accounting of the allocated times. We adopt the following criteria:

- Observations that are scheduled once (which are the majority of cases): They are naturally accounted for only once.
- Observations that were not executed (replaced with decontamination campaigns or for other reasons) but are not rescheduled, usually skipped calibrations that do not require to be recovered: They are accounted for under “skipped”, and do not contribute to the total time of their observation type.
- Observations that were not executed and are rescheduled for a second observation in *#version_rsd*, such as skipped EWS observations: They need to be accounted for twice since both instances contribute to the total RSD time. The rescheduled observation contributes to

the total time of its observation type while the original skipped observation is accounted for under "skipped".

- Observations that were flagged as unusable (due to solar activity, instrument failure or other reasons) but are not rescheduled, usually calibrations that do not require to be recovered: They contribute to the total time of their observation type, since they were executed as such and were not replaced in the rescheduling.
- Observations that were flagged as unusable and are rescheduled for a second observation in *#version_rsd*, such as EWS observations: They need to be accounted for twice since both instances contribute to the total RSD time. The rescheduled observation contributes to the total time of its observation type. However, the original observation that turns out to be unusable, even though executed as part of a given observing type is accounted for under "lost". This avoids counting the time of the same EWS observation twice which would be inconsistent with the area count.

6.2.1 Targets budget

Table 6.7 shows the distribution of the time allocated in *#version_rsd* to the various targeted observations, i.e, instrument calibrations, auxiliary fields, Deep fields (including CPC) and additional surveys. We note that the self-calibration field is here included in the EAFs budget and not in the instrument calibrations, since its repeated observations make it the deepest of the Euclid fields. Grism sanity observations, which are usually at the center of a Deep field, are also included in the EAFs.

Instrument Calibrations	F-007: VIS non-linearity	29.5 d	166.2 days
	F-008: VIS PSF model	29.3 d	
	F-009: NISP-S non-linearity	82.7 d	
	F-010: NISP-S wavelength dispersion	6.9 d	
	F-011: NISP reciprocity failure	2.3 d	
	F-012: VIS flat-band voltage shift	1.3 d	
	F-013: Photometric calibration	2.8 d	
	F-015: VIS serial trap pumping	4.8 d	
	F-016: VIS charge injection timing	1.4 d	
	F-018: NISP persistence	5.2 d	
Auxiliary Fields	F-005: Photo-z calibrations	31.9 d	103.5 days
	F-004: Color gradient calibrations	2.8 d	
	F-001: Self-Calibration	68.7 d	
	F-017: Grism sanity	0.1 d	
Deep Fields	F-002/3: EDF-North	86.0 d	261.7 days
	F-002/3: EDF-South	114.4 d	
	F-002: EDF-Fornax	61.3 d	

Additional surveys	Galactic Bulge Survey	1.2 d	1.2 days
			532.6 days (25.0 % of the RSD duration)

Table 6.7: Time budget for the Calibration and Deep observations

The breakdown in the four categories is:

- Instrument calibrations: 31.2%
- Auxiliary fields: 19.4%
- Deep fields: 49.2%
- Additional surveys: 0.2%

while the breakdown per target is shown in Figure 6.8.

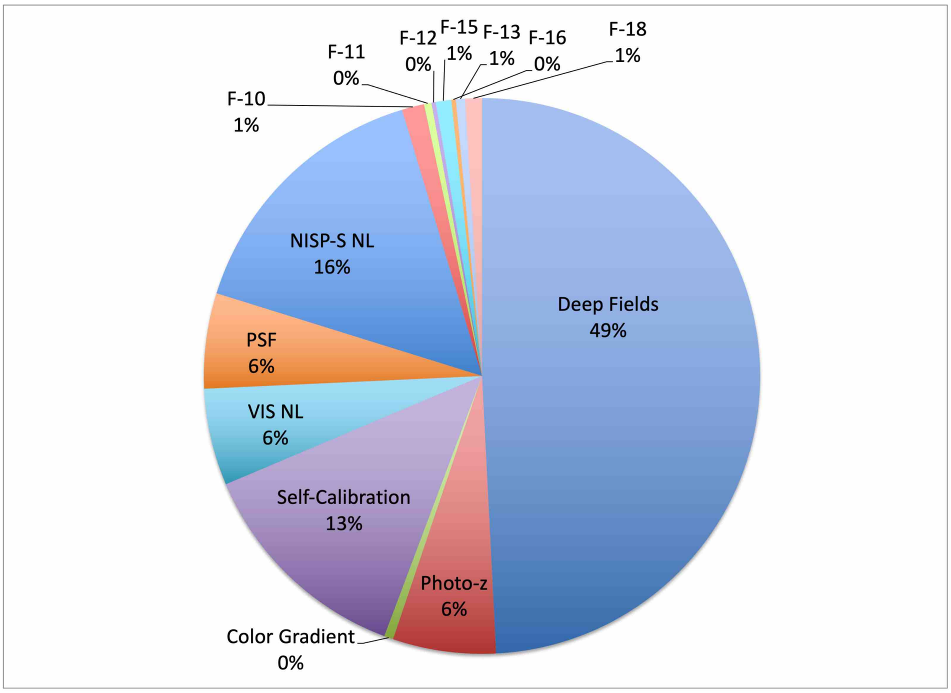

Figure 6.8: Breakdown of the time used to complete the EDS and all calibration observations, per calibration block

The presented document is Proprietary information of the Euclid Consortium.
This document shall be used and disclosed by the receiving Party and its related entities (e.g. contractors and subcontractors) only for the purposes of fulfilling the receiving Party's responsibilities under the Euclid Project and that the identified and marked technical data shall not be disclosed or retransferred to any other entity without prior written permission of the document preparer.

6.2.2 Full RSD budget

The time taken in *#version_rsd* by the various components of the RSD is shown in Table 6.8 and in Figure 6.9.

EWS	Global tessellation	1305.3 d	1374.3 days
	Polar caps	69.0 d	
Euclid Fields	EDS	261.7 d	365.2 days
	EAFs	103.5 d	
Instrument calibrations			166.2 days
Unallocated time			106.4 days
Lost observations	EWS	61.0 d	81.3 days
	EDS	15.4 d	
	EAFs	4.9 d	
SOPS			19.0 days
Skipped observations	Decontamination #1	8.4 d	14.2 days
	Decontamination #2	5.5 d	
	Others	0.3 d	
Patch-to-patch slews			6.7 days
Additional surveys	EGBS	1.2 d	1.2 days
			2134.5 days (100% of the RSD duration)

Table 6.8: Time used by each component of the RSD in *#version_rsd*

Besides EWS, Euclid fields and calibrations, the total amount of time of executed lost observations and non-executed skipped ones is also given. All observations include two components: (i) the duration of a pointing in the sequence (which includes exposure times and dither slews for ROS observations) and (ii) the slew time to reach the next pointing in the sequence (dither or field slews in the case of non-ROS observations, and tile-to-tile field or large slews in the case of ROS observations). Patch-to-patch slew times at the end of the observing sequences (either between EWS patches, or from/to EWS to other observations) are the only slews not included in the observing sequences times and are given separately. Table 6.8 also shows the duration of the SOPS windows, the EGBS, and the total time remaining unallocated.

The presented document is Proprietary information of the Euclid Consortium.
This document shall be used and disclosed by the receiving Party and its related entities (e.g. contractors and subcontractors) only for the purposes of fulfilling the receiving Party's responsibilities under the Euclid Project and that the identified and marked technical data shall not be disclosed or retransferred to any other entity without prior written permission of the document preparer.

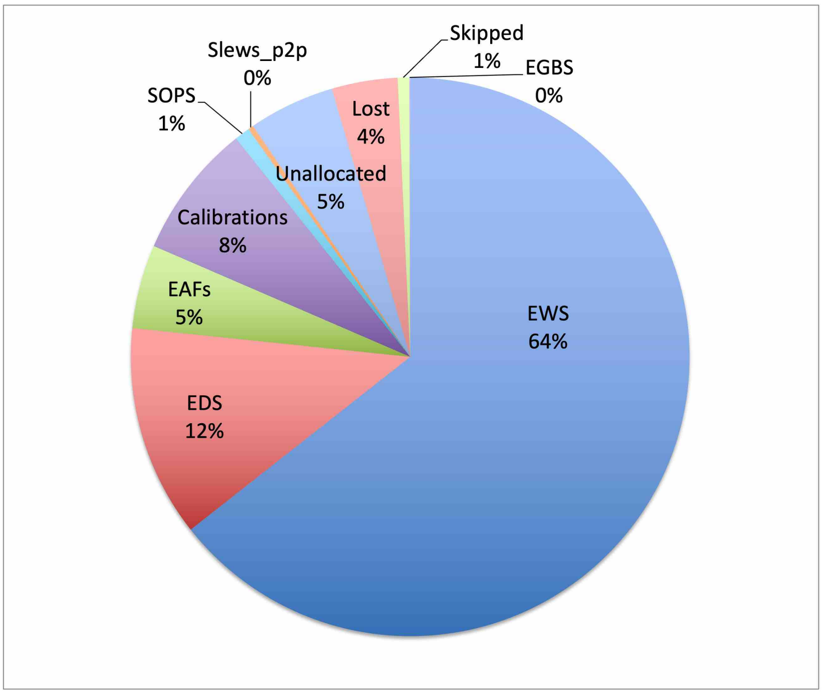

Figure 6.9: Breakdown of the time usage in *#version_rsd*

6.3 Survey statistics

6.3.1 Number of observations

As defined in [AD04], each observation has a unique *pointing-id*. For ROS observations one set of four dithered pointings is identified by one *obs-id*. For non-ROS observations all the pointings of a single visit share a single obs-id, with the exception of F-009 and F-010 that consist of 2 and 11 sub-sequences, respectively, each with its own obs-id. One obs-id and one pointing-id are also assigned to the SOPS, while the EGBS is scheduled as reserved time with no ids assigned. A spatially contiguous sequence of pointings is assigned one *patch-id*. For EWS observations one survey window may contain various patches, while for non-EWS ROS observations one full visit to a EDF or a EAF is one patch consisting of several obs-ids. For most non-ROS observations one visit defines one patch, with the exception of F-009 and F-010 where each of its sub-sequences defines a patch.

[AD01] constrains the total number of *fields*. In this context, a set of dithered frames counts as one field. Thus, in the case of ROS observations, one field corresponds to one obs-id, while for non-ROS observations, each pointing-id is one field. We count lost fields twice (the original executed one and its reschedule), and skipped fields only once (the reschedule, since the original one was not executed). The skipped fields are: 6 initial EWS tiles; 1 monthly block + 1 biannual block (decontamination #1); 8 EWS + North-cap-06 (decontamination #2), and they form 5 non-EWS patches and 1 EWS patch. *#version_rsd* thus contains:

- *#count_fields_total* fields, *#count_fields_wide* of which in the EWS
- *#count_patches_total* observation sequences, *#count_patches_wide* of which are EWS patches

We note that the number of EWS fields quoted in Table 6.4 is smaller than *#count_fields_wide* where, for the purpose of computing the effective overlap, the number of lost fields was only counted once.

6.3.2 Pointing angles

The distribution of SAA and AA values implemented in *#version_rsd* is shown in Figure 6.10. The shape of the SAA histogram reflects the fact that observations are not always made in transit. They are made either de-pointing towards the Sun with SAA peaked at 89 deg or de-pointing away from the Sun using a broad range of SAA forming the tail of the histogram. Roughly *#solar_saapeak* of the observations have SAA values between 89 and 92 deg, in contrast with the 70% used in pre-launch RSDs. The SAA values implemented range from *#solar_saamin_used* to *#solar_saamax_used*. In contrast, the histogram of AA values is narrower than in pre-launch configurations, since the tilt tolerance allows us to keep a narrow AA range in the EWS observations. Roughly *#solar_aapeak* of the observations keep AA between -5 and -4 deg. The AA values implemented range from *#solar_aamin_used* to *#solar_aamax_used*.

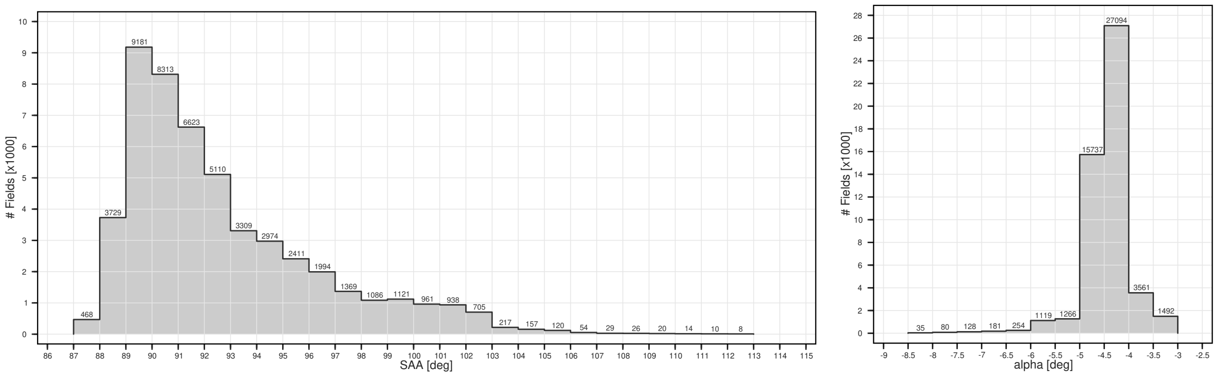

Figure 6.10: Distribution of pointing angles for all fields in the survey: SAA (left panel) and AA (right) panel

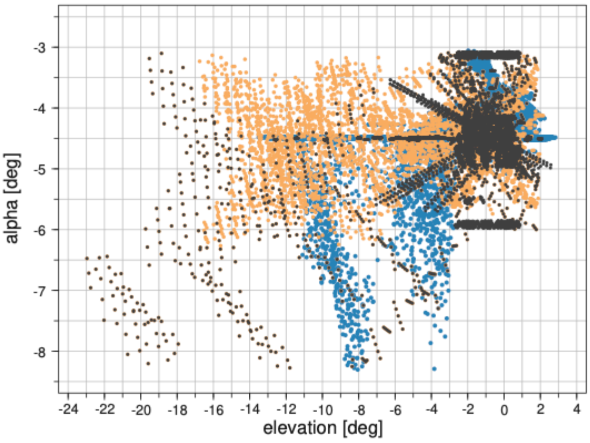

Figure 6.11: Distribution of pointing angles for all fields in the survey in the AA vs elevation plane, where elevation = 90 deg - SAA. Colors show the pointing type: EWS (orange), EDS (blue), Calibrations (black)

The presented document is Proprietary information of the Euclid Consortium.
This document shall be used and disclosed by the receiving Party and its related entities (e.g. contractors and subcontractors) only for the purposes of fulfilling the receiving Party's responsibilities under the Euclid Project and that the identified and marked technical data shall not be disclosed or retransferred to any other entity without prior written permission of the document preparer.

The solar angles used in every pointing of *#version_rsd* are shown in Figure 6.11, with colors representing the pointing type (EWS, EDS, calibrations). Figure 6.12 is a binned representation (in logarithmic bins) of the same information for four sub-sets of the RSD data.

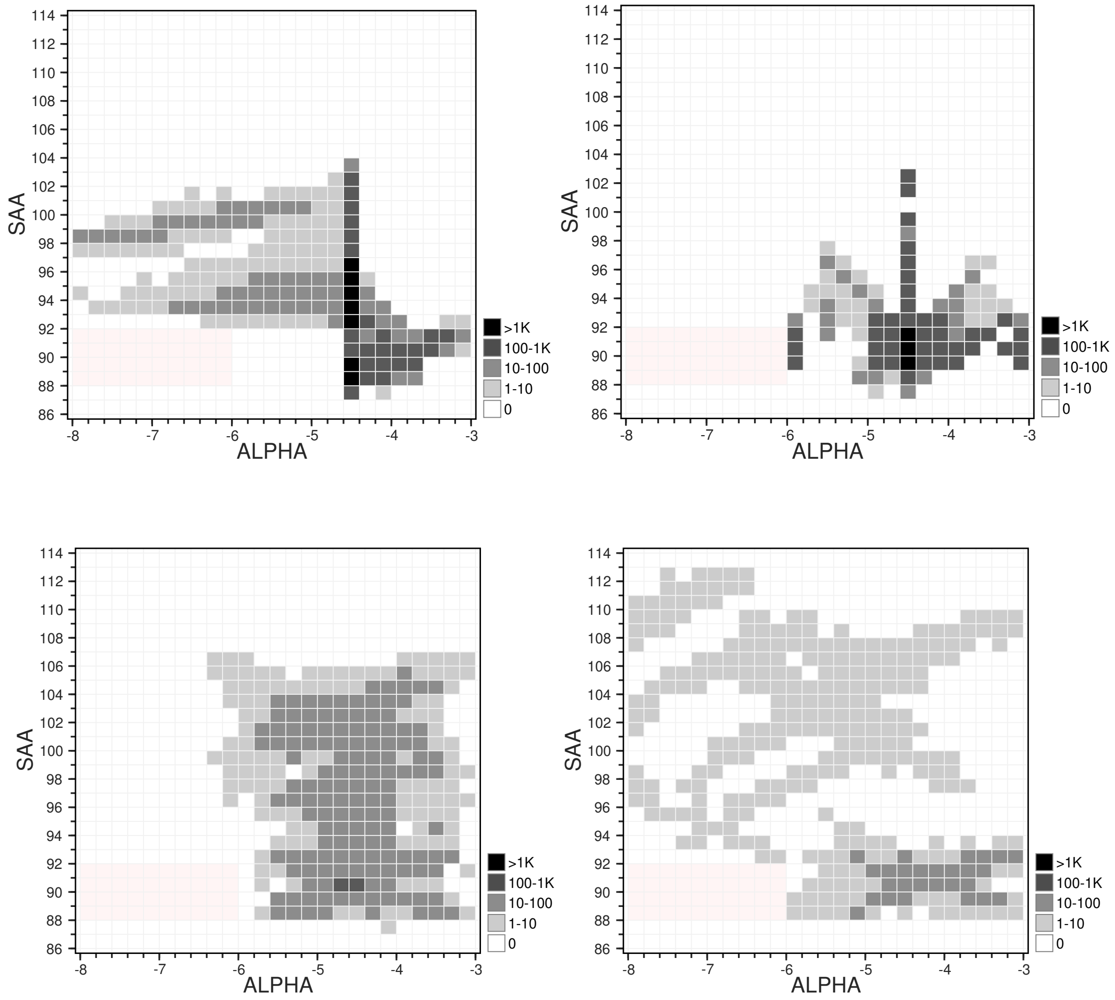

Figure 6.12: Binned distribution of pointing angles for all fields in the survey in the AA, SAA plane, for sub-sets of the RSD data. Upper left panel: EWS. Upper right panel: instrument calibrations and EAFs. Lower left panel: EDS, excluding CPC observations. Lower right panel: CPC observations

It is clear that the stray light leak region of SAA = [88, 92] deg with AA < -6 deg is successfully avoided (light pink areas on the lower left side of the panels in Figure 6.12). Most observations of the EWS are made with AA = -4.5 deg, with very few observations below AA = -6.5 deg or above AA = -3.5 deg and none above SAA = 104 deg. There is an anti-correlation in the EWS plot, with observations with low SAA being taken with high AA values. Calibrations are even more confined in the AA, SAA plane and do not show the same correlation as EWS ones. EDS extends less into low values of AA and slightly more into high SAA values, and we note that AA was not kept fixed in these observations. CPC observations are the only ones using the largest SAA values, which are needed to fulfill the required spectra directions.

Figure 6.13 shows the progression of SAA along the survey. The largest excursions in SAA are the “saw-like” structures in the first year, corresponding to CPC-South observations that use the longitude reach to be able to be scheduled with the required directions. In the fifth year, the EWS patches are generally observed with higher SAA values due to the fact that by then, on lower latitudes, the patches are shorter and extend in longitude, deviating more from transit. The progression of the SAA field-to-field variation along the time is shown in Figure 6.14. The large spikes in the first year are the transitions to CPC-South. In the following years the occasional double spikes, reaching up to 20 deg, are transitions to/from EDF-S. During EWS observations the variation is mostly smooth under 1 deg, promoting thermal stability (cf. Sect. 4.3.9). There are however, two spikes of 14 deg amplitude (around MJD_2000 10540 and 10910) that occur during EWS observations in transitions between low latitude patches.

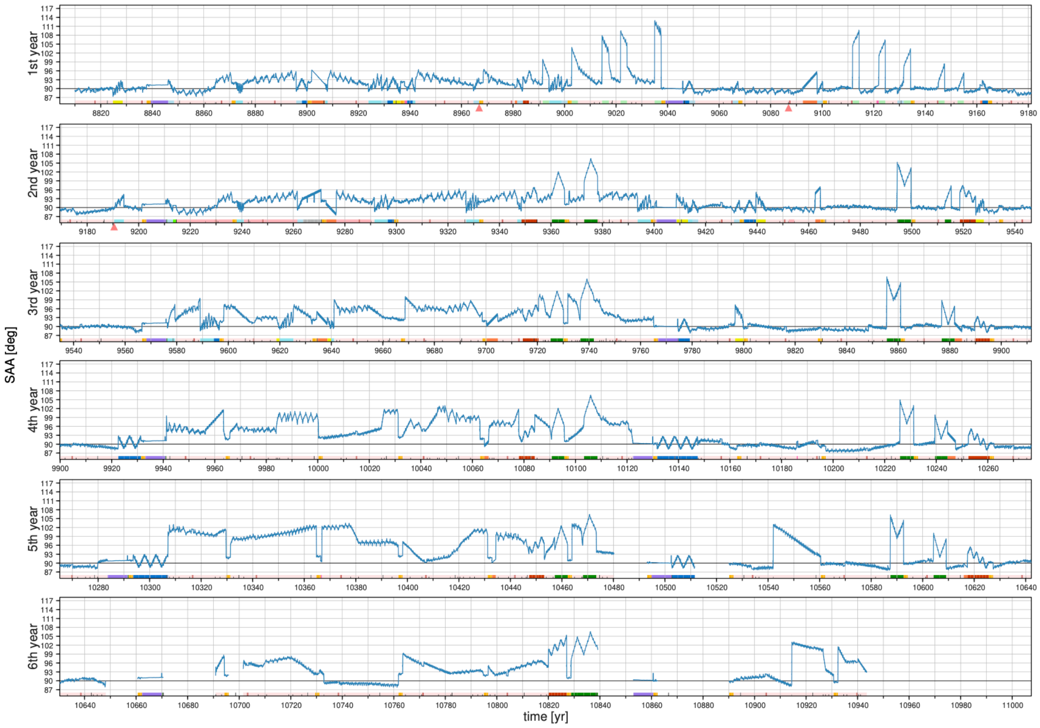

Figure 6.13: Progression of SAA during the survey. Time given in MJD_2000

Figure 6.14: Progression of SAA field-to-field variation during the survey. Time given in MJD_2000

Figure 6.15 shows the progression of AA along the survey. The most prominent feature is the fact that AA is kept constant for very large intervals of time, during the observation of EWS patches.

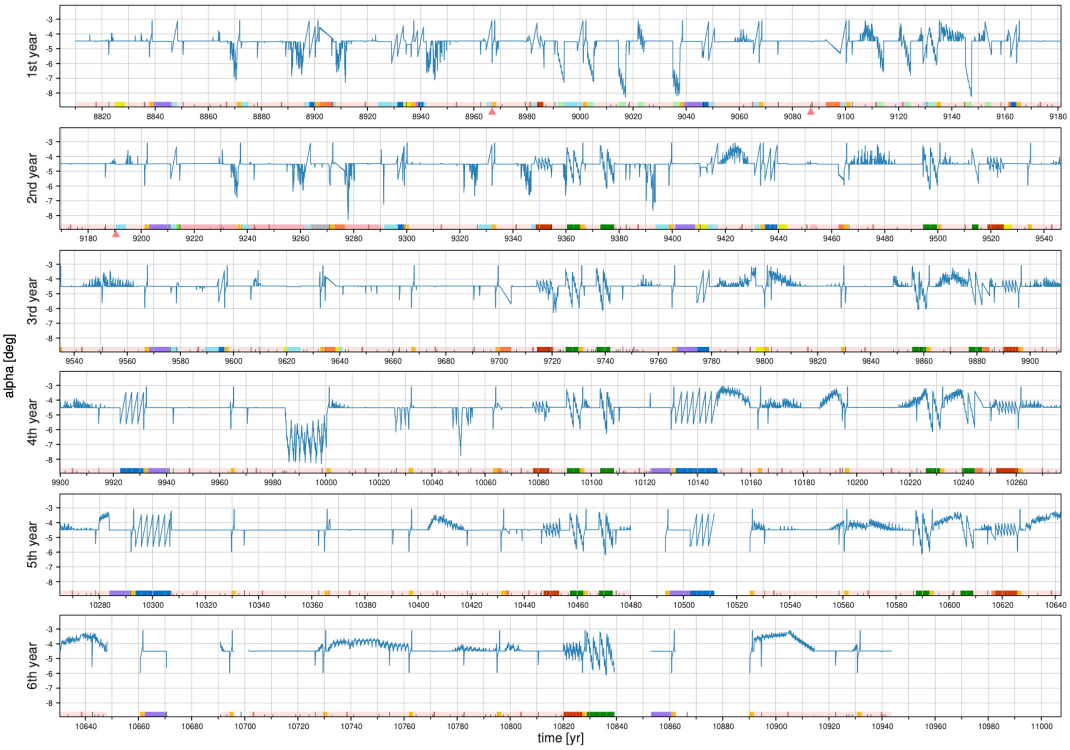

Figure 6.15: Progression of AA during the the survey. Time given in MJD_2000

Figure 6.16: Progression of AA field-to-field variation during the the survey. Time given in MJD_2000

The progression of AA field-to-field variations along the survey is shown in Figure 6.16. Variations are smaller than in SAA, being exactly zero for large periods of time. Spikes are mostly kept below 1.5 deg, with very few cases reaching 3 deg. There is a rapid AA variation around MJD_2000 9990 distinct from the other patterns present. It corresponds to a patch that was pushed to the limit to fill a gap between two patches.

In general, both SAA and AA field-to-field variations are below 1 deg throughout the survey, as shown in Figure 6.17. We note that the SAA histogram has *#solar_saadelta_outlier* of outliers with large SAA variations (larger than 4 deg) not shown in Figure 6.17.

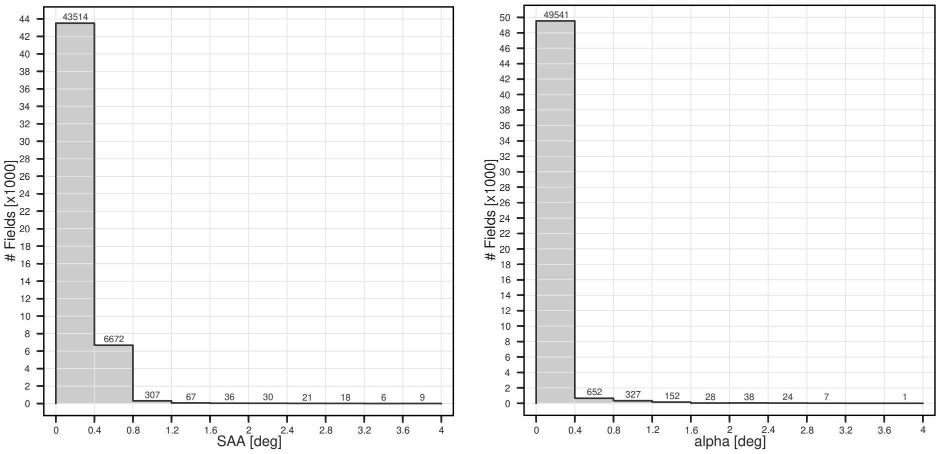

Figure 6.17: Distribution of field-to-field variations in the pointing angles: SAA (left panel) and AA (right panel)

The presented document is Proprietary information of the Euclid Consortium.
This document shall be used and disclosed by the receiving Party and its related entities (e.g. contractors and subcontractors) only for the purposes of fulfilling the receiving Party's responsibilities under the Euclid Project and that the identified and marked technical data shall not be disclosed or retransferred to any other entity without prior written permission of the document preparer.

6.3.3 Slews

Figure 6.18 shows the distribution of field (left panel) and large (right panel) slews. There is a total of *#count_slews_field* field slews. The total time spent in performing the field slews amounts to *#slewtime_total_field* over the RSD duration. There is a total of *#count_slews_large* large slews, with sizes distributed over the full range up to 180 deg. Large slews are applied a maximum of *#count_slews_large_month_max* times in a single month.

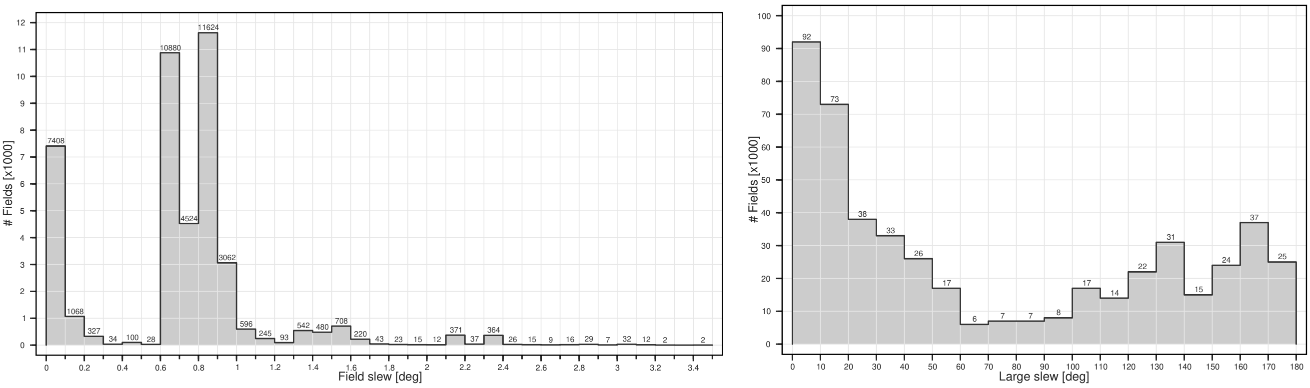

Figure 6.18: Size distribution of field-to-field slews

The presented document is Proprietary information of the Euclid Consortium.
This document shall be used and disclosed by the receiving Party and its related entities (e.g. contractors and subcontractors) only for the purposes of fulfilling the receiving Party's responsibilities under the Euclid Project and that the identified and marked technical data shall not be disclosed or retransferred to any other entity without prior written permission of the document preparer.

7 Verification control tables

This section starts by summarizing some of the RSD_2025A features. It then proceeds with the detailed verification of its compliance with MOCD-A requirements and CalF specifications.

7.1 Summary

RSD_2025A introduces the recovery capability to the replanning. It requires the user to specify a restarting point in the form of a patch id, the first patch to replan. Plus, it requires a calibration plan compatible with the basis survey, the survey to replan and recover, with an identical set of calibrations up to the breakpoint. Recovery introduces the possibility to repeat observations of EWS tiles already observed in the basis survey. The user specifies a backlog of previously skipped or lost observations to be recovered, and specifies in a new wide-plan the survey windows where to make the recoveries. The respective tiles then become available for rescheduling during the EWS computation.

A list of features of RSD_2025A follows:

- RSD_2025A contains a large reobservation campaign aimed at recovering the full intra-decontamination period of 2.5 months. Together with the recovery of other lost or skipped observations, the total recovery of tessellated EWS patches, polar caps, and 6 CPC and EDF-N visits, required the displacement of around 690 deg^2 of RSD_2024C area.

- Reserved time for a new additional survey: the Euclid Galactic Bulge Survey.

- New F-013 and F-018 calibrations.

- The new calibrations plus the EGBS reserved time require around 60 deg^2 of EWS time-equivalent area.

- The enclosed area of the EWS is compact, without gaps other than the bright start avoidance regions and totals 13 025 deg^2, which is 350 deg^2 less than in RSD_2024C. This is an improvement over the potential decrease of 750 deg^2 required for the recovery and for the time taken by the new calibrations. This result was possible at the expense of reducing the unallocated time.

- The unallocated time is 106 days, 50 days less than in RSD_2024C, and it starts only in the 5th year.

- RSD_2025A is identical to RSD_2024C up to the restarting date, hence including the original schedule of lost and skipped observations. Those amount to around 100 days, or 5% of the survey time.

- EWS allocated time is now slightly under 2/3 of the total survey time, and the unallocated time decreased to 5%.

- In winter season the reduced visibility favors the appearance of gaps between patches. In RSD_2024C most of these gaps were only filled in the summer season or in later years of the survey. RSD_2025A improved the interactive process of EWS building by allowing to extend the time limits of the survey windows case by case (while always keeping the solar angle constraints). This allowed us to extend some patches such as to fill the gaps immediately. One example is the region between EDF-F and EDF-S that is now connected earlier.

- The effect of tuning the margins of the patches to fill gaps may produce unwanted effects on the behavior of the solar angles. There is one patch observed with oscillating AA values, in contrast with all the other where AA is kept constant or varies smoothly or kept. There are also two large spikes on the SAA variation, during the 55th and 6th years that should be revised in a future RSD revision.

- Seven of the 21 polar caps patches are only observed in the 3rd year. Some of them were pushed by the reobservation campaign. In other cases, they were postponed to increase the size of a neighboring survey window such that it could include a PSF visit.

- As before, priority was given in the first year to the southern mainland. However, some of the scheduled area is outside the DES footprint and does not have ground-based data available. The coverage is thus not optimized for DR1, but it was considered too late to optimize that aspect of RSD_2025A [RD12].

- In the 6th year, when observing at low latitudes, priority was given to the southern mainland and to the southern island. This allowed to reach the ecliptic latitude of -15 deg in a more uniform way than before, and to have a more compact coverage of the southern island in detriment of scattered observations on the northern island.

- The (small and low S/N) northern island is not covered at all.

- The mean S/N is slightly higher in the three observed quadrants than in RSD_2024C.

- The quality metric in the lowest quality field is 0.68, an improvement from the 0.62 achieved by RSD_2024C.

- There is one EDF-N visit missing. It is a blue grism visit, and it will be included in a future RSD revision.

- The first EDF to be completed is EDF-N in the 10th semester.

- EDF-F reaches the required BGS:RGS ratio at the end of the 2nd year, while the other deep fields are dominated by RGS visits and only reach the balance in the 5th year.

- CPC-S is completed in the first year, but CPC-N has 4 visits left for the second year (the final two in the 4th semester of the survey).

The presented document is Proprietary information of the Euclid Consortium.
This document shall be used and disclosed by the receiving Party and its related entities (e.g. contractors and subcontractors) only for the purposes of fulfilling the receiving Party's responsibilities under the Euclid Project and that the identified and marked technical data shall not be disclosed or retransferred to any other entity without prior written permission of the document preparer.

- The reobservation of COSMOS delays its completion to the 5th semester.

- SXDS and VVDS, even though inside the RoI are outside the EWS footprint.

- There is one more visit to a PSF field, with respect to RSD_2024C. There are two instances (one shortly after the restarting date) where the presence of short survey windows does not allow the scheduling of a PSF visit, leaving a gap of 60 days in the PSF schedule. In the 5th and 6th years the presence of unallocated time also prevents the scheduling of PSF visits.

- PSF fields PSF-17 and PSF-20 are never observed.

- There is one SOPS window occurring outside the required time, which was accepted by MOC.

- F-010 is scheduled in the preferred target.

- F-011 is scheduled in 2025-03-20, 5 weeks into the 2nd year, not immediately at the beginning of the year.

- Most calibrations are done in blocks: Monthly block is now F-001+F-018+F-007. Biannual calibration is F-009+F-016 (+F-011 yearly) as before. PSF block is now F-012+F-015+F-013+F-008.

- RSD_2025A avoids implementing EDF BGS visits next to non-ROS visits to avoid grism errors. RGS visits are saved for those occasions. However, given that there are fewer RGS visits than BGS ones, this is not always possible. In the cases a BGS visit needs to be done, it is accompanied by the new F-017 buffer (a single ROS). There are nevertheless 12 instances where a BGS Deep field is followed by F-001, and 1 instance where a COSMOS visit ends in BGS and is followed by F-001. It was assumed that SOC deals with this type of transitions and an F-017 was not scheduled.

- The final observation scheduled is at longitude 170 deg, which leaves 70 deg (over 2 months) after the end of the survey for an eventual extended survey to progress efficiently before reaching the low-stress period.

7.2 Compliance with MOCD-A requirements

Table 7.1 summarizes the sky survey system requirements and the WL and GC requirements defined in *#version_mocda* [AD02] and verifies the compliance of the *#version_rsd* implementation with them.

Label	Parameter	Requirement	Survey design	Compliance
Sys-001	Survey duration	≤ 6 years	5 years and 10 months	Compliant
Sys-002	SAA range	[87.1, 120.9]	[87.16, 113.00]	Compliant

The presented document is Proprietary information of the Euclid Consortium.
This document shall be used and disclosed by the receiving Party and its related entities (e.g. contractors and subcontractors) only for the purposes of fulfilling the receiving Party's responsibilities under the Euclid Project and that the identified and marked technical data shall not be disclosed or retransferred to any other entity without prior written permission of the document preparer.

		if using an orbit file		
Sys-003	AA range	[-8.4, -3.0] if using an orbit file	[-8.33, -3.05]	Compliant
Sys-004	Deleted			
Sys-005	Number of scientific observations and field to field slews (field + large)	N_obs ≤ 55,000 N_slews ≤ 55,000	N_obs = 50,526 N_slews = 43,519	Compliant
Sys-005a	Deleted			
Sys-006	Deleted			
Sys-007	Number and amplitude of large slews	≤ 950 > 3.5 deg	563 Implemented	Compliant
Sys-008	Deleted			
Sys-009	ROS duration	(20s) + 996s + 70s + 996s + 70 s + 996s + 70s + 1006s + slew time estimator	Implemented	Compliant
Sys-009b	Deleted			
Sys-010	Deleted			
Sys-011	Deleted			
Sys-012	Slew duration	According to slew time estimator	Implemented	Compliant
Sys-012b	Minimum time between slews	According to slew type	Implemented	Compliant
Sys-012c	Lead time	20s	Implemented	Compliant
Sys-013	Deleted			
Sys-013b	Amplitude of dither slews	[37.5’’, 130’’]	[73.0’’, 130.0’’]	Compliant
Sys-013c	Dither geometry	Revised S-pattern	Implemented	Compliant
Sys-014	Deleted			
Sys-015	Deleted			
Sys-016	Deleted			
Sys-017	Deleted			
Sys-018	Deleted			
Sys-019	SOPS window	6h every 28 days (starting Mondays	76 SOPS	Compliant*

The presented document is Proprietary information of the Euclid Consortium.
This document shall be used and disclosed by the receiving Party and its related entities (e.g. contractors and subcontractors) only for the purposes of fulfilling the receiving Party's responsibilities under the Euclid Project and that the identified and marked technical data shall not be disclosed or retransferred to any other entity without prior written permission of the document preparer.

		10-14 UTC) ending with t_largeslew + 5 min SAA in [89.1, 118.9] AA in [-6.4, -3.0]	Implemented	*SOPS #17 is scheduled at 20:52 UTC, with the agreement of MOC
Sys-020	Deleted			
Sys-021	Tiles	Size defined from the common FoV No gaps if pointing uncertainty is 7.5’’ (3σ)	Tile size defined from common FoV, pointing uncertainty and tilting tolerance, ensuring no gaps by construction [RD11]	Compliant
Sys-022	VIS FoV	Coordinates of 9 points specified	Implemented	Compliant
Sys-023	NISP FoV	Coordinates of 9 points specified	Implemented	Compliant
Sys-024	Common FoV	Coordinates of 4 corners specified, corresponding to the intersection of Sys-022 and Sys-023 (not required to compute the Euclid FoV)	A different method is implemented to define the Euclid FoV from Sys-022 and Sys-023	Compliant
Sys-025	Uncertainty on line-of-sight with respect to S/C reference frame	0.1 deg per axis	No impact in survey design	N/A Note: target quaternions will need to be recomputed after in-flight characterization
Sys-026	Deleted			
Sys-027	Deleted			
Sys-028	Deleted			
Sys-029	Blinding stars avoidance	Magnitude limit is $m_{AB} \leq 4$	Tessellation include avoidance radius around blinding stars	Compliant
Sys-030	Planets straylight avoidance	Avoidance radius given	Implemented by excluding the affected areas from the RoI	Compliant
Sys-031	Deleted			
WL-001	WL survey area	> 14,000 deg^2	13,025 deg^2	Non-compliant*

	(EWS enclosed area)			*impossible to achieve simultaneously with Sys-001, given the lower survey mapping efficiency
WL-002	Mean WL galaxies density in RoI	> 30 arcmin^{-2} which implies that almost all source galaxies have S/N ($I_{\rm E}$) > 10, S/N ($Y_{\rm E}$, $J_{\rm E}$, $H_{\rm E}$) > 5 and are thus useful for WL [RD06]	Only outliers below the values: S/N ($I_{\rm E}$) = 11.4 S/N ($Y_{\rm E}$), = 5.0 S/N ($H_{\rm E}$) = 5.7 S/N ($J_{\rm E}$) = 5.7	Compliant* *compliant for S/N, the number density is non-verifiable at survey level
WL-003	WL dither coverage	95% (90%) of VIS (NISP) covered by ≥ 3 dithers	VIS: 95.2% NISP: 89.8% [RD11]	Compliant
WL-003a	Deleted			
WL-004	Area lost to bright objects avoidance	< 1.5%	1.3%	Compliant
WL-005	Deleted			
WL-006	Deleted			
WL-007	Deleted			
GC-001	GC survey area (EWS enclosed area)	> 14,000 deg^2	13,025 deg^2	Non-compliant* * impossible to achieve simultaneously with Sys-001, given the lower survey mapping efficiency
GC-002	Deleted			
GC-003	Deleted			
GC-004	Deleted			
GC-005	Deleted			
GC-006	GC dither coverage	90% (50%) of NISP covered by ≥ 3 (4) exposures	≥3: 89.8% ≥4: 52.2% [RD11]	Compliant
GC-006a	Deleted			

GC-007	Area lost to bright objects avoidance	< 1.5%	1.3%	Compliant
DS-001	EDS area	> 40 deg^2	53 deg^2	Compliant
DS-002	EDS number of visits	≥ 40 in each field	EDF-N: 39 visits EDF-S: 45 visits EDF-F: 52 visits	Non-compliant* *One additional visit needs to be scheduled in a future RSD
DS-003	Deleted			
DS-004	Depth of images VIS and NISP-P (stacked)	> 2 mag deeper than EWS implying ≥ 40 ROS visits	Implemented with the number of visits given in DS-002 (one ROS per tile per visit)	Non-Compliant* *EDF-N lacks one visit
DS-005	Deleted			
DS-006	Deleted			
DS-007	Deleted			
CA-001	Calibration observations	To be implemented according to CalF unless if conflicting with other requirements	See Table 7.2	Compliant
CA-002	Consecutive dither slews per calibration	< 10	Implemented	Compliant

Table 7.1: Compliance check with MOCD-A requirements

7.3 Compliance with calibration specifications

Table 7.2 summarizes the calibration specifications defined in *#version_calf* [AD03] and verifies the compliance of the *#version_rsd* implementation with them.

Label	Requirement	Implementation	Compliance
F-001 Self-Cal	Target: Selfcal center with specified pointings in fixed order Sequence: ROS_D1, B-R angular separation Sequence duration (estimated): 24.3 h	Target: implemented Sequence: implemented Sequence duration: 26.2h Cadence: 28-41 days	Compliant* *Cadence has one instance of 41 days

The presented document is Proprietary information of the Euclid Consortium.
This document shall be used and disclosed by the receiving Party and its related entities (e.g. contractors and subcontractors) only for the purposes of fulfilling the receiving Party's responsibilities under the Euclid Project and that the identified and marked technical data shall not be disclosed or retransferred to any other entity without prior written permission of the document preparer.

	Cadence: 25–40 days		
F-002 Deep fields	Area ≥ 40 deg^2 Sequence: ROS, B:R ratio Depth: 2 mag deeper than EWS Noise bias: progression as EWS	Area: 53 deg^2 Sequence: implemented Depth: 2 mag deeper (n_visits function of zodi), except for EDF-N Noise bias: progression slower than EWS on the 3rd year, but still compliant when considering the excess area with respect to the minimum 40 deg^2 required	Non-Compliant* * EDF-N has 39 visits, one visit less than required. To be corrected in a future RSD revision (no deadline)
F-003 CPC	Area ≥ 40 deg^2 Cadence: 10 visits with minimum separation no less than 4 deg between the reference directions, to be completed in the first year of the survey Sequence: ROS	Area = 43 deg^2 Cadence: min separation of 6.4 deg deg (CPC-N) and 4.0 deg (CPC-S), last visit (replanned CPC-N) in year 1.7 Sequence: implemented	Non-Compliant* *16/20 visits completed in first year (unavoidable due to the reobservations)
F-004 Color gradient	Target: 5 fields (AEGIS, GOODS-N, COSMOS, CDFS, UDS) Sequence: ROS, B:R ratio, in two visits Depth: 4 x S/N EWS Cadence: AEGIS in first year, at least one per year Total time (estimated): 2.8 d (AEGIS + GOODS-N)	Target: AEGIS + GOODS-N (the other 3 already observed with 5xS/N for F-005) Sequence: implemented, ending and starting with red Depth: implemented Cadence: as required (cf. Table 5.2) Total time: 2.8 d	Compliant
F-005 Photo-z	Target: 4 fields (COSMOS, SXDS, CDFS, VVDS) Sequence: ROS, B:R ratio Depth: 5 x S/N EWS Cadence: CDFS in 1st year, COSMOS observed in 4 visits to be started in 1st year Total time (estimated): 32.0 d	Target: COSMOS, SXDS, CDFS, VVDS Sequence: implemented, ending and starting with red Depth: implemented Cadence: as required (cf. Table 5.2) Total time: 31.9 d	Compliant* *COSMOS completed in the 3rd year (unavoidable due to the reobservations)
F-006 Wide survey	Target: EWS Sequence: ROS	As required	Compliant

The presented document is Proprietary information of the Euclid Consortium.
This document shall be used and disclosed by the receiving Party and its related entities (e.g. contractors and subcontractors) only for the purposes of fulfilling the receiving Party's responsibilities under the Euclid Project and that the identified and marked technical data shall not be disclosed or retransferred to any other entity without prior written permission of the document preparer.

F-007 VIS NL	Target: Selfcal-faint Sequence: special VIS sequence + bias + flats Sequence duration (estimated): 11.5h Cadence: 25–40 days	Target: implemented Sequence: implemented Sequence duration: 11.7 h Cadence: with F-001 in monthly block	Compliant
F-008 VIS PSF	Target: choice from list such as to minimize SAA and AA variations Sequence: special VIS sequence Sequence duration (estimated): 9.5 h Cadence: "loose month" (2-6 weeks) when an EWS patch is available	Target: optimal choice from list Sequence: implemented Sequence duration: 11.7 h Cadence: 60 visits in total: up to 100 days, 12 instances above 42 days, all instances more than 3 days after a SOPS	Non-compliant* *5 instances above 50 days for lack of survey windows large enough to enable thermalization, or for lack of contemporary EWS observations
F-009 NISP NL	Target: Selfcal-center Sequence: Validation + measurements Sequence duration (estimated): 6.9 d Cadence: 5-7 month	Target: implemented Sequence: as required Sequence duration: 6.7 d Cadence: 6 months	Compliant
F-010 NISP Dispersion	Target: PN (choice from list) + self-cal field Sequence: PN scan + special NISP-S sequence alternating between sef-cal and PN Cadence: once, after 11-16 months Total time (estimated): 7.0 d	Target: preferred PN Sequence: implemented, Cadence: once, after 15 months Total time: 6.9 d	Compliant
F-011 NISP reciprocity failure	Target: Selfcal-center Sequence: special NISP-P sequence with and without LED illumination Sequence duration (estimated): 8.5 h Cadence: Annual, starting one year into the survey	Target: implemented Sequence: implemented Sequence duration: 11h Cadence: annual, starting on month 13, with every other biannual block	Compliant
F-012 VIS Flatband voltage shifts	Target: off-sky Sequence: special VIS sequence Sequence duration (estimated): 36 min Cadence: with every F-08	Target: PSF field Sequence: implemented Sequence duration: 36 min Cadence: same as F-008	Compliant

	observation, in a F-012/F-015/F-013/F-008 sequence		
F-013 Photometric calibration	Target: PSF field Sequence: 4 ROS-D1 pointings Sequence duration (estimated): 1.4 h Cadence: with every F-08 observation, in a F-012/F-015/F-013/F-008 sequence	Target: PSF field Sequence: implemented Sequence duration: 1.4 h Cadence: same as F-008	Compliant
F-015 VIS Serial trap pumping	Target: VIS PSF field Sequence: special sequence Sequence duration (estimated): 1.9 h Cadence: with every F-08 observation, in a F-012/F-015/F-013/F-008 sequence	Target: PSF field Sequence: implemented Sequence duration: 1.9 h Cadence: same as F-008	Compliant
F-016 Charge injection timing	Target: unspecified, but avoiding the stray light leak Sequence: special sequence Sequence duration (estimated): 2.7 h Cadence: 5 -7 month	Target: high latitude, avoiding forbidden angles Sequence: as required Sequence duration: 2.8 h Cadence: same as F-009 in biannual block	Compliant
F-017 Grism sanity	Target: an EDF Sequence: 1 ROS (red) Sequence duration (estimated): 1.2 h Cadence: after or before a EDF blue visit that precedes or follows (respectively) a non-ROS observation	Target: center of the relevant EDFs Sequence: as required Sequence duration: 1.2 h Cadence: applied in two instances	Compliant* * There are 13 instances of ROS transitions to F-001 where F-017 could have been scheduled optionally and it was not
F-018 NISP Persistence	Target: unspecified Sequence: special sequence Sequence duration (estimated): 2.3 h Cadence: in every monthly block, in a F-001/F-018/F-007 sequence	Target: high latitude, avoiding forbidden angles Sequence: as required Sequence duration: 2.3 h Cadence: same as F-001	Compliant

Table 7.2: Compliance check with CalF specifications

The presented document is Proprietary information of the Euclid Consortium.
This document shall be used and disclosed by the receiving Party and its related entities (e.g. contractors and subcontractors) only for the purposes of fulfilling the receiving Party's responsibilities under the Euclid Project and that the identified and marked technical data shall not be disclosed or retransferred to any other entity without prior written permission of the document preparer.